FACTORS AFFECTING MATURATION OF BOVINE OOCYTES; HORMONAL ENVIRONMENT, FOLLICULAR AND MATERNAL AGING

A Thesis Submitted to the College of

Graduate Studies and Research

In Partial Fulfillment of the Requirements

For the Degree of Doctor of Philosophy

Department of Veterinary Biomedical Sciences

University of Saskatchewan

Saskatoon

By

DINESH DADARWAL

TABLE OF CONTENTS

page

PERMISSION TO USE i
ABSTRACT ii
LIST OF TABLES vii
LIST OF FIGURES viii
LIST OF ABBREVIATIONS xi

CHAPTER 1: GENERAL INTRODUCTION 1
1.1 Estrous cycle and follicular dynamics in cattle 2
1.2 Hormone and follicular dynamics in cattle 4
1.3 Progesterone level and duration of proestrus during follicle development 8
1.4 Superstimulation 9
1.5 Oocyte quality and cytoplasmic organelles 10
1.5.1 Nuclear maturation 11
1.5.2 Cytoplasmic maturation 14
1.5.2.1 Role of mitochondria in oocyte competence 16
1.5.2.2 Role of lipid droplets in oocyte competence 18
1.6 Maternal aging and oocyte competence 20
1.7 Follicular aging and oocyte competence 21
1.8 FSH starvation 22
1.9 Confocal Microscopy 23
1.10 Mitochondrial and lipid droplet staining 24

CHAPTER 2: OBJECTIVES AND HYPOTHESES 25
2.1 Specific Objectives 25
2.2 Specific Hypotheses 26

CHAPTER 3: EFFECT OF PROGESTERONE CONCENTRATION AND DURATION OF PROESTRUS ON FERTILITY IN BEEF CATTLE AFTER FIXED-TIME ARTIFICIAL INSEMINATION 27
3.1 Abstract 28
3.2 Introduction 29
3.3 Materials and methods 31
3.3.1 Animal groups and treatment protocol 32
3.3.2 Blood sampling and radioimmunoassay 34
3.3.3 Statistical analyses 35
3.4 Results 36
3.4.1 Blood plasma progesterone concentration 36
3.4.2 Ovulation and pregnancy rates 38
3.4.3 Size of the preovulatory follicle 40
3.4.4 Size of the CL, and progesterone concentrations 40
3.4.5 Reproductive end points in subset of data after hormone….. 43
3.5 Discussion 44

CHAPTER 4: ORGANELLE REORGANIZATION IN BOVINE OOCYTES AT DIFFERENT STAGES OF DOMINANT FOLLICLE GROWTH AND MATURATION **48**
4.1 Abstract *49*
4.2 Introduction *50*
4.3 Materials and Methods *52*
4.3.1 Collection of cumulus-oocyte-complexes (COCs) 52
4.3.2 Processing of oocytes for transmission electron microscopy 54
4.3.3 Analyses of cytoplasmic organelle parameters 55
4.3.4 Statistical analyses 57
4.4 Results *57*
4.4.1 Mitochondria 57
4.4.2 Mitochondrial relation with lipid droplets and SER profiles 58
4.4.3 Lipid droplets 61
4.4.4 Other organelles 63
4.5 Discussion *65*

CHAPTER 5: EFFECT OF FOLLICULAR AGING ON THE NUCLEAR MATURATION AND DISTRIBUTION OF LIPID DROPLETS IN BOVINE OOCYTES **73**
5.1 Abstract *74*
5.2 Introduction *75*
5.3 Materials and Methods *77*
5.3.1 Experimental design and protocol 78
5.3.2 Collection of Cumulus-Oocyte Complexes 80
5.3.3 Processing of COCs for Nuclear staining 81
5.3.4 Processing of COCs for Lipid staining 83
5.3.5 Image processing and segmentation of 3D volume sets 83
5.3.6 Statistical analyses 88
5.4 Results *88*
5.4.1 Follicle numbers and collection efficiency 88
5.4.1. Nuclear maturation 90
5.4.2 Oocyte volume, lipid volume and surface area 92
5.4.3 Lipid droplets number and distribution 94
5.5 Discussion *96*

CHAPTER 6: EFFECT OF FOLLICULAR AND MATERNAL AGING ON ATP CONTENT AND DISTRIBUTION OF MITOCHONDRIA IN *IN VIVO* MATURED OOCYTES **101**
6.1 Abstract *102*
6.2 Introduction *104*
6.3 Materials and methods *107*
6.3.1 Follicular aging: experimental design and protocol 107
6.3.2 Maternal aging: experimental design and protocol 108
6.3.3 Grading of COCs 109
6.3.4 ATP assay 109
6.3.5 Processing of COCs for mitochondrial staining 110
6.3.6 Image processing, segmentation of 3D volume sets 111

6.3.7 Statistical analyses 116
6.4 Results *116*
6.4.1 Follicular Aging: collection efficiency and grades 116
6.4.2 Follicular Aging: total ATP content 117
6.4.3 Follicular aging: mitochondrial population and distribution pattern 119
6.4.4 Follicular aging: Mitochondrial activity and size 122
6.4.5 Maternal Aging: collection efficiency and grades 124
6.4.1 Maternal aging: total ATP content 125
6.4.6 Maternal aging: mitochondrial population 126
6.4.7 Maternal aging: average intensities and voxel numbers of mitochondria 129
6.5 Discussion *131*

CHAPTER 7: GENERAL DISCUSSION **136**

CHAPTER 8: GENERAL CONCLUSIONS **151**
8.1 Progesterone concentration and length of proestrus during dominant follicle growth *151*
8.2 Oocyte ultrastructure with respect to changes dominant follicle growth, regression and maturation *151*
8.3 Follicular aging: nuclear maturation, lipid droplets, mitochondrial number and distribution and ATP content *152*
8.4 Maternal aging: ATP content and mitochondrial number and distribution. *152*

CHAPTER 9: BIBLIOGRAPHY **154**

APPENDIX A **179**

10 WORK FLOW FOR SEGMENTATION OF 3D DATA (MITOCHONDRIAL STAINING) **179**
10.1 Preliminary steps to consider before performing deconvolution (in Imaris 7.4) *179*
10.2 Deconvolution in Autoquant X2 *180*
10.3 Segmentation of mitochondrial intensities *183*
10.3.1 Threshold cutoff 183
10.3.2 Surface build up 184
10.3.3 Distance transformation to surface 187
10.3.4 Identification of mitochondria as Spots 188
10.3.5 Identification of spots in clusters or isolated spots (individual mitochondria) 190
10.3.6 Identification of peripheral vs central spots 194
10.3.7 Identification of intensities in within the spots and clusters 195

Permission to Use

In presenting this thesis in partial fulfilment of the requirements for a Postgraduate degree from the University of Saskatchewan, I agree that the Libraries of this University may make it freely available for inspection. I further agree that permission for copying of this thesis in any manner, in whole or in part, for scholarly purposes may be granted by the professor or professors who supervised my thesis work or, in their absence, by the Head of the Department or the Dean of the College in which my thesis work was done. It is understood that any copying or publication or use of this thesis or parts thereof for financial gain shall not be allowed without my written permission. It is also understood that due recognition shall be given to me and to the University of Saskatchewan in any scholarly use which may be made of any material in my thesis.

Requests for permission to copy or to make other use of material in this thesis in whole or part should be addressed to:

Head of the Department of Veterinary Biomedical Sciences

University of Saskatchewan

Saskatoon, Saskatchewan (S7N 5B4)

ABSTRACT

Hormonal environment in which follicle grows has been shown to affect the oocyte competence. Our objective was to identify factors that affect oocyte competence and characterize the structural and functional changes induced by these factors.

Fertility was compared in cattle following alterations in levels of progesterone and length of proestrus during dominant follicle growth. We hypothesized that subluteal-phase progesterone will mitigate the effect of a shorter proestrus on pregnancy rates. A shorter duration of proestrus during a fixed-time AI protocol in cattle resulted in a smaller preovulatory follicle, smaller and less functional CL with lower progesterone secretion, and lower fertility ($P<0.01$). A subluteal-phase progesterone milieu during ovulatory follicle growth induced higher pregnancy rates ($P<0.01$) and compensated for the effect of a short proestrus on pregnancy rates.

Organelle behavior was characterized in oocytes obtained from follicles at different phases of dominant follicle growth. We hypothesized that ooplasmic organelles undergo changes in population and spatial distribution in a phase-specific manner. The growing phase oocytes have least area of mitochondria in contact with lipid droplets ($P=0.04$) and a peripheral distribution of lipids compared to an even distribution in oocytes from other phases. The regression phase oocytes showed an increase in mitochondrial number ($P=0.03$) and even distribution of mitochondria compared to peripheral in other phases. Moreover, oocytes from regression phase had higher ($P<0.01$) lipid content per unit volume of oocyte than other phases.

Effect of follicular aging on nuclear maturation rates and, size and distribution of lipid droplets and mitochondria in *in vivo* matured oocytes were compared. We hypothesized that follicular aging after FSH starvation will result in maturation failure with accumulation of larger lipid droplets and altered distribution of mitochondria as compared to superstimulation with

continued FSH support (4-d and 7-d). A 7-d FSH protocol resulted in greater proportion ($P<0.01$) of mature oocytes compared to other groups. FSH starvation lead to more poor quality oocytes that had ATP contents similar to short FSH group. Further, organization of mitochondria as intense and bigger clusters ($P=0.01$) alongwith increased size of lipid droplet ($P=0.03$) within the oocytes from FSH starvation group might indicate atresia. Effect of maternal aging on mitochondrial numbers, distribution and ATP content of *in vivo* matured bovine oocytes was studied. We hypothesized that *in vivo* matured oocytes from old cows will have reduced number of mitochondria, altered distribution of mitochondria and decreased the ATP content compared to those from young cows. Maternally aged oocytes had significantly less ATP content ($P=0.01$) although mitochondrial population and distribution pattern did not differ.

ACKNOWLEDGMENTS

I am grateful to Dr Jaswant Singh, for accepting me as a PhD student in his lab. His patience, knowledge, dealing with students and "always ready with a question" attitude is unmatched. I hope that I have lived up to his expectations.

I would like to thank my committee members, Dr Gregg Adams, Dr Carl Lessard and Dr Suresh Tikoo for their valuable time, suggestions and critics throughout my PhD program. I thank Dr Baljit Singh (Associate Dean) and Dr Gilian Muir (graduate chair), without their directions and wisdom completion of my PhD would not have been possible.

I would also like to express my gratitude towards Dr Reuben Mapletoft for his guidance. I am deeply touched by his age defying hard work, promptness and humbleness. I also thank Dr Poul Hyttel for collaborating and sharing his knowledge with me. I thank Dr GS Dhaliwal and Dr SPS Ghuman from India for suggesting me to join Dr Singh's lab.

I have very fond memories that I share with my friends Gary, Shankar, Jaipal, Aman, Ravi, Deepak, Srinivas, Alisha, Irfan, Ajeet, Mrigank and their families. Their presence made my stay much more enjoyable and Saskatoon my home. I would like to thank all my RRL team members; Fernanda, Jennifer, Manuel, Miriam, Hayder, Bilal, Orleitta, "awesome" Luiz's and summer students Cody, Amber, Tegan, Chris, Dhruv, Rand Davis, Kelly, Dally, and Shiny, who helped in best of their capacities and mean more than colleagues to me. I also appreciate help extended by Kosala Rajapaksa and Lyle Boswall in lab.

It was unfortunate that three people that I admired and loved, my mom Mohini Devi, my father-in-law Dr Ram Deo and, my friend and colleague Dr Jagir Singh, left for their heavenly abode during my PhD. I would have loved to share my achievements with them.

Last but not least, I thank my wife, Pooja, my son Abhi, my father Dr KR Dadarwal and my mother-in-law Mohini Devi for being patient and making my life complete. I hope I will be able to spend more time with them after my PhD.

Last but not least, I am thankful to University of Saskatchewan and Province of Saskatchewan for the financial support and GADVASU, Ludhiana for allowing me to pursue my PhD at University of Saskatchewan.

Dedication

I would like to dedicate this thesis to my family, my teachers, Guru Angad Dev Veterinary and Animal Sciences, Ludhiana and University of Saskatchewan, Saskatoon. Without their faith and support I would not have succeeded in this venture.

LIST OF TABLES

Table 3.1. Effect of treatments designed to induce luteal-phase progesterone concentrations and a normal proestrus (LN), luteal-phase progesterone and a short proestrus (LS), subluteal-phase progesterone and a normal proestrus (SuN) , and subluteal-phase progesterone and a normal proestrus (SuS) in cattle (heifers and cows combined). Data represent the subset of animals in each group in which the intended progesterone profile was achieved. …44

Table 4.1. Volume (percent of ooplasm) and surface density (Mean±SEM, $\mu m^2/\mu m^3$ of ooplasm) of mitochondria, SER profiles and vesicles; and number (Mean±SEM, per $1000\mu m^3$ of ooplasm) of SER profiles and vesicles in oocytes at different stages of follicular development. …65

Table 5.1. Mean number (±SE) of follicles in different size categories at 12h after LH administration. …89

Table 5.2. Proportion of COCs collected to follicles aspirated (percent collection efficiency) and different grades of expanded COCs in different superstimulation protocols …89

Table 5.3. Mean (±SEM) number and relative proportion lipid droplets in oocytes collected following superstimulation protocols. …95

Table 6.1. Percent collection efficiency and proportion (percent) of different grades of COCs obtained from follicles aspirated at 18-20 h after LH administration. …117

Table 6.2. Proportion of oocytes from Short FSH, FSH starvation and Long FSH groups different distribution pattern of mitochondria within the ooplasm. …119

Table 6.3. Effect of superstimulatory treatment on the mean **(**±SEM) number**,** proportion, and distribution of individual mitochondria and clusters within the oocyte. …121

Table 6.4. Percent collection efficiency and proportion (percent) of different grades of COCs obtained from follicles aspirated at 18-20 h after LH administration. …124

Table 6.5. Proportion of oocytes from young and old cows with different distribution pattern of mitochondria within the ooplasm. …127

Table 6.6. Mean **(**±SEM) number and proportion of individual mitochondria and clusters within the oocyte of superstimulated young and old cows. …128

LIST OF FIGURES

Figure 3.1 Treatment groups designed to induce luteal-phase progesterone levels and a normal proestrus (LN), luteal-phase progesterone levels and a short proestrus (LS), subluteal-phase progesterone levels and normal proestrus (SuN), or subluteal-phase progesterone levels and short proestrus (SuS) in cows (n= 79) and heifers (n=61).. 34

Figure 3.2 Blood plasma progesterone concentrations (mean±SEM) in cattle (cows and heifers combined) treated to induce luteal-phase progesterone concentrations and a normal proestrus (LN), luteal-phase progesterone and a short proestrus (LS), subluteal-phase progesterone and a normal proestrus (SuN), and subluteal-phase progesterone and a normal proestrus (SuS). 37

Figure 3.3 Ovulation (a) and pregnancy rates (b) in cattle (cows and heifers combined) treated to induce luteal-phase progesterone concentrations and a normal proestrus (LN) luteal-phase progesterone and a short proestrus (LS), subluteal-phase progesterone and a normal proestrus (SuN) and subluteal-phase progesterone and a normal proestrus (SuS). Ovulation was evaluated 22 h post-AI and pregnancy was diagnosed at Day 60 post-AI. 39

Figure 3.4 Size of preovulatory follicle (mm, mean ±SEM) at fixed-time AI in cattle (cows and heifers combined) treated to induce luteal-phase progesterone concentrations and a normal proestrus (LN) luteal-phase progesterone and a short proestrus (LS), subluteal-phase progesterone and a normal proestrus (SuN), and subluteal-phase progesterone and a normal proestrus (SuS). 41

Figure 3.5 Diameter of the CL (a; mm, mean ±SEM) and plasma progesterone concentration (b; ng/ml, mean ±SEM) 9 days after fixed-time AI in cattle (cows and heifers combined) treated to induce luteal-phase progesterone concentrations and a normal proestrus (LN), luteal-phase progesterone and a short proestrus (LS), subluteal-phase progesterone and a normal proestrus (SuN), and subluteal-phase progesterone and a normal proestrus (SuS). 42

Figure 4.1 Diameter profiles (Mean +SEM, mm) of dominant follicles of Wave 1 (anovulatory) and Wave 2 (ovulatory). Mean days of follicular aspirations on Day 3 of Wave 1 (D3W1), Day 6 of Wave 1 (D6W1), Day 1 of Wave 2 (D1W2) and preovulatory during estrus (Day ≥17) are indicated by dotted vertical lines. 53

Figure 4.2 (a, b, c, d) Electron micrographs (photographed at a primary magnification of 3000x) representing peripheral (a), perinuclear (b), and central (c) regions of ooplasm as well as the peripheral region overlayed with the transparent grid for stereology (d). (e, f, g, h) Cortical granules (CG), Golgi complex (G), hooded (HM) and non-hooded mitochondria (N-HM), vesicles (V), smooth endoplasmic reticulum (SER), and lipid droplets LD) identified for the quantitative data..... 56

Figure 4.3 Percent distribution of mitochondria in different regions of ooplasm (a) and percentage of mitochondrial surface in contact with lipid droplets (b) and smooth

endoplasmic reticulum (c) in oocytes collected at different stages of follicular growth and maturation. 59

Figure 4.4 Number (Mean + SE) of total (a), non-hooded (b) and hooded (c) mitochondria per 1000μm^3 of oocyte from follicles at different stages of follicular growth and maturation. 60

Figure 4.5 Volume (a, percent of oocyte volume), surface density (b, μm^2/ μm^3 of oocyte) and number (c, per 1000 μm^3 of oocyte) of lipid droplets..... 62

Figure 4.6 Number of Golgi complexes (a) and cortical granules (b) in 1000 μm^3 of oocyte from follicles at different stages of follicular growth and maturation. 64

Figure 5.1 Experimental protocols designed to give Short FSH, FSH Starvation and Long FSH superstimulation treatments in heifers (n=12). 79

Figure 5.2 Flow chart showing steps involved in identifying lipid droplets of an oocyte stained with Nile Red. 86

Figure 5.3 Images representative of distribution patterns observed in bovine oocytes, uniformly scattered (a), peripherally scattered (b), peripherally clustered (c), centrally scattered (d) and centrally clustered (e). The images are maximum intensity projection of 10 μm z-stacks around the largest diameter of the oocytes. 87

Figure 5.4 Percent rates of immature (A), intermediate (B) and mature (C) oocytes following Short FSH, FSH starvation and Long FSH treatments. Nuclear envelop of oocytes was immunostained with anti-Lamin A/C followed by Alex 488 (pseudo-colored yellowish green to enhance visualization) as secondary. Chromatin material (Aqua color) was stained with DAPI..... 91

Figure 5.5 Mean (+ SE) volume of individual lipid droplets (10^{-3} picoliter, a), total lipid volume (picoliter, b), surface area of individual lipid droplets (μm^2, c) and total surface area (10^3 μm^2, d) within the oocytes collected following three superstimulatory treatments. 93

Figure 6.1 Supertimulation protocol applied to mother-daughter pairs (n=7). PGF = prostaglandin F2α; FSH = Follicular Stimulating Hormone; LH = Lutropin. FSH injections were administered at 12 h intervals. 109

Figure 6.2 Pictures depicting steps of segmentation in Imaris Pro 7.4.2 to identify individual and clustered mitochondria. 114

Figure 6.3 Confocal microscopy showing mitochondrial distribution patterns observed in oocytes stained with Mitotracker Deep Red FM (D to H). Unstained negative control oocyte show no mitochondrial staining (A, Transmission light and B, He Ne 633 nm laser)..... 115

Figure 6.4 Total ATP content (mean±SE) in the oocytes from compact and extended COCs of Short FSH, FSH starvation and Long FSH groups. Both compact and extended COCs included all grades..... 118

Figure 6.5 Average intensity (±SE) and average number voxels (±SE) in individual mitochondria and clusters in the oocytes from COCs of Short FSH (n=5), FSH starvation (n=30) and Long FSH (n=12) groups.. 123

Figure 6.6 Total ATP content (mean±SE) in the oocytes from compact (A) and expanded (B) COCs of mother and daughter groups... 125

Figure 6.7 Mean intensity (±SE) and mean number of voxels (±SE) in individual mitochondria and clusters in the oocytes from COCs of young (N=20) and old cows (N=42)..... 130

Figure 7.1 Schematic presentation of changes in organelle characteristics with development of dominant follicle. 141

LIST OF ABREVIATIONS

AI	artificial insemination
ATP	Adenosine triphosphate
C	celsius
CIDR	controlled internal drug release
CL	corpus luteum
COC	cumulus oocyte complex
d	day
fmol	femto mol
FSH	follicle stimulating hormone
GV	germinal vesicle
GVBD	germinal vesicle breakdown
h	hours
im	intramuscular
IVF	in vitro fertilization
LH	luteinizing hormone
pmol	pico mol
MHz	megahertz
min	minute
mL	milliliter
mm	millimeter
mM	millimolar
ng	nanogram
pL	picoliter
ROS	reactive oxygen species
SAS	statistical analysis system
SEM	standard error of the mean
SER	smooth endoplasmic reticulum
vs.	versus
µg	microgram
µL	microlitre
µm	micron
NIH	National Institute of Health

CHAPTER 1

1 GENERAL INTRODUCTION

An understanding of the factors that influence oocyte maturation is of immense value to improve fertility in livestock species and humans during the natural and assisted breeding programs. Improvements in our understanding of follicular growth characteristics and our ability to manage follicular growth have helped to design protocols that allow scientists to test the effect of different hormonal environments on the quality of oocyte and its developmental competence. Studies have indicated that level of progesterone (Savio et al., 1993; Bisinotto et al., 2010; Denicol et al., 2012), its duration (Mihm et al., 1999; Santos et al., 2010) and duration of proestrus (Bridges et al., 2008; Bridges et al., 2010) during the growth of dominant follicle affect fertility. However, it is not fully understood how do different levels of progesterone during early part combined with different durations of progesterone-free environment during later part of dominant follicle growth, affect fertility in cattle.

Despite advances in our ability to culture oocyte and embryos *in vitro*, the blastocyst number derived from *in vitro* fertilization (IVF) programs are still lower than those from oocytes matured *in vivo*. Studies in cattle have indicated that differences in the duration of growth of follicle during *in vitro* maturation compared to *in vivo* obtained oocytes fail to bring certain desired changes in the morphology of the oocyte (Hyttel et al., 1989a). Organelles, especially mitochondria (Stojkovic et al., 2001; Nagano et al., 2006) and lipid droplets (Sutton-McDowall et al., 2012) have been associated with the attainment of oocyte competence. However, maturation changes in oocyte, especially

with respect to cytoplasmic organelles, are of descriptive nature and have not been characterized based on the well-defined stages of follicular growth.

In the following sections, I review our current knowledge of factors that influence bovine oocyte maturation. Wherever there is lack of information in cattle, available literature from other species has been incorporated.

1.1 Estrous cycle and follicular dynamics in cattle

Estrous cycle represents the duration between two consecutive estrus events and is on average 21 days in cattle (Adams et al., 2008; Adams et al., 2012). Cattle assume regular estrous cyclicity at the onset of puberty, the age (average 15 months) of which can vary depending on genotype, plane of nutrition, season and social interaction with bulls (Patterson et al., 1992; Funston et al., 2012; Perry, 2012). More than 50% of the cattle cease to undergo regular estrous cycles (reproductive senescence) by the age of ≥13 years (Erickson, 1966). Estrous cycle of cattle has been divided into four phases: proestrus, estrus, metestrus and diestrus. These phases depend on the signs of receptivity, ovarian structures and hormonal environment. Proestrus is the period (2-3 days) from luteolysis to onset of receptivity, when progesterone decreases following luteolysis and reach basal levels while estradiol levels gradually increase (Forde et al., 2011). Estrus represents the period when a cow exhibits receptive behavior towards male for mating due to effect of blood plasma estradiol concentrations on brain in presence of basal levels of progesterone (Vailes et al., 1992; White et al., 2002; Roelofs et al., 2010). The duration of standing estrus varies between 8-18 hours depending on the type of cattle (dairy or beef), lactational status, milk yield and method used for estrus detection (White et al., 2002; Forde et al., 2011). Ovulation occurs 20-30 h after the onset of estrus (White

et al., 2002; Forde et al., 2011). During next 3 to 4 days following ovulation, the granulosa and theca cells of the follicle wall develop into luteal tissue, plasma progesterone levels gradually rise to luteal levels and the period is often referred to as metestrus. During the proceeding diestrus period (13-16 days), luteal tissue (corpus luteum) is fully functional (Forde et al., 2011). The corpus luteum secretes progesterone during the entire diestrus period or for the entire duration of pregnancy in pregnant cattle.

The introduction of ultrasonography into cattle reproduction in early 1980's allowed scientists and veterinary practioners to track changes in ovarian structures i.e. follicles and corpus luteum over the entire estrous cycle. New concepts of follicular growth from a spontaneous growth to wave-like growth pattern emerged, a phenomenon that has been tested in other mono-ovular species including humans (Baerwald et al., 2003; Adams et al., 2012; Baerwald et al., 2012). Cattle can have one to four waves of follicle growth in a given cycle, but majority has either a 2-wave or 3-wave growth pattern in an estrous cycle (Pierson and Ginther, 1984; Pierson and Ginther, 1988; Savio et al., 1988a; Sirois and Fortune, 1988; Knopf et al., 1989; Jaiswal et al., 2009; Adams et al., 2012). The number of waves in estrous cycle has been reported to remain constant in about 2/3rd of cattle (Jaiswal et al., 2009). During each wave, a group of follicles (4 mm) begin to grow and after 2-3 days of growth, one (Pierson and Ginther, 1988) of them becomes dominant to continue its growth, while others undergo atresia. The phenomenon of selecting a dominant follicle was observed to occur under the influence of estradiol and inhibin secreted collectively by all growing follicles (Gibbons et al., 1997a; Ginther et al., 2000a; b). The dominant follicle (except from ovulatory wave) and subordinate follicles have been shown to undergo well-defined stages of growth (where follicle

continues to grow), static (follicle diameter remains constant) and regression (follicle undergoes reduction in diameter) phases. The last wave i.e. 2nd and 3rd in a two- or three- wave animal is ovulatory and is represented by the continuous growth of dominant follicle culminating in ovulation (Pierson and Ginther, 1988; Savio et al., 1988a; Sirois and Fortune, 1988; Knopf et al., 1989).

1.2 Hormone and follicular dynamics in cattle

Each wave of follicular growth is initiated by a transient rise in FSH, secreted from pituitary in response to GnRH (Baenziger and Green, 1988). Both FSH and LH are glycoproteins that share a species-specific α-subunit and differ in their hormone-specific β-subunit (Baenziger and Green, 1988). Transient rise in FSH surge consistently occurred on the day before follicles ≥ 4 mm were detected (Adams et al., 1992b). A decline in FSH following the peak FSH levels, was related with one of the follicles being selected to become dominant (Gibbons et al., 1997a; Ginther et al., 1999). The decline in FSH levels was observed to happen due to the estradiol and inhibin secreted collectively by all follicles ≥ 5 mm in size (Gibbons et al., 1997a). In cattle, follicle selection occurred when dominant follicle reaches ≥8.5mm antral diameter and exceeded the size of subordinate follicles by at least 1 mm (Gibbons et al., 1997a). Recently, growth of follicles sized 1-3mm were tracked through ultrasound and were shown to have a wave pattern closely linked with FSH surge (Jaiswal et al., 2004; Adams et al., 2012). Moreover, a hierarchy of growth was observed in the study as the follicle that emerged earliest (at least 6 to12 h earlier than other follicles) was destined for being selected as dominant follicle (Jaiswal et al., 2004). If the hierarchy designates selection, it raises questions about our current understanding of dominant follicle selection. Follicles of all sizes (1-14 mm) have been

shown to have FSH receptors but lower levels of FSH at the time of selection were reported to be insufficient for further growth of subordinate and smaller follicles (Xu et al., 1995). These lower levels of FSH were proposed to be critical in order to sustain the growth of largest follicle as further reduction in FSH concentrations slowed the growth of largest follicle. A rebound in FSH levels was reported to bring the growth rate back to normal allowing continuous growth of the largest follicle (Bergfelt et al., 2000). Moreover, granulosa cells of future dominant follicle acquired LH receptors around the time of selection, so that it can continue to grow from available LH support (Bao et al., 1997a; Luo et al., 2011). The increase in LH receptor concentration in granulosa cells of dominant follicle has recently been shown to occur under the influence of circulating LH (Luo et al., 2011). While, subordinate follicles became atretic due to lack of sufficient FSH levels in circulation and failed to respond to circulating LH due to lack of LH receptors in granulosa cells (Bao et al., 1997a; Luo et al., 2011). Concomitant to the difference in LH receptors concentration in the granulosa cells of dominant vs subordinate follicles, the dominant follicle have had an increase in secretion of estradiol and insulin like growth factor-1 and, decreased IGF binding proteins (IGFBP-2 and -5) levels (Austin et al., 2001; Shahiduzzaman et al., 2010). Before selection, all follicles ≥ 5 mm have the ability to become dominant follicle (Gibbons et al., 1997a). Indirect evidence to the above-mentioned concept is provided by the ability of exogenous FSH administration to prevent the subordinate follicles to undergo atresia during the superstimulatory treatments.

In cattle, inhibin-A from the dominant follicle, rather than estradiol, has been reported to keep the FSH levels to basal secretion (Kaneko et al., 1993; Kaneko et al.,

1997; Kaneko et al., 2002). For dominant follicle, basal levels of FSH may still be needed for continued growth, as exogenous estradiol could cause dominant follicle atresia (Adams et al., 1992b; Bergfelt et al., 2000), which explains why dominant follicle ablation and exogenous estradiol administration consistently result in an emergence of a new follicular wave emergence. Both these methods are used quite extensively to synchronize emergence of a new wave, approximately 1 to 2 days after dominant follicle ablation (Bergfelt et al., 1994) or cautery (Ko et al., 1991) and approximately 4 days after estradiol administration in presence of luteal levels of progesterone (Bo et al., 1994). Alternatively, GnRH can be administered to cause ovulation or luteinization of follicles ≥9 mm and synchronize the emergence of new wave 2 days later (Martinez et al., 2000). However, only 56% of heifers and 85% of cows respond favorably to GnRH treatment (Pursley et al., 1995; Roche and Mihm, 1997), which makes ablation and estradiol administration as the preferred methods of synchronizing new wave emergence over GnRH in cattle. However, ablating follicles require expertise and costly equipment, while, estradiol has been banned in many countries due to suspected adverse effects on human health through meat or milk consumption. Exogenous estrogens from animal meat and milk have been associated with precocious puberty (Aksglaede et al., 2006), increasing testicular and breast cancer incidents in humans (Meireles et al., 2010; Pape-Zambito et al., 2010; Zhong et al., 2011).

During the first wave in a cattle, the dominant follicle continues to grow but does not ovulate and undergo regression as the progesterone from corpus luteum keep the LH pulses at low levels (Rahe et al., 1980). Moreover, the granulosa cells of dominant follicles in presence of luteal-phase progesterone lost their LH receptors, thus failed to

continue growth and undergo atresia (Xu et al., 1995). Progesterone have been shown to suppress the GnRH secretion through it's nuclear receptors, thereby keeping LH pulsatility at low levels (Skinner et al., 1998; Mihm et al., 2002). In sheep, it was observed that progesterone receptors are present on dopaminergic, beta-endorphin, dynorphin B and NPY neurons in the arcuate nucleus of hypothalamus (Dufourny et al., 2005a; b). These neurons were shown to project into preoptic area of hypothalamus that is rich in GnRH neurons responsible for pulsatile GnRH secretion (Dufourny et al., 2005a; b).

In the ovulatory wave, the LH pulsatility increases following luteolysis (due to removal of progesterone inhibition on GnRH pulsatility), which increases the steroidogenic capacity of the dominant follicle and allows follicle to grow bigger (Rathbone et al., 2001a; Ginther et al., 2012a). Resulting increase in circulating estradiol concentrations reaches a peak level to indirectly induce GnRH surge, which in turn cause LH surge (Rathbone et al., 2001a; Reames et al., 2011; Ginther et al., 2012a). Approximately 24 to 27 h following LH surge, the preovulatory follicle undergo certain changes to release the mature oocyte (Rathbone et al., 2001a; Siddiqui et al., 2010). In order to circumvent the cost involved with estrus detection, different hormones have been used to induce synchronous ovulation in large group of animals, reviewed earlier (Mapletoft et al., 2003; Macmillan, 2010; Wiltbank et al., 2011). Exogenous administrations of GnRH analogues, estradiol and porcine LH have been shown to induce ovulation at different time points with varying degree of synchrony (Mapletoft et al., 2003; Macmillan, 2010; Wiltbank et al., 2011).

1.3 Progesterone level and duration of proestrus during follicle development

Progesterone is the primary determinant of the fate of dominant follicle as to whether the follicle will ovulate or regress during an estrous cycle. Luteal levels of progesterone have been shown to suppress LH pulsatility that keep estradiol production from follicle at low levels and do not allow dominant follicle to ovulate (Rathbone et al., 2001a; Ginther et al., 2012a). Circulating Progesterone levels inversely affected the size of growing dominant follicle in a dose dependent manner (Adams et al., 1992a). Subluteal-phase levels of progesterone that are observed during initial growth of dominant follicle of wave 1 or otherwise maintained using exogenous sources have been related to decline in fertility (Savio et al., 1993; Bisinotto et al., 2010; Denicol et al., 2012). These studies proposed that higher LH pulse frequency due to subluteal-phase levels were allowing the oocytes within follicles to mature earlier than needed, thereby adversely affecting fertility. When progesterone was administered exogenously to maintain luteal levels of progesterone during the 1st wave, the pregnancy rates increased and were comparable to those observed in lactating dairy cattle that ovulated follicle from 2^{nd} wave (Denicol et al., 2012). Despite an increased preovulatory follicle diameter due to subluteal-phase progesterone during dominant follicle growth, no adverse or beneficial effects on fertility in beef cattle were observed when compared to groups with luteal levels of progesterone (Colazo et al., 2004b; Pfeifer et al., 2009; Cerri et al., 2011). Contrary to aforementioned studies, larger size follicles have been shown to develop into larger corpora lutea and more functional following ovulation, which is beneficial for embryo development and hence improve pregnancy rates (Perry et al., 2005).

Dominant follicles of ovulatory waves complete its final (2-3 days) growth in a relatively progesterone free environment that is commonly referred as proestrus period. Proestrus period is characterized by increased estradiol production by follicle that in turn increases LH amplitude acting via modulating GnRH secretion from hypothalamus and an increase in LH pulse frequency due to basal progesterone concentrations (Rathbone et al., 2001a; Ginther et al., 2012a). Also, a 5d progesterone dependent growth plus 3d progesterone free growth increases fertility in cattle compared to 7d progesterone dependent plus 2.5d progesterone free growth (Bridges et al., 2008; Bridges et al., 2010). The duration of growth from wave emergence to ovulation is another key factor that determines the outcome of breeding/insemination. Longer period of growth in luteal or subluteal-phase environment were reported to decrease the oocyte quality and hence fertility compared to a short period of growth in the luteal environment (Mihm et al., 1999; Santos et al., 2010). However, the effect of short duration of dominant follicle growth under subluteal-phase progesterone environment has not been studied especially in conjunction with different durations of proestrus.

1.4 Superstimulation

Both equine chorionic gonadotropin (eCG) and FSH have been used to develop superstimulation protocols for both clinical and research purposes (Bo et al., 2011; Mapletoft and Bo, 2011). The end goal is to obtain maximum number of embryos per animal from a single superstimulation protocol. Due to a shorter half-life of FSH (Laster, 1972), single dose induces lower superovulatory response (Looney et al., 1981; Walsh et al., 1993), therefore, multiple doses of constant or decreasing amount are given to achieve optimal superstimulation (Mapletoft et al., 2002). However, recent study have shown that

a single-split dose of FSH with hyaluronan is capable of yielding on an average 5 transferable embryos, quite similar to traditional repeated dose protocol (Tríbulo et al., 2012). A higher response of superstimulatory treatment in cattle have been shown to occur if the treatment was initiated around the time of follicular wave emergence (Nasser et al., 1993). As wave emergence occurs on 2 to 3 occasions during an estrous cycle, very limited time is available to initiate superstimulation at the time of spontaneous wave emergence. For that reason, superstimulation protocols are often preceded by estradiol plus progesterone or transvaginal follicular ablation to synchronize the follicular wave with superstimulatory protocols (Mapletoft et al., 2003; Jaiswal, 2007). Furthermore, the progesterone levels during the superstimulatory treatment have been shown to affect the embryo quality but it is not yet clear whether the effect favorable or detrimental (Rivera et al., 2011). One of the studies have shown that subluteal-phase progesterone during superstimulation produce poor quality embryos (Jaiswal, 2007; Rivera et al., 2011) while other study have shown improved embryo quality compared to protocols with luteal levels of progesterone (Jaiswal, 2007).

1.5 Oocyte quality and cytoplasmic organelles

Various studies have reflected on the role played by different organelles on the quality and competence of oocytes. Recent study in mouse has shown that mitochondria and lipid droplets are needed for ATP production for the energy demanding processes of maturation, fertilization and cleavage (Dunning et al., 2010). Mitochondria along with SER are the Ca^{2+} storehouses, which is exchanged between the two organelles to create membrane potential in order to regulate different cell functions (Iino, 2010). Resumption of meiosis in bovine oocytes has been related to Ca^{2+} signaling as Ca^{2+} chelator prevents

oocyte nuclear maturation (He et al., 1997). SER along with Golgi bodies are also believed to be the source of lipid droplets that are needed for ATP generation and membrane synthesis during cleavage (Ost et al., 2005). Golgi bodies function as specialized regions for the transport and processing of proteins (Rothman, 1994; Allan and Balch, 1999). In addition, Golgi bodies produce cortical granules that were recently shown to be essential for blocking polyspermy in mice (Liu, 2011; Burkart et al., 2012). Actin microfilaments have been shown to assist cortical granules in their movement to periphery in mice oocytes in order to block polyspermy (Connors et al., 1998). Microtubules and microfilaments have also been considered crucial for nuclear maturation of bovine oocytes as they were reported to aid in proper alignment of chromosomes with the spindles (Kim et al., 2000). Furthermore, microtubules have been shown to assist the movement of active mitochondria to the inner cytoplasm and localization around peri-nuclear area during pig oocyte maturation (Sun et al., 2001).

1.5.1 Nuclear maturation

Although oocytes enter the meiotic cell cycle during the fetal life, the completion of meiosis occurs only in adult life when ovulated oocytes are fertilized *in vivo* or oocytes are matured and fertilized *in vitro*. During the fetal life, the primary oocytes within the primordial follicles are arrested at Prophase I. As the primordial follicles enters the growth phase and become antral follicles (around 0.3 mm size; (Lussier et al., 1987) the oocyte diameter increases from 30 microns to 90 microns. Oocytes from small antral follicles (0.4-0.9 mm) were shown to resume meiosis but only 1/10th could complete it to Metaphase II (Führer et al., 1989). By the time follicles reached 2 mm of antral diameter about 50% of the oocytes could develop a Metaphase II spindle (Führer et al., 1989; Fair

et al., 1995). Mammalian oocytes have been shown to resume meiosis if they are removed from the antral follicles (Pincus and Enzmann, 1935; Edwards, 1965; Palma et al., 2012) or within the preovulatory follicles under the influence of LH surge (Kruip et al., 1983; Hyttel et al., 1986b). The ability of oocytes arrested at prophase I to resume meiosis, release half set of chromosomes as polar body and develop into Metaphase II (MII) is referred as nuclear maturation. The process of nuclear maturation has further been categorized into distinct stages. In the germinal vesicle (GV) stage, oocytes have an intact nuclear envelope and enclose filamentous chromatin material with various degrees of clumping (Motlik et al., 1978; Chohan and Hunter, 2003; Liu et al., 2006). In the germinal vesicle breakdown (GVBD), the nuclear envelope was shown to undergo degeneration, get rippled and the nuclear material got condensed (Hyttel et al., 1987). In cattle, majority of the oocytes reached GVBD by 6 hours after of IVM, which is often considered as an indicator of meiosis resumption (Motlik et al., 1978; Hyttel et al., 1986b). In superstimulated cattle, the GVBD occurred at 9-12 h after LH surge and no difference in ultrastructure was shown to exist when PMSG or FSH was used for superstimulation (Hyttel et al., 1986a). Around the time when GVBD occurred, there was retraction of contacts between the oocyte and surrounding cumulus cells (Hyttel et al., 1986a). Following GVBD, the chromosomes were arranged as Metaphase I spindle. Next, the oocyte released the polar body and developed Metaphase II spindle to complete the nuclear maturation. In cattle, a major proportion of oocytes reached MII at 20 h of IVM (Hyttel et al., 1986b) or 20 h after spontaneous or induced LH-surge (Kruip et al., 1983; Hyttel et al., 1986a; Hyttel et al., 1989c). In heifers superstimulated with PMSG, the percent of MII oocytes from >8mm follicles increased from 22% at 48 hours after

prostaglandin injection to 65% about 12 hours later (Bousquet et al., 1995). The effect of duration of FSH treatment in a superstimulation protocol and gonadotropin free period on the nuclear maturation rates of bovine oocytes is not known.

It appears that several mechanisms are involved in resumption of meiosis and completion of nuclear maturation. Cyclic nucleotides, cyclic AMP and cyclic GMP, are considered as the primary inhibitors of meiotic resumption in oocyte (Törnell et al., 1990). The cGMP produced by granulosa cells have been proposed to enter the oocyte through the gap junctions between oocyte and cumulus cells to keep the levels of primary cAMP phosphodiesterase 3A (PDE3A) in mouse oocyte at low levels (Norris et al., 2009). Lowered PDE3A were reported to permit the cAMP, produced within the oocyte by constitutive GPCR3 (Mehlmann, 2005) to remain at higher levels and thus maintain the meiotic arrest in mouse oocytes. The LH exposure has been shown to decrease the cGMP production by granulosa cells through yet unknown mechanisms and close the gap junctions (by phosphorylation of connexin-43) via mitogen activated protein kinase (MAPK) (Norris et al., 2008; Norris et al., 2009; Conti et al., 2012). Both of these events reportedly decreased the amount of cGMP entering the mouse oocyte. Reduced cGMP in turn increased the PDE3A that hydrolyses cAMP and initiated resumption of meiosis. The LH peak before the ovulation have been indicated to cause granulosa cells to undergo luteinization to produce more of progesterone, which is reflected in the steroid content of the bovine follicular fluid (Fortune et al., 2009). Recent study has proposed that an increase in progesterone within the follicular fluid initiated meiotic resumption in bovine oocytes (Siqueira et al., 2012). Same study also showed that higher progesterone induces PGE2 production. The later is needed for epidermal growth factors (EGF) like

factors mediated maintenance of MAPK secretion in cumulus cells (Yamashita et al., 2011).

The preovulatory LH surge is also crucial for the cumulus cell expansion that is often used as an indicator of oocyte maturation. The LH surge have been shown to increase the levels of EGF-like factors such as amphiregulin (AREG), epiregulin (EREG) and b-cellulin (BTC) in the follicular fluid of preovulatory follicles, while the epidermal growth factor (EGF) itself remained at low levels (Hsieh et al., 2009; Zamah et al., 2010; Kawashima et al., 2012). Recently, LH stimulated mouse oocytes have been shown to secrete crucial factors, growth differentiation factor 9 and bone morphogenic protein 15, that increased the expression of epidermal growth factor receptor in the cumulus cells (Su et al., 2010). The EGF like factors secreted from granulosa cells bind to its receptor on cumulus cells to cause cumulus cell expansion (Kawashima et al., 2012). Existence of mutual interaction between the oocyte and surrounding cumulus cells in cattle has been indirectly observed in a recent study as adding denuded oocytes and COCs during IVM increased the blastocyst rates (Dey et al., 2012). Recent reports that atrial natriuretic peptides (Zhang and Xia, 2012) and angiotensin II (Reis et al., 2012; Siqueira et al., 2012) might be involved in the oocyte meiosis have indicated that our understanding of the mechanisms involved in nuclear maturation is far from clear.

1.5.2 Cytoplasmic maturation

Cytoplasmic maturation is a poorly defined process that refers to the changes in organelles morphology, their inter-relationships and functions within the oocytes of dominant follicles. These modulations in organelles are expected to help the oocytes to store enough mRNA and proteins that will be required during nuclear maturation,

fertilization and early embryonic life before genomic activation of embryo (Sirard, 2001; Ferreira et al., 2009). A classical ultrastructural study was undertaken on bovine oocytes in order to evaluate the qualitative changes in organelles as the dominant follicles grow until the time close to ovulation following induced luteolysis (Assey et al., 1994). As dominant follicle of the ovulatory wave grew in presence of luteal levels of progesterone from CL, the contacts between oocyte and cumulus cells remained intact. Cortical granules moved in clusters towards peripheral ooplasm, while there was a decline in microvilli and an increase in the contact between lipid droplets and mitochondria (Assey et al., 1994). At 24-48 h after prostaglandin injection, the contacts between oocyte and surrounding cumulus cells decreased, cumulus cells began to expand, cortical granules became solitary and lipids became larger (Assey et al., 1994). At 72 h after induced luteolysis, perivitelline space appeared, mitochondria showed even distribution, lipid droplets were larger and centrally located, and the contacts between different organelles decreased. Completion of cytoplasmic maturation had been defined by the localization of cortical granules to just inside of ooplasmic membrane (Kruip et al., 1983; Assey et al., 1994). During IVM, a heterogenous population of oocytes are aspirated from 3-8 mm follicles and cultured for 24 h before being fertilized *in vitro*. It has been suggested short-time (24 h) of maturation period is not enough for the oocytes, especially from the smaller follicles, to undergo cytoplasmic changes as observed during growth and maturation of follicles *in vivo*. In that regard, previous studies have indicated some differences between the *in vivo* and *in vitro* matured oocytes with regards to the changes in organelle morphology and distribution (Hyttel et al., 1989a). These changes in oocyte organelles could be the reason why *in vivo* matured oocytes have better developmental

competence than those *in vitro* matured (van de Leemput et al., 1999; Hendriksen et al., 2000).

1.5.2.1 Role of mitochondria in oocyte competence

Mitochondria are organelles primarily responsible of ATP generation but in addition they act as source of reactive oxygen species, store Ca^{2+}, and mediate apoptosis (Ramalho-Santos et al., 2009; Van Blerkom, 2011; St John, 2012). Structurally, mitochondria have outer and inner membranes. The later is thrown into shelf-like cristae surrounding a matrix (Zick et al., 2009). The morphology of mitochondria vary with cell type and functioning of cell (Zick et al., 2009). In oocytes from growing follicles, the mitochondria have large number of cristae (Wassarman and Josefowicz, 1978). Whereas mitochondria represent a more quiescent morphology as they are round in shape with less cristae in matured oocytes (Assey et al., 1994).

Mitochondria are unique organelles as they have their own DNA (mtDNA) coding for 13 genes of proteins needed for oxidative phosphorylation (Scarpulla, 2008; St John et al., 2010). These proteins are crucial subunits of electron transport chain, which reside in the inner mitochondrial membrane. The remaining subunits are coded by nuclear DNA and are imported into the mitochondria (St John, 2012). In oocytes, each mitochondrion has been proposed to have 2-5 copies of mtDNA. The MII oocytes of cattle on an average have approximately $3.8x10^5$ copies of mtDNA (Tamassia et al., 2004; May-Panloup et al., 2005). The mtDNA copies have been observed to reduce to approximately half from 4-cell stage until morula and increase to $6.8x10^5$ copies in blastocysts (Tamassia et al., 2004; May-Panloup et al., 2005). Concomitant to the increase in mtDNA copies in blastocyst stage, there was an increase in the regulators of mtDNA transcription namely

nuclear respiratory factor 1 (NRF1) and the mitochondrial transcription factor A (Tamassia et al., 2004; May-Panloup et al., 2005; Kanka et al., 2012). Recent reports have indicated that mtDNA copy number is more critical for development of embryo but not for oocyte maturation (Wai et al., 2010; Ge et al., 2012). Based on silencing one copy of mitochondrial transcription factor A gene, the mouse oocyte has been reported to need 40-50,000 mtDNA copies for embryonic development (Wai et al., 2010).

Several studies have related changes in mitochondrial distribution and mitochondrial activity with oocyte maturation and developmental competence (Ge et al., 2012; Sato and Sato, 2012). The distribution pattern of mitochondria have been reported to vary with species and stage of oocyte maturation (Tarazona et al., 2006; Ambruosi et al., 2009; Valentini et al., 2010; Machatkova et al., 2012; Marei et al., 2012). Based on dyes targeted towards mitochondrial membrane potential, immature bovine oocytes were shown to have lower mitochondrial activity compared to *in vitro* matured oocytes (Tarazona et al., 2006). A recent study has shown a decrease in mitochondrial activity and mitochondrial clustering when bovine oocytes from healthy follicles were compared with those from atretic follicles (Machatkova et al., 2012). The presence of mitochondria in clusters have been proposed to be the areas of localized ATP production by oxidative phosphorylation thereby limiting the deleterious effects of reactive oxygen species (Van Blerkom et al., 2003; Van Blerkom, 2011). As mtDNA is not protected by histone and lack DNA repair system, it has been proposed to undergo mutations due to oxidative stress especially with aging (Croteau and Bohr, 1997; Stuart and Brown, 2006). In that regard, a significant increase in point mutations have been observed in oocytes from older women that could affect DNA replication (Barritt et al., 2000; Bentov et al., 2011).

The ATP generated by mitochondria is needed for variety of events such as oocyte maturation, fertilization and early embryonic development until embryonic genome activation (Van Blerkom et al., 1995; Bavister and Squirrell, 2000; Stojkovic et al., 2001; Nagano et al., 2006; Van Blerkom, 2011). Further, the ATP content of oocyte has been related to developmental competence of the oocyte as good quality bovine oocytes have higher ATP content (Stojkovic et al., 2001; Nagano et al., 2006; Machatkova et al., 2012). The amount of ATP within the porcine oocytes was influenced by presence or absence of surrounding cumulus cells as incubating denuded oocytes with cumulus cells during IVM increased the ATP content of the porcine oocytes (Cui et al., 2009). The chances of aneuploidy, meiotic arrest and fertilization failure increases in the event of low ATP content in aged oocytes or poor quality oocytes (Van Blerkom et al., 1995; Ramalho-Santos et al., 2009; Zhao and Li, 2012).

1.5.2.2 Role of lipid droplets in oocyte competence

Lipid droplets are dynamic organelles that store triglycerides in the central core surrounded by phospholipids, cholesterol and variety of proteins (Martin and Parton, 2006; Olofsson et al., 2009). They have been proposed to originate from the plasma membrane (Marchesan et al., 2003), endoplasmic reticulum (Robenek et al., 2006) or Golgi (Ost et al., 2005). The origin of lipid droplets in oocytes have not been studied, but these structures have been observed in close association with smooth endoplasmic reticulum within the bovine oocytes (Assey et al., 1994). Recently, Perilipin 2, a protein that regulates both triglyceride accumulation and lipolysis, was found to be increased in mouse oocyte after hCG injection with a concomitant increase in lipid droplet accumulation (Yang et al., 2010). The Perilipin 2 mRNA and protein did not increase

after IVM despite an increase in lipid droplet amount indicating that other proteins might be involved in the lipid droplet dynamics. According to the morphological grading of COCs based on homogeneity of cytoplasm, larger lipid droplets were observed in Grade 3 and 4 COCs (de Loos et al., 1989). It is not clear whether the accumulation of lipids in oocytes with poor competence is due to an increase in lipid production or due to decrease in utilization of lipids by the oocytes.

Till date, the maturation and culture media have been developed based on the concept that carbohydrates are the crucial energy substrate used by oocytes and embryos. As one mole of palmitic acid yields thrice the amount of ATP produced by 1 M glucose, only recently the focus has shifted towards lipid droplets as energy substrates (McKeegan and Sturmey, 2011; Sutton-McDowall et al., 2012). The morphological Grade 1 immature bovine COCs (de Loos et al., 1989) have triglycerides as major lipid type with palmitic, oleic and stearic acids as the primary components of triglycerides in the lipid droplets. The immature bovine oocytes have more triglyceride content that decrease as the oocytes mature, get fertilized and cleave to two-cell stage (Ferguson and Leese, 1999). Subsequent studies further substantiated the claim that triglycerides act as important source of energy during oocyte maturation and early embryonic development in cattle (Ferguson and Leese, 2006; Jeong et al., 2009), pig (Somfai et al., 2011) and mouse (Downs et al., 2009). The rate-limiting enzyme for β-oxidation of lipids, carnitine-palmitoyl-transferase-I (CPT1B), is located in the outer mitochondrial membrane component, and regulates the entry of lipids into mitochondria for ATP synthesis (Gentile et al., 2004; Dunning and Robker, 2012). Inhibiting CPT1B during oocyte maturation and post-fertilization period significantly decreased the blastocyst rate in mouse (Dunning et

al., 2010). Further, adding L-carnitine, an amino acid needed for transporting fatty acids to mitochondria, improved the *in vitro* development of bovine embryos (Sutton-McDowall et al., 2012). It appears that both carbohydrates and lipids are needed as energy source by the oocyte and developing embryo. This could be the reason why combination of L-carnitine and carbohydrates increased the blastocyst rates over carbohydrate alone supplementation during *in vitro* culture of bovine embryos (Sutton-McDowall et al., 2012).

1.6 Maternal aging and oocyte competence

Maternal aging refers to that state of follicle when it is recruited into growth phase at an older age. Age related decline in fertility due to poor oocyte quality is well documented in women as patients >37 years of age have higher rates of fertilization failure (Yie et al., 1996). Even the primordial and primary follicles of older women have been shown to differ with respect to morphology of different organelles when compared to the follicles from younger women aged 25-32 years (de Bruin et al., 2004). It has been observed that mouse oocytes loose the ability to store the mRNAs required for maturation and subsequent development with the advancing age (Hamatani et al., 2004). A reduced expression of genes involved in cell cycle regulation, oxidative phosphorylation and oxidative stress was observed in oocytes from older women aged >38 years (Eichenlaub-Ritter et al., 2004; Steuerwald et al., 2007; Eichenlaub-Ritter et al., 2011). As a result, oocytes from older women are affected at multiple levels. They suffer from more oxidative stress due to reduced reactive oxygen species scavengers such as glutathione and superoxide dismutase (Tarin et al., 2004; Steuerwald et al., 2007). Other effects observed in older women are increased mitochondrial damage (both DNA and coded

proteins) and higher incidence of aneuploidy due deregulated cell-cycle (Tatone, 2008; Eichenlaub-Ritter et al., 2011).

Older cows (13-14 yrs.) have been validated to be an ideal model to study reproductive function of older women as there are similarities in follicular dynamics and hormonal profiles of these species with advancing age (Malhi et al., 2005). When older cows were superstimulated and oocyte competence compared to those of younger cows, about 2/3rd of the oocytes from older cows experienced fertilization failure (Malhi et al., 2007). However, the embryos from older cows and younger cows did not differ with regards to their potential to develop and both groups carried to full term. The advancing age of cows or women have been shown to affect the oocytes ability to undergo *in vitro* fertilization (Su et al., 2012). In oocytes from older cows, rate of oocyte nuclear maturation was not affected (Yamamoto et al., 2010). However, a large proportion of oocytes from older cows failed to get fertilize (Yamamoto et al., 2010), a finding that has been observed in oocytes from older women too (Yie et al., 1996).

1.7 Follicular aging and oocyte competence

Follicular aging refers to the phenomenon when a dominant follicle in the ovulatory wave is allowed to grow for longer period before it ovulates. In 2-wave cattle, the dominant follicle of an ovulatory wave grows for 9 d before it ovulates compared to 6 d in a 3-wave animals (Ginther et al., 1989; Jaiswal et al., 2009). In a recent study, shorter duration of growth period of ovulatory follicle (analogous to a 3-wave animal), lead to a smaller preovulatory follicle compared to 2-wave animals without affecting the fertility (Dias et al., 2012b). When cattle were superstimulated, longer growth period resulted in poor quality cleavage-stage embryos (Dias et al., 2012a); however, the embryos from

both groups did not differ with regard to their ability to grow during *in vitro* culture. There seems to be an upper limit to the duration of dominant follicle growth such that the oocyte within follicle is still competent to get fertilized and develop into embryo. When follicles were allowed to grow for >10 days, the oocyte showed sign of asynchrony between the nuclear and cytoplasmic maturation (Revah and Butler, 1996) and fertility was reduced (Stock and Fortune, 1993; Austin et al., 1999).

1.8 FSH starvation

The FSH starvation or withdrawal refers to the period from the last FSH injection of superstimulatory treatment to the spontaneous or induced LH peak (Dias et al., 2012a; García Guerra et al., 2012) or collection of oocytes (Blondin et al., 1997b; Sirard et al., 1999). The concept of FSH starvation was proposed when higher *in vitro* blastocyst rates were observed using oocytes aspirated from follicles 48 h after single bolus FSH injection (Blondin et al., 1997b). A 48 h waiting period induced some degree of atresia in oocytes that has been shown as beneficial for future embryo development (Blondin et al., 1997a). Further, when follicles were aspirated in superstimulated heifers at 36 h, 48 h and 60 h after the last FSH treatment, a 48 h-FSH free window improved the blastocyst rates (Sirard et al., 1999). However, when a 84 h starvation period (60 h in presence of luteal levels of progesterone plus 24 h under decreasing levels of progesterone) was provided, about half of the dominant follicles lost their ovulatory capacity (Dias et al., 2012a). Further introducing a still longer starvation period (144 h) in heifers under a subluteal-phase levels of progesterone caused all follicles to loose their ovulatory capacities (Jaiswal, 2007). More recently, a range of starvation period (44-68 h) was defined that have been proposed to increase the blastocyst rates (Nivet et al., 2012). These studies

indicated that oocyte undergo certain undefined changes during the FSH starvation period that improves the developmental competence which should be tested against the groups that are given continuous FSH support.

1.9 Confocal Microscopy

Confocal microscopy works on the principal of illuminating an object under review with a point source light of which the image is gathered and projected through a pinhole aligned in a conjugate focal plane (Minksy, 1961). The pinhole removes out-of-focus light, which is the primary reason for clarity of confocal images compared to those obtained in wide-field microscopy. The specimen is illuminated repeatedly in the same focal plane to gather the entire 2D-image. Once a focal plane has been scanned, the light can be focused on different focal planes at specified depths in Z-direction to obtain 3-D image sets. In further improvement to the confocal microscopy systems, multi-photon laser allows deeper penetration of specimen and less photobleaching of flurophores compared to conventional confocal laser scanning microscopy (CLSM) (Bush et al., 2007). Despite these improvements, the resolution of both conventional confocal microscopy and multi-photon confocal microscopy is limited by the point-spread function (PSF) (van der Voort and Strasters, 1995; Kirshner et al., 2012). The PSF is blurring/convolution of a confocal image due to diffraction of light by the point of object in focus and by the edge of aperture (van der Voort and Strasters, 1995; Dong et al., 2003). The blurring is more in the Z-direction (radial PSF) rather than in X-Y plane (transaxial PSF) (Dong et al., 2003; Biggs, 2010). Thus, it is necessary to remove the out-of-focus light i.e. deconvolution by using theoretical PSF (based on algorithms) or PSF based on fluorescent beads (Biggs, 2010; Cole et al., 2011).

1.10 Mitochondrial and lipid droplet staining

Functional status of mitochondria if often assessed by using dyes that accumulate in the mitochondria based on inner mitochondrial potential, which indicates ATP synthesis capabilities of cell (Chazotte, 2009; 2011; Perry et al., 2011). Mitotracker probes, including Mitotracker Deep Red, are positively charged that have been shown to permeate through the cell membrane and distribute in a Nernstian fashion into active mitochondria (Ehrenberg et al., 1988; Chazotte, 2009). Compared to other cationic dyes such as rhodamine 123 and JC1, carbocyanine based Mitotracker dyes (including Mitotracker Deep Red) have the advantage of being stable to aldehyde fixation (Poot et al., 1996; Perry et al., 2011). The rhodamine 123 has phototoxic effects on cells and JC1 gives non-mitochondrial staining (Chen, 1989). Both these stains wade off as soon as mitochondria looses its membrane potential and are not fixation resistant (Chen, 1989).

Cytoplasmic lipids can be easily stained with Nile Red, which is a fluorescent (yellow to gold fluorescence) derivative of otherwise non-fluorescent Nile blue stain (Fowler et al., 1985; Greenspan et al., 1985). The fluorescent capability and excitation and spectra emission spectra of Nile Red are dependent on solvents as it is least fluorescent in water and high in organic solvents (Greenspan and Fowler, 1985). Previous studies have shown the Nile Red to be an excellent dye for staining lipids in mammalian oocytes (Genicot et al., 2005; Barcelo-Fimbres and Seidel, 2011; Romek et al., 2011).

CHAPTER 2

2 OBJECTIVES AND HYPOTHESES

The overall hypothesis is that hormonal environment, stage and duration of follicle development and age of animal influence the bovine oocyte maturation. The overall objective is to study the effects of hormonal environment on fertility and aspects of bovine oocyte maturation.

2.1 Specific Objectives

1. To compare the effects of changes in duration of proestrus and progesterone concentration on follicular development and fertility after fixed-time artificial insemination in beef cows and heifers.
2. To define the changes in number, size and distribution of organelles in the ooplasm during different phases of dominant follicle development.
3. To study the effect of follicular aging with or without FSH starvation on:

a) Nuclear maturation.

b) Lipid droplets number and distribution in the ooplasm.

4. To determine the effect of follicular aging with or without FSH starvation on:

a) Number and distribution of mitochondria within the ooplasm

b) ATP content of bovine oocytes.

5. To evaluate the effect of maternal aging on:

a) Number and distribution of mitochondria within the ooplasm

b) ATP content of bovine oocytes.

2.2 Specific Hypotheses

1. a) Exposure of the growing dominant follicle to luteal-phase plasma progesterone concentrations followed by a short duration of proestrus will result in lower fertility than longer duration of proestrus.

   b) Exposure of the growing dominant follicle to subluteal-phase progesterone concentrations will overcome the negative effects of short proestrus.
2. Organelles within an oocyte undergo changes in number and spatial distribution depending on the stage of dominant follicle growth and maturation.
3. a) Follicular aging of oocytes after FSH starvation will result in failure of nuclear maturation and accumulation of larger lipid droplets as compared to those with continued FSH support for short or long duration.

   b) Follicular aging of oocytes after FSH starvation will cause an abnormal mitochondrial distribution across the ooplasm and a lower ATP content compared to those with continued FSH support.
4. Maternal aging will alter the distribution of active mitochondria across the ooplasm and reduce the ATP content of *in vivo* matured oocytes.

CHAPTER 3

3 EFFECT OF PROGESTERONE CONCENTRATION AND DURATION OF PROESTRUS ON FERTILITY IN BEEF CATTLE AFTER FIXED-TIME ARTIFICIAL INSEMINATION

Dadarwal D, Mapletoft RJ, Adams GP, Pfeifer LFM, Creelman C, Singh J

Relationship of this study to the dissertation

The dominant follicle of the ovulatory wave in cattle initiates its final growth in a luteal-phases progesterone levels and completes the differentiation in decreasing or basal levels of progesterone (proestrus period). In this first study of my dissertation, I examined how alterations in hormonal environment during dominant follicle development affect the fertility in beef cattle. We tested the hypotheses that a) an exposure of the growing dominant follicle to luteal-phase plasma progesterone concentrations followed by a short duration of proestrus will result in lower fertility than longer proestrus, and b) an exposure of the growing dominant follicle to subluteal-phase progesterone concentrations will overcome the effects of short proestrus.

3.1 Abstract

Our objective was to determine the effect of plasma progesterone concentration and the duration of proestrus during growth of the ovulatory follicle on fertility in beef cattle. Heifers (n=61) and postpartum cows (n=79) were assigned randomly to four groups in a 2-by-2 design involving luteal-phase versus subluteal-phase plasma progesterone concentration and normal versus short proestrus. To synchronize follicular wave emergence, estradiol-17β was given im during the mid-luteal phase (Day 0) and a once-used CIDR device was placed intravaginally same day. In the subluteal-phase progesterone groups, a luteolytic dose of prostaglandin F2α (PGF) was given on Day 0 and again 12 h later. In the luteal progesterone groups, PGF was not given so as to retain a functional CL. The CIDR was removed and PGF was given on Day 7 or 8 in the short- and normal-proestrus groups, respectively. Cattle were given pLH im 12 h or 36 h later in the short- and normal-proestrus groups, respectively, and artificially inseminated (AI) 12 h after pLH treatment. Transrectal ultrasonography was used to monitor ovarian response during treatments and to diagnose pregnancy 60 d post-AI. Cattle (heifers and cows combined) with subluteal-phase levels of progesterone and those with normal proestrus had a larger follicle at the time of AI and larger CL 9 days after AI that secreted higher concentrations of progesterone than cattle with luteal levels of progesterone or those with short proestrus (progesterone, $P<0.03$; proestrus, $P<0.01$). A higher incidence of ovulation ($P<0.01$) was detected the day after AI in heifers (55/61; 90.2%) than in cows (44/79; 55.6%), and ovulation rate was affected by the duration of proestrus in cows ($P=0.01$) but not in heifers ($P=0.98$). The pregnancy rate was higher in cattle (heifers and cows combined) in the subluteal-phase progesterone groups and normal proestrus groups

than in the luteal progesterone or short proestrus groups, respectively, (progesterone, P<0.02; proestrus, P<0.01; 53.8%, 37.1%, 46.7% and 11.1%, in subluteal-phase progesterone-normal proestrus, subluteal-phase progesterone-short proestrus, luteal progesterone-normal proestrus and luteal progesterone-short proestrus groups, respectively). In conclusion, a short proestrus interval resulted in a lower pregnancy rate following fixed-time AI in beef cattle. A low progesterone environment during growth of the ovulatory follicle increased the preovulatory follicle size and subsequent CL size and function, and compensated for the effect of a short proestrus on pregnancy rates.

Key words: Progesterone, proestrus, beef cattle, timed insemination, fertility.

3.2 Introduction

The purpose of fixed-time artificial insemination protocols is to permit insemination during a preplanned window of time eliminating the necessity of estrus detection and minimizing time and labor costs. Fixed-time artificial insemination protocols involve synchronization of follicular wave emergence and ovulation. Synchronization of follicular wave emergence may be achieved by GnRH-induced ovulation (Martinez et al., 2000), ultrasound-guided follicular ablation (Bergfelt et al., 1994; Bergfelt et al., 1997), or treatment with estradiol and progesterone (Bo et al., 1994; Bergfelt et al., 1997; Martinez et al., 2001; Rathbone et al., 2001a; Martinez et al., 2002). Synchronization protocols often involve the use of an intravaginal progesterone-releasing device for 5-9 days, prostaglandin-F2α at the time of device removal, and treatment with LH, GnRH, or estradiol 24-56 hours later to induce ovulation, reviewed earlier (Mapletoft et al., 2003). Progestin devices have been used for periods up to 15 days (Munro, 1987) and may be used more than once to minimize cost. Previously used intravaginal devices

induce subluteal-phase plasma progesterone ranging from 0.5 to 2 ng /ml (Pfeifer et al., 2009).

Progesterone has a negative feedback effect on LH secretion (Ireland and Roche, 1982) and subluteal-phase plasma concentrations of progesterone resulted in elevated LH pulse-frequency in cattle (Stock and Fortune, 1993; Kinder et al., 1996). The effect of negative feedback on LH secretion was demonstrated in an earlier study in which progesterone suppressed the growing phase of the dominant follicle in a dose-dependent manner (Adams et al., 1992). Administration of exogenous progesterone for 10 days resulted in lower fertility, possibly due to occurrence of nuclear maturation and redistribution of organelles oocyte prior to gonadotropin surge (Mihm et al., 1999). However, fertility did not differ when progesterone device was inserted into vagina of beef heifers for 6 days or 3 days (Dias et al., 2012b). In more recent reports (Colazo et al., 2004a; Pfeifer et al., 2009) where a previously used intravaginal progesterone device was inserted for a shorter duration, no adverse effects on fertility were observed, despite an increase in diameter of preovulatory follicle (Pfeifer et al., 2009). In that regard, an increase in fertility has been reported when larger follicles ovulate within a protocol (Perry et al., 2005). Recent data from our research group (Jaiswal, 2007) have shown that maintaining subluteal-phase progesterone for a short period during follicular growth results in an oocyte with improved *in vitro* fertilization capabilities compared to those growing in a high progesterone environment. Based on these findings, we propose to utilize subluteal-phase progesterone levels during dominant follicle growth to attain a larger preovulatory follicle and greater fertility compared to normal luteal levels.

Another aspect of dominant follicle growth in the preovulatory wave is the progesterone-free interval (i.e. proestrus) between spontaneous luteolysis and onset of estrus. In a natural estrous cycle the duration of proestrus is 3 to 4 days. While an exogenous hormonal induction of ovulation in most fixed-time AI protocols involves exogenous administration of estradiol at 24 h or GnRH or pLH at 48h after progestin device removal (Martinez et al., 2004). Therefore, fixed-time AI protocols tend to have a shortened proestrus interval, with potential impact on fertility. This notion has been addressed in a recent study (Bridges et al., 2008) in which a 5d CIDR estrus synchronization protocol with longer proestrus (72h) resulted in an increased of the pregnancy rate compared to a 7d CIDR protocol with shorter proestrus (60h).

We hypothesized that a) an exposure of the growing dominant follicle to luteal-phase plasma progesterone concentrations followed by a short duration of proestrus will result in lower fertility than longer proestrus, and b) an exposure of the growing dominant follicle to subluteal-phase progesterone concentrations will overcome the effects of short proestrus. The experiment was designed to compare the effects of changes in duration of proestrus and progesterone concentration on follicular development and fertility after fixed-time artificial insemination in beef in cows and heifers. We show that subluteal-phase progesterone during the growth of dominant follicle overcame the negative effects of short proestrus of fertility in beef cattle.

3.3 Materials and methods

Hereford-cross cows (n=85) and pubertal heifers (n=62) were used during the months of May to August. The cows were between 2 and 8 years of age, weighed 400 to 750 kg, and were ≥35 d postpartum and lactating. The heifers were between 14 to 24

months of age and weighed 280 to 425 kg. The cattle were maintained on pasture except on days of examination or treatment when they were placed in corrals and fed alfalfa hay and barley silage with free access to fresh water and mineral blocks. The experimental protocol was approved by the University Committee on Animal Care and Supply and conducted in accordance with the guidelines of the Canadian Council on Animal Care.

3.3.1 Animal groups and treatment protocol

Cattle were assigned randomly into four groups based on a 2-by-2 design with two levels of progesterone (luteal versus subluteal-phase) and durations of proestrus (normal versus short; Figure 3.1). The experiment was done in 2 replicates and all groups and parities were represented in both replicates. The level of progesterone was classified as luteal-phase (>1.5 ng/ml) and subluteal-phase (0.5 to 1.5 ng/ml) during the growing phase of the ovulatory follicle. The duration of proestrus was classified as normal (36 hr) and short (12 hr). Thus, the formed groups are referred to as: luteal-phase progesterone with normal proestrus (LN), luteal-phase progesterone with short proestrus (LS), subluteal-phase progesterone with normal proestrus (SuN) and subluteal-phase progesterone and short proestrus (SuS).

At the beginning of the treatment protocol, all animals were given 500 μg cloprostenol im (PGF; Estrumate, Schering-Plough Animal Health, Pointe-Claire, OC, Canada) twice, 11d apart to synchronize ovulation. At the time of the second PGF treatment, the ovaries were examined by transrectal ultrasonography using a 7.5 MHz linear-array transducer (Aloka SSD-900, Tokyo, Japan) and animals were assigned randomly to the four treatment groups (Figure 3.1). Animals in which a CL was not detected (n=6) were distributed evenly among treatment groups.

Nine days later (5 to 8 d after ovulation), cattle were given an intramuscular dose of 1 mg (heifers) or 1.5 mg (cows) estradiol-17β (Catalog # E8875, Sigma-Eldrich St. Louis, MO, USA) dissolved in canola oil (0.5 mg estradiol-17β per ml of canola oil) to synchronize follicular wave emergence (Bo et al., 1994). A CIDR (uCIDR, Pfizer Animal Health) device that has been used once for 7 d was placed in the vagina to maintain subluteal-phase plasma progesterone concentrations similar to earlier report (Pfeifer et al., 2009). At the same time (Day 0), cattle in the subluteal-phase progesterone groups (SuN, SuS) were given a luteolytic dose of PGF and another 12 h later, whereas cattle in the luteal-phase progesterone groups (LN, LS) were allowed to retain the functional CL. The uCIDR were removed on Day 7 (LN, SuN) or Day 8 (LS, SuS). All animals were given PGF on the day of uCIDR removal and 12.5 mg pLH (Lutropin, Bioniche Inc, Canada) im 12 h (LS, SuS) or 36 h (LN, SuN) later to induce ovulation. Fixed-time artificial insemination was done 12 h after pLH treatment.

Ultrasonographic examinations of the ovaries were done on Day 0 (uCIDR insertion), Day 5, Day 7/8 (day of uCIDR removal), on the day of artificial insemination, and 1 and 9 days after insemination. Ovulation was considered to have occurred if the dominant follicle detected on the previous day was not perceived on the day after insemination. Ovulation was confirmed 9 days after insemination by detection of a CL in the same ovary and elevated plasma progesterone concentrations (>1ng/ml). Pregnancy was diagnosed by transrectal ultrasonography 60 d after insemination.

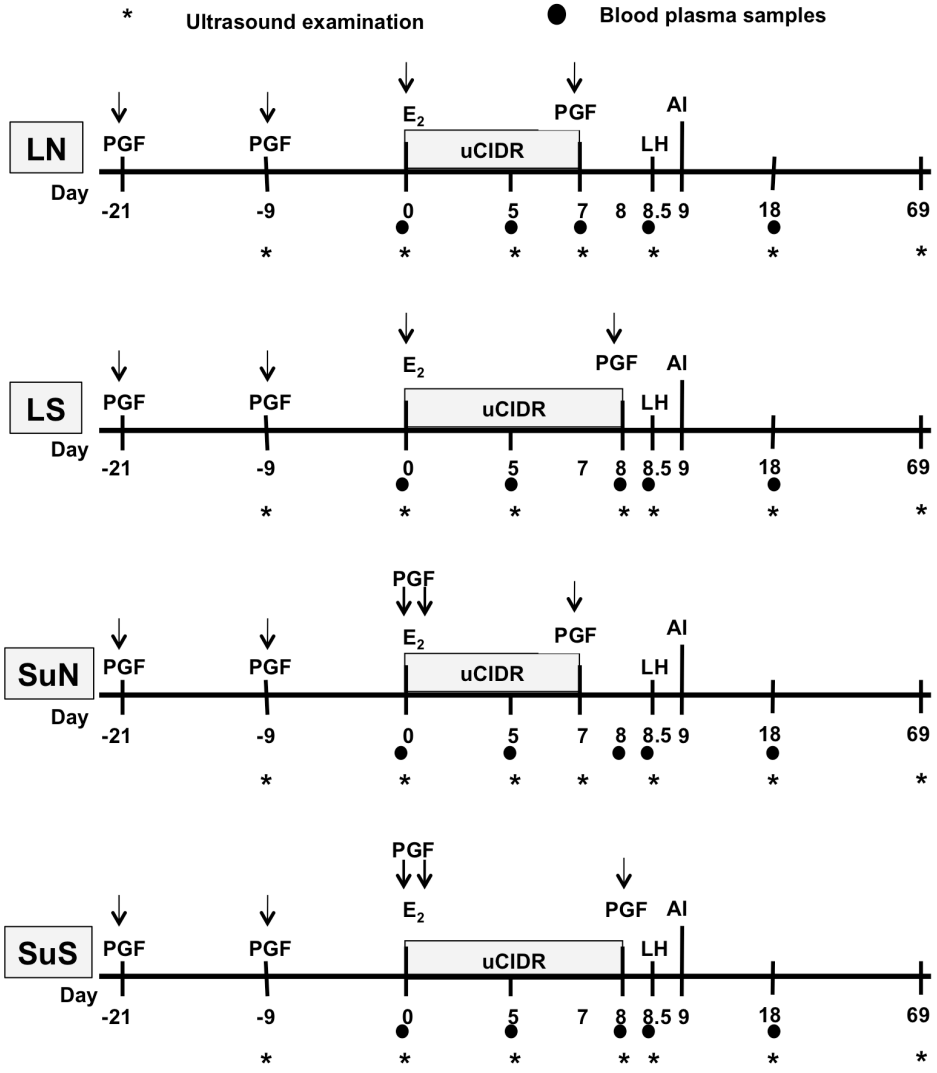

Figure 3.1 Treatment groups designed to induce luteal-phase progesterone levels and a normal proestrus (LN), luteal-phase progesterone levels and a short proestrus (LS), subluteal-phase progesterone levels and normal proestrus (SuN), or subluteal-phase progesterone levels and short proestrus (SuS) in cows (n= 79) and heifers (n=61). PGF = prostaglandin F2α; E_2 = estradiol-17β; uCIDR = once-used CIDR; pLH = Lutropin; AI = artificial insemination.

3.3.2 Blood sampling and radioimmunoassay

Blood samples were collected by caudal venipuncture on Day 0, Day 5, the day of uCIDR removal, the day of insemination, and 9 days after insemination to determine the

plasma progesterone concentration. Blood samples were taken in heparinized 10 ml vacutainer tubes (Becton and Dickinson Vacutainer Systems, Franklin Lakes, NJ, USA), and were centrifuged at 1500xg for 15 min to harvest plasma. Plasma samples were stored at -20°C until radioimmunoassay.

Plasma progesterone concentrations were measured using a commercial solid-phase kit (Coat-A-Count; Diagnostic Products Corporation, Los Angeles, CA, USA, (Pfeifer et al., 2009). The intra-assay coefficients of variation were 4.8% and 4.3% for low- and high-reference samples (means, 1.46 and 13.42ng/ml, respectively). The inter-assay coefficients of variation were 6.8% and 6.1% for low- and high-reference samples, respectively.

3.3.3 Statistical analyses

Statistical analyses were performed using the Statistical Analysis System software package (SAS 9.2; SAS Institute Inc., Cary, NC, USA). The preliminary statistical model included treatments (progesterone level and proestrus duration), parity (cow and heifer) and replicate (1 and 2) as explanatory variables. There was no significant effect of replicate on any of the response variables; therefore, replicate was omitted from the final model. By design, we analyzed cow and heifer data separately as well as a combined dataset. Binomial data (pregnancy and ovulation rates) and single-point measurements (preovulatory follicle diameter, CL diameter, and plasma progesterone concentration) were analysed using the GLIMMIX procedure. The logit link function and Newton-Raphson optimization technique were used for binomial data. Single-point data had a Gaussian distribution; hence, an identity link was used. Tukey's post-hoc test was used for multiple comparisons. All data are reported as mean ± SEM. Probabilities ≤0.05 were

considered significant, whereas $P > 0.05$ but ≤ 0.10 were considered trends approaching significance.

3.4 Results

Records of 6 cows and 1 heifer were excluded from the analyses due to either animal lost the progesterone device or missed a crucial day during the protocol due to illness. Further, 4 heifers from LN group were shifted to SuN group on the 2nd day of the protocol as they were accidently administered PGF at the beginning of the protocol. Thus, the number of cattle (n= 61 heifers and 79 cows) in different groups were; LN (n= 11 heifers and 19 cows), LS (n= 16 heifers and 20 cows), SuN (n= 18 heifers and 21 cows) and SuS (n= 16 heifers and 19 cows).

3.4.1 Blood plasma progesterone concentration

As expected, all animals had luteal levels of progesterone (≥ 1.5 ng/ml) at the commencement of the protocol (Figure 3.2). There was an expected drop in progesterone concentration to 0.5-1.5ng/ml in the low progesterone groups (SuN and SuS). However, 14 cows and 21 heifers did not fit the expected plasma progesterone concentrations on Day 5 and Day 7/Day 8 of the protocol. Therefore, we performed some analyses excluding these animals (see section 3.4.5).

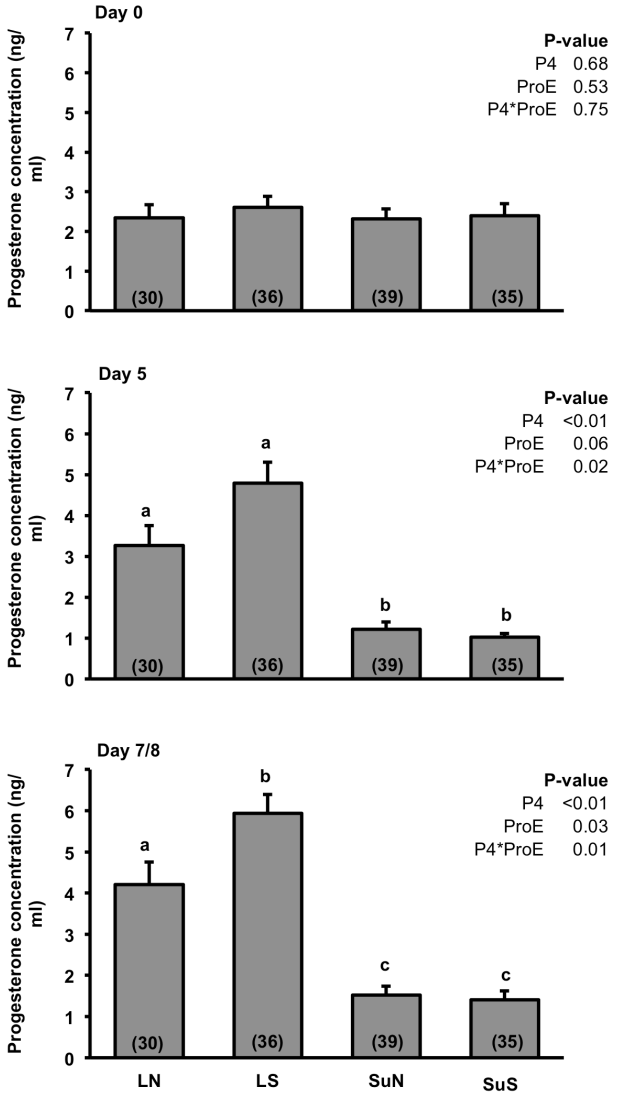

Figure 3.2 Blood plasma progesterone concentrations (mean±SEM) in cattle (cows and heifers combined) treated to induce luteal-phase progesterone concentrations and a normal proestrus (LN), luteal-phase progesterone and a short proestrus (LS), subluteal-phase progesterone and a normal proestrus (SuN), and subluteal-phase progesterone and a normal proestrus (SuS). Day 0 = day of uCIDR insertion; Day5 = one day after expected follicular wave emergence; Day 7/8 = day of uCIDR removal in the normal proestrus groups (Day 7) and short proestrus groups (Day 8); P4 = progesterone treatment; ProE = proestrus duration. Values in parentheses at the inside-bottom of each bar indicate the number of animals in each group. [ab] Values with no common superscripts are different ($P<0.05$). Parity had no effect on progesterone concentration ($P>0.15$); P4 = progesterone; ProE = proestrus. The number of animals is indicated in parentheses.

3.4.2 Ovulation and pregnancy rates

A higher proportion of heifers (55/61; 90%, P<0.01) ovulated by the day after AI as compared to cows (44/79; 56%). Therefore, data for heifers and cows were analyzed separately and combined (Figure 3.3). Overall (heifers and cows combined), higher ovulation rates (P=0.02) were observed in animals with subluteal-phase progesterone than those with luteal levels. A shorter proestrus resulted in lower ovulation rate (P<0.01) than a normal length proestrus. Cows and heifers separately analyzed, a shorter proestrus lowered the ovulation rate in cows (P=0.01) than the normal length proestrus but not in heifers.

A total of 30 cows out of 79 (38%) and 22 heifers out of 61 (36.1%) were diagnosed as pregnant at Day 60 after fixed-time AI. A larger proportion of cattle (heifers and cows combined) with subluteal-phase levels of progesterone became pregnant than those with luteal levels of progesterone (P=0.02, Figure 3.3b). A shorter proestrus resulted in lower pregnancy rate when compared to cattle (heifers and cows combined or separate) having normal length proestrus (P<0.01 for combined analysis; P=0.02 for heifers and P=0.03 for cows by separate analyses).

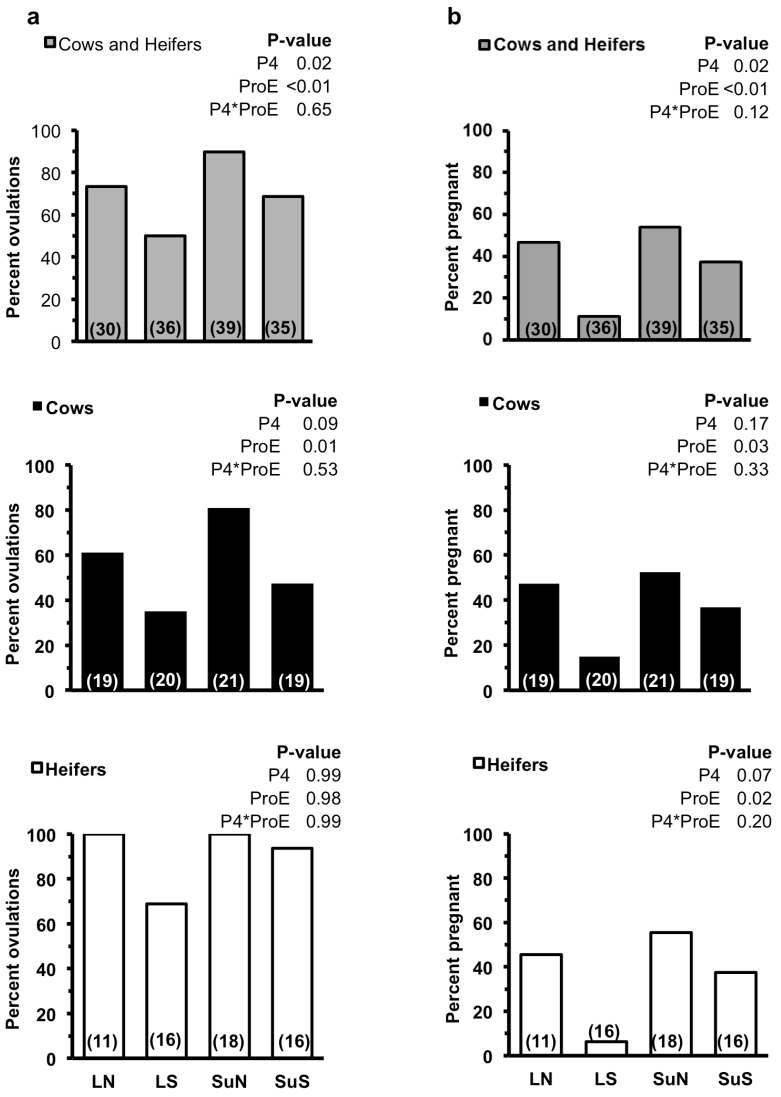

Figure 3.3 Ovulation (a) and pregnancy rates (b) in cattle (cows and heifers combined) treated to induce luteal-phase progesterone concentrations and a normal proestrus (LN) luteal-phase progesterone and a short proestrus (LS), subluteal-phase progesterone and a normal proestrus (SuN) and subluteal-phase progesterone and a normal proestrus (SuS). Ovulation was evaluated 22 h post-AI and pregnancy was diagnosed at Day 60 post-AI. Values in parentheses at the inside-bottom of each bar indicate the number of animals in each group. [ab] Values with no common superscripts are different ($P<0.05$). Parity had no effect on ovulation and pregnancy rates ($P>0.15$); P4 = progesterone; ProE = proestrus. The number of animals is indicated in parentheses.

3.4.3 Size of the preovulatory follicle

Cattle (heifers and cows combined) with subluteal-phase levels of progesterone or normal length proestrus had larger follicles at AI than cattle with luteal levels of progesterone or shorter proestrus, respectively (progesterone and proestrus, P<=0.01). When the data were analyzed separately for cows and heifers (Figure 3.4), cows in the LS group had a smaller size of preovulatory follicle than the SuN, SuS and LN groups (progesterone*proestrus interaction P=0.03). In heifers, a normal proestrus (versus short, P<0.01) or subluteal-phase progesterone (versus luteal, P=0.03) resulted in larger preovulatory follicle.

3.4.4 Size of the CL, and progesterone concentrations

Cattle (heifers and cows combined) with subluteal-phase levels of progesterone during dominant follicle growth had a larger CL with higher levels of circulating progesterone 9 days after fixed-time AI than cattle with luteal levels of progesterone (P=0.03 for CL size and, P<0.01 for plasma progesterone, Figure 3.5). Cattle (heifers and cows combined) with short proestrus had a smaller CL and lower circulating levels of progesterone 9 days after fixed-time AI than cattle with normal length proestrus (P<0.01 for both CL and plasma progesterone). The CL diameter in cows was not different across the treatment groups (Figure 3.5a). The CL size in heifers with short proestrus was smaller than normal proestrus heifers (P=0.02) and tended to differ (P=0.06) with progesterone level during dominant follicle growth. The progesterone concentration on Day 9 after fixed-time AI (Figure 3.5b) was lower in both cows and heifers (analyzed separately) with a shorter proestrus (P<0.01). In cows, the subluteal-phase progesterone

during the growth of dominant follicle resulted in higher progesterone (P=0.02) on Day 9 after fixed-time AI but the effect was less evident in heifers (P=0.08).

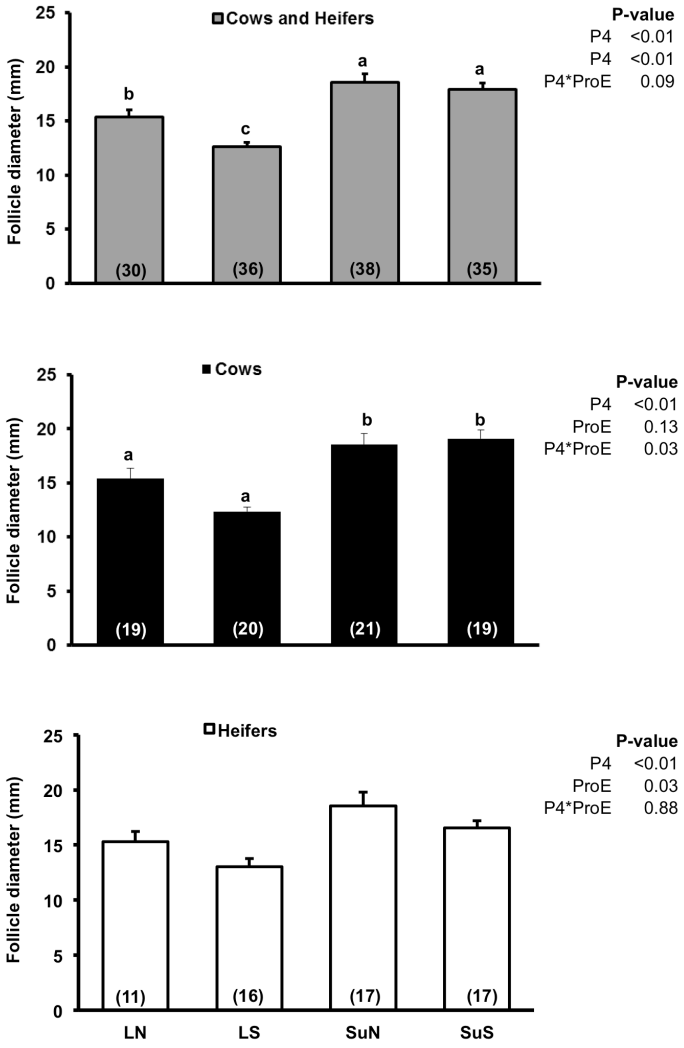

Figure 3.4 Size of preovulatory follicle (mm, mean ±SEM) at fixed-time AI in cattle (cows and heifers combined) treated to induce luteal-phase progesterone concentrations and a normal proestrus (LN) luteal-phase progesterone and a short proestrus (LS), subluteal-phase progesterone and a normal proestrus (SuN), and subluteal-phase progesterone and a normal proestrus (SuS). Values in parentheses at the inside-bottom of each bar indicate the number of animals in each group. [ab] Values with no common superscripts are different (P<0.05). Parity had no effect on follicle diameter (P=0.42); P4 = progesterone; ProE = proestrus. The number of animals is indicated in parentheses.

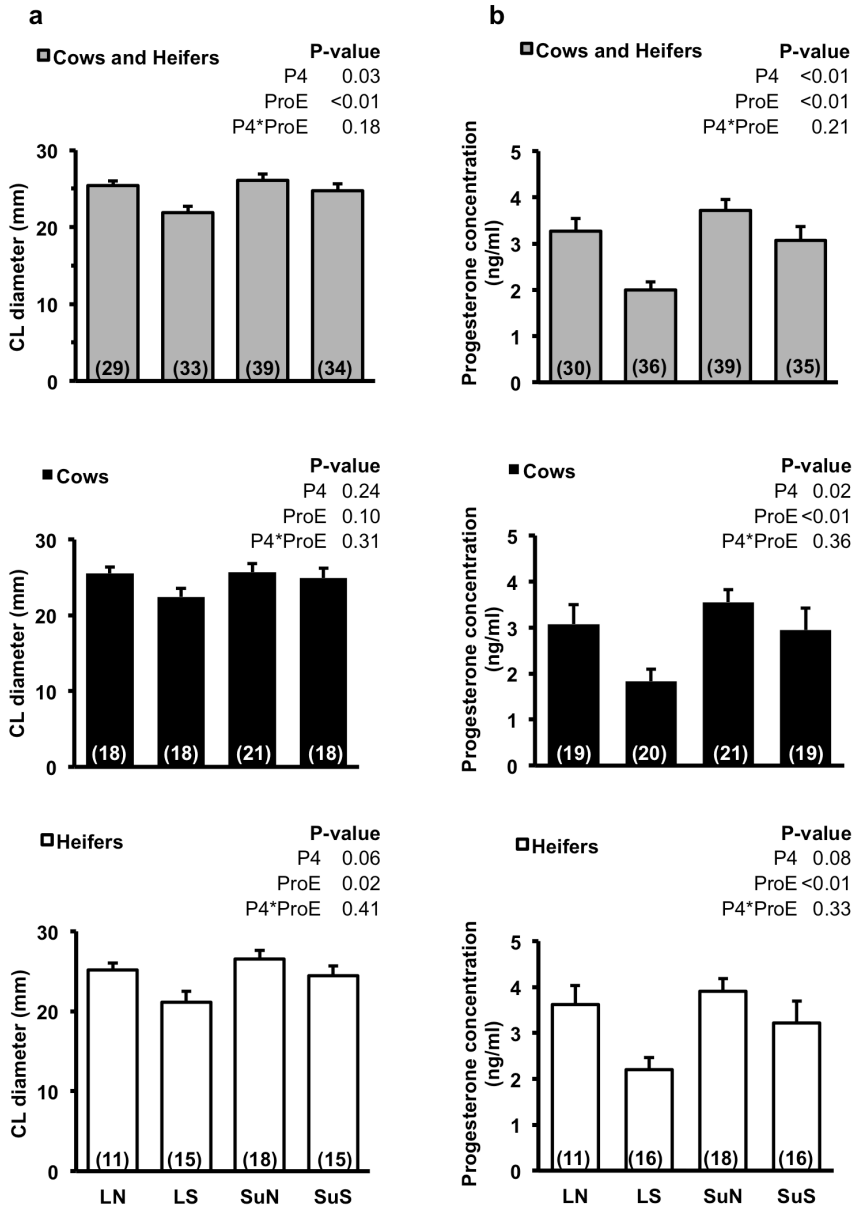

Figure 3.5 Diameter of the CL (a; mm, mean ±SEM) and plasma progesterone concentration (b; ng/ml, mean ±SEM) 9 days after fixed-time AI in cattle (cows and heifers combined) treated to induce luteal-phase progesterone concentrations and a normal proestrus (LN), luteal-phase progesterone and a short proestrus (LS), subluteal-phase progesterone and a normal proestrus (SuN), and subluteal-phase progesterone and a normal proestrus (SuS). Values in parentheses at the inside-bottom of each bar indicate the number of animals in each group. [ab] Values with no common superscript are different ($P<0.05$). Parity had no effect on CL diameter ($P=0.70$) or progesterone concentration 9 days after fixed-time AI ($P=0.14$); P4 = progesterone; ProE = proestrus. The number of animals is indicated in parentheses.

3.4.5 Reproductive end points in subset of data after hormone-based reclassification:

The expected plasma levels on Day 5 and Day 7/Day 8 for subluteal-phase progesterone groups (SuS and SuN) were 0.5-1.5ng/ml and for luteal progesterone groups (LS and LN) were >1.5ng/ml. Some animals did not meet this strict criterion. Including only those animals that met these criteria created a subset of data and the data sub-set was analyzed as described above. A total of 105 cattle (65 cows; 82.3% and 40; 65.5% heifers) strictly met the expected progesterone pattern during the protocol in the different groups (Table 3.1).

The subset of heifers and cows behaved similar (Table 3.1) to the parent dataset with one exception. Pregnancy rate (heifers and cows combined) for the LS group was lower (progesterone $P<0.01$, proestrus $P<0.01$ and progesterone*proestrus interaction $P=0.03$) compared to other groups (LN, SuN and SuS), which did not differ from each other. The ovulation rate for this subset of cattle was affected by the duration of proestrus ($P=0.01$) but not by the level of progesterone ($P=0.12$). The subset of cattle (heifers and cows combined) with subluteal-phase levels of progesterone and those with normal proestrus had a larger follicle at the time of AI and a larger CL 9 days after AI that secreted higher concentrations of progesterone than cattle with luteal levels of progesterone and those with short proestrus (progesterone, $P<0.01$; proestrus, $P=0.03$).

Table 3.1 Effect of treatments designed to induce luteal-phase progesterone concentrations and a normal proestrus (LN), luteal-phase progesterone and a short proestrus (LS), subluteal-phase progesterone and a normal proestrus (SuN), and subluteal-phase progesterone and a normal proestrus (SuS) in cattle (heifers and cows combined). Data represent the subset of animals in each group in which the intended progesterone profile was achieved. Values presented as proportions or mean±SEM.

Endpoints	**Groups**			
	LN	**LS**	**SuN**	**SuS**
Proportion of cattle with intended progesterone profiles	20/30 (67%)	31/36 (86%)	27/39 (69%)	27/35 (77%)
Proportion that ovulated (%)	14/20 (70%)	16/31 (52%)	24/27 (89%)	17/27 (63%)
Proportion pregnant (%)	8/20 [a] (40%)	1/31 [b] (3%)	13/27 [a] (48%)	11/27 [a] (41%)
Preovulatory follicle size (mm)	14.8±0.8	12.2±0.3	19.3±0.8	18.6±0.6
CL size (mm) 9 d after AI	24.5±0.8	21.5±1.0	26.6±1.1	25.1±0.9
Blood plasma progesterone (ng/ml) 9 d after AI.	3.3±0.3	1.9±0.2	3.7±0.3	3.2±0.4

[ab] Values with different superscripts are different ($P<0.05$). Analyses were done on proportions, not percentages.

3.5 Discussion

In the present study, a shorter proestrus interval resulted in lower pregnancy rates after fixed-time AI, supporting our first hypothesis. A subluteal-phase progesterone environment resulted in increased pregnancy rates and compensated for the adverse effects of a short proestrus supporting our second hypothesis. These findings emphasize the importance of the endocrine environment during ovulatory follicle growth and maturation on the outcome of fertility.

An important aspect that governs success of a fixed-time AI protocol is the timing of ovulation relative to AI. Ovulation occurred in majority of heifers within 1 day after AI but in cows. Ovulation rates in heifers are similar to that reported in an earlier study (Pfeifer et al., 2009). However, the duration of proestrus was 48 h in the former study

compared to 36 h in the present study. The 36 h interval between PGF and LH in beef cows appeared to be less than optimal as approximately one-third of them failed to ovulate by the day after AI (Figure 3.3a). A crucial finding reported earlier (Pfeifer et al., 2009) is that approximately one-third of animals with subluteal-phase progesterone came into estrus before the scheduled time of AI. These findings must be interpreted carefully with regards to the difference in the life-span of the ovulatory follicles (5 d in present study and 6 d in above-mentioned report). We speculate that if we would have delayed LH treatment by 12 h for cows, most will have ovulated which may have improved the pregnancy rate.

Pregnancy rates reported in other studies (Lucy et al., 2001; Martinez et al., 2001; Baruselli et al., 2004; Colazo et al., 2004a; Kasimanickam et al., 2006; Schafer et al., 2007) in which progestin-based ovulation synchronization protocols were used in postpartum cows range from 45% to 70%, which is similar to the rate observed in the normal proestrus groups in the present study (Figure 3.3b). Similar to previous reports (Colazo et al., 2004a; Pfeifer et al., 2009) that compared levels of progesterone during follicular growth, pregnancy rates for LN groups were not different from SuN groups (Figure 3.3b). However, when both short and normal proestrus animals were compared in the present study, the subluteal-phase progesterone groups had higher pregnancy rates than the luteal-phase groups.

Progesterone suppresses secretion of hypothalamic GnRH and pituitary derived LH (Mihm et al., 2002). The negative feedback effect of progesterone on LH and FSH differs as FSH may increase in the presence of high progesterone while LH pulsatility is suppressed (Mihm et al., 1999). However, in the presence of subluteal-phase levels of

progesterone, LH pulsatility is elevated and growing dominant follicles reach a larger size in presence of subluteal-phase levels of progesterone (Adams et al., 1992a; Stock and Fortune, 1993; Pfeifer et al., 2009). This finding is consistent with the results of the present study; preovulatory follicles were larger in subluteal-phase progesterone groups compared to luteal-phase progesterone groups (Figure 3.4). Ovulation of these larger follicles resulted in a larger CL that secreted more progesterone into circulation (Figure 3.5). Similar findings following subluteal-phase levels of circulating progesterone were observed in an earlier study from our group (Pfeifer et al., 2009).

Recent reports (Mussard et al., 2007; Bridges et al., 2008) have indicated that fertility increases in CIDR based protocols if the duration of luteal progesterone exposure is shortened and duration of proestrus is increased. When follicles were allowed to grow for 3-4 d in a normal luteal progesterone environment followed by 72 h of gonadotropin support (proestrus period), pregnancy rates rose by 10.3 percentage points when compared to 5-6d growth in a normal luteal progesterone environment and 60 h of gonadotropin support (Bridges et al., 2008). In a subsequent study by same group (Bridges et al., 2010), a shorter duration of proestrus adversely affected fertility even in animals with larger ovulatory follicle diameters. Ovulations following short proestrus were associated with shortened subsequent luteal phases and lower plasma progesterone concentrations. In the present study, short proestrus groups had smaller follicle diameters (by 1.5 mm compared to normal proestrus groups, Figure 3.4) at AI, probably due to a shortened period of gonadotropin support. The small sized preovulatory follicle ovulated and developed into smaller sized and less functional CL that resulted in reduced fertility in these animals. Lower pregnancy rates have also been observed in beef cattle induced to

ovulate smaller follicles in estrus synchronization protocol (Lamb et al., 2001; Perry et al., 2005). Although we did not carry out frequent blood sampling, but there is a possibility that shorter proestrus groups may have had a delayed rise in progesterone after ovulation. There is evidence that an early rise of progesterone after ovulation and maintaining higher progesterone levels shortly after conception favors embryo elongation that result in better fertility (Lonergan, 2011; Walsh et al., 2011).

Unexpectedly, about one-fourth of heifers failed to adhere to the expected progesterone secretion pattern in the different groups. The majority (70%) of these heifers were from subluteal-phase progesterone groups. Because we did not conduct intensive ultrasonography and blood sampling for progesterone data, it is difficult to provide a plausible explanation. Based on this sub-sample subluteal-phase progesterone was able to compensate for the adverse effect of fertility because of short proestrus. However, it is interesting that animals in this sub-sample did not behave differently with regard to the various reproductive endpoints measured.

In summary, a shorter duration of proestrus during a fixed-time AI protocol in cattle resulted in a smaller preovulatory follicle, smaller and less functional CL with lower progesterone secretion, and lower fertility. A subluteal-phase progesterone milieu during ovulatory follicle growth induced follicles to grow to a larger size resulting in larger CL and higher pregnancy rates following fixed-time AI and, compensated for the negative effects of short proestrus on fertility. A once used CIDR to maintain subluteal-phase progesterone environment during dominant follicle development can be successfully used in fixed time AI protocols to obtain pregnancy rates similar to luteal progesterone plus normal proestrus.

CHAPTER 4

4 ORGANELLE REORGANIZATION IN BOVINE OOCYTES AT DIFFERENT STAGES OF DOMINANT FOLLICLE GROWTH AND MATURATION

Dadarwal D, Adams GP, Hyttel P, Brogliatti GM, Caldwell S, Singh J

Relationship of this study to the dissertation

In my previous study (Chapter 3), I have shown that how different hormonal environment affects the dominant follicle development and fertility. In this study, I focused on how the dominant follicle development affects the oocyte ultrastructure. Previous studies have indicated an increase in developmental capacity of oocytes with the growth of follicles, therefore, an understanding of the quantitative subcellular changes in the organelles within the oocyte is very crucial. In this study, I used transmission lectron microscopy to test the hypothesis that oocyte undergoes changes in its organelle structure and distribution in a manner specific for each stage of follicle development.

4.1 Abstract

A study was designed to understand the changes in number, size and distribution of organelles in the ooplasm during the growing, static, regressing and preovulatory phases of dominant follicle development in cattle. We hypothesized that ooplasmic organelles undergo changes in number and spatial distribution in a manner specific for phase of follicle development. Hereford heifers were monitored daily by transrectal ultrasonography and cumulus-oocyte-complexes were collected by transvaginal ultrasound-guided follicular aspiration on Days 3 to 4 (growing dominant follicles, n=5; Day 0 = ovulation), Days 6 to 7 (static dominant follicles, n=5), Days 10 to 12 (regressing dominant follicles, n=7) of Wave 1 and on Days ≥17 (preovulatory follicles, n=5). Oocytes were processed and transmission electron micrographs were obtained of the ooplasm representing peripheral (ooplasm within 10μm of plasma membrane) and central regions. The surface area density ($\mu m^2/\mu m^3$), volume density ($\mu m^3/\mu m^3$), and numerical density (number/1000μm^3) of organelles were recorded using standard stereological methods, and were analyzed by 2-way analysis of variance (region and day). The numerical density of mitochondria was higher (P=0.03) in oocytes from regressing follicles (193.0 ±10.4 /μm^3) compared to those from growing, static and preovulatory stages (118.7±14.4, 125.6±20.8 and 150.5±28.7 /μm^3, respectively). More than 70% of mitochondria in oocytes from growing, static and preovulatory follicles were located in the peripheral regions, whereas oocytes from regressing follicles had an even distribution (region*day interaction P<0.001). The volume occupied by lipid droplets was higher (P<0.01) in oocytes from regressing follicles (3.5±0.7%) than in those from growing and preovulatory follicles (1.1±0.3 and 1.6±0.2%) while oocytes from static follicles were

intermediate (2.3±0.5%). Oocytes from growing follicles had a greater proportion of lipid droplets in the peripheral region than in the central region (86.9 vs 13.1%), whereas all other stages had an even distribution (region*day interaction P≤0.01). The percent surface area of mitochondria in contact with lipid droplets was lower (P≤0.04) in the oocytes from growing follicles (2.3±0.9%) than static, regressing and preovulatory follicles (8.9±0.2, 6.1±1.2 and 6.2±1.4%, respectively). The amount, size and distribution of smooth endoplasmic reticulum, vesicles, cortical granules, and Golgi did not differ among phases (P>0.11). Our hypothesis was partially supported in that mitochondrial number increased and translocation occurred from a peripheral to an even distribution as follicles entered the regression phase. In addition, lipid droplets underwent spatial reorganization from a peripheral to an even distribution during the growing phase and mitochondria-lipid contact area increased with follicle maturation.

Keywords: Oocyte, ultrastructure, cattle, dominant follicle, oocyte maturation, mitochondria, lipid, stereology, electron microscopy.

4.2 Introduction

Oocyte quality determines the success of fertilization and subsequent embryonic. Bovine oocytes achieve the competence to sustain fertilization and initial embryonic development to the blastocyst stage by the time the surrounding follicles reach 2-3 mm (Lonergan et al., 1994; Blondin and Sirard, 1995). The proportion of oocytes that developed to the blastocyst stage was higher for oocytes from follicles >6 mm compared to those from 2-6 mm follicles (Lonergan et al., 1994). Similarly, higher blastocyst rates were observed for oocytes obtained from follicles >13 mm compared to those from 5-8 mm follicles (Hagemann et al., 1999). Furthermore, higher proportions of blastocyst were

reported from IVF of *in vivo* matured oocytes (obtained after LH surge) than those matured *in-vitro* (van de Leemput et al., 1999; Hendriksen et al., 2000). The follicles (3-8 mm) that were aspirated for *in vitro* maturation had grown for short duration (1-4 days) compared to follicles that were aspirated after LH surge (6-9 days) (van de Leemput et al., 1999; Hendriksen et al., 2000). Above mentioned findings suggest that oocytes undergo maturational changes as the follicle grows. The processes in the oocyte, which are most likely influenced by the difference in follicular growth, are cytoplasmic events as the transcriptional activity of the oocyte is reduced to a minimum at the end of the growth phase at a follicle diameter of about 3 mm (Fair et al., 1995, 1996). Further, the nuclear maturation, i.e. the meiotic resumption, is not initiated *in vivo* until after LH surge (Assey et al., 1994) and is well simulated during 24 h *in-vitro* maturation of bovine oocytes.

Among cytoplasmic organelles considered crucial for acquisition of oocyte competence, mitochondria and lipid droplets are critical for energy (ATP) production (Dunning et al., 2010). Moreover, mitochondria along with smooth endoplasmic reticulum (SER) are the primary source of Ca^{2+} oscillations that govern the events such as nuclear maturation, fertilization and activation of embryonic development (Machaca, 2007; Ajduk et al., 2008). The events of nuclear maturation following preovulatory LH surge have been well-characterized by transmission electron microscopy (Kruip et al., 1983; Hyttel et al., 1986b; Hyttel et al., 1987; Assey et al., 1994). After resumption of meiosis, the majority of the oocytes reach metaphase II at 19-22 hours after LH surge (Assey et al., 1994). The events of cytoplasmic development before the LH surge during follicular dominance, however, are much less studied. An electron microscopy based

qualitative study has indicated that structural changes with respect to different organelles occur even before the LH surge (Assey et al., 1994).

Therefore, we set out to evaluate structural changes in oocytes obtained from phase-specific dominant follicles by using objective quantitative criteria. The specific objective of this study was to characterize, quantitatively, the changes in numbers and distribution of mitochondria, lipid droplets, SER within the oocyte at different stages of dominant follicle growth and maturation. We tested the hypothesis that the number and spatial distribution of organelles within the ooplasm change in a phase-specific manner.

4.3 Materials and Methods

4.3.1 Collection of cumulus-oocyte-complexes (COCs)

Twenty-two crossbred Hereford heifers were maintained in corrals at the Goodale Research Farm, University of Saskatchewan (Saskatoon, Canada). The heifers were between 14 to 22 months of age and had free access to hay, minerals and water. The experimental protocol was approved by the University Committee on Animal Care and Supply, and the study was conducted in accordance with the guidelines of the Canadian Council on Animal Care.

The ovarian follicular development was monitored daily by transrectal ultrasonography (Aloka SSD-500 echocamera with 7.5 MHz linear array transducer, UST 5821-7.5 Aloka Co. Ltd, Tokyo, Japan). The location and antral diameter of individual follicles (>4 mm) in both ovaries were recorded on data sheets (Knopf et al 1989). Following spontaneous ovulation (Day 0), heifers were assigned randomly for COC collection from dominant follicles on Day 3 to 4 (growing phase of the Wave 1 dominant

follicle, D3W1, n=5), Day 6 to 7 (static phase of the Wave 1 dominant follicle, D6W1, n=5), one day after the emergence of second follicular wave (Days 10 to 12; regression phase of the Wave 1 dominant follicle, D1W2, n=7), and on Days ≥17 (preovulatory follicle after detection of signs of estrus, D17, n=5, Figure 4.1).

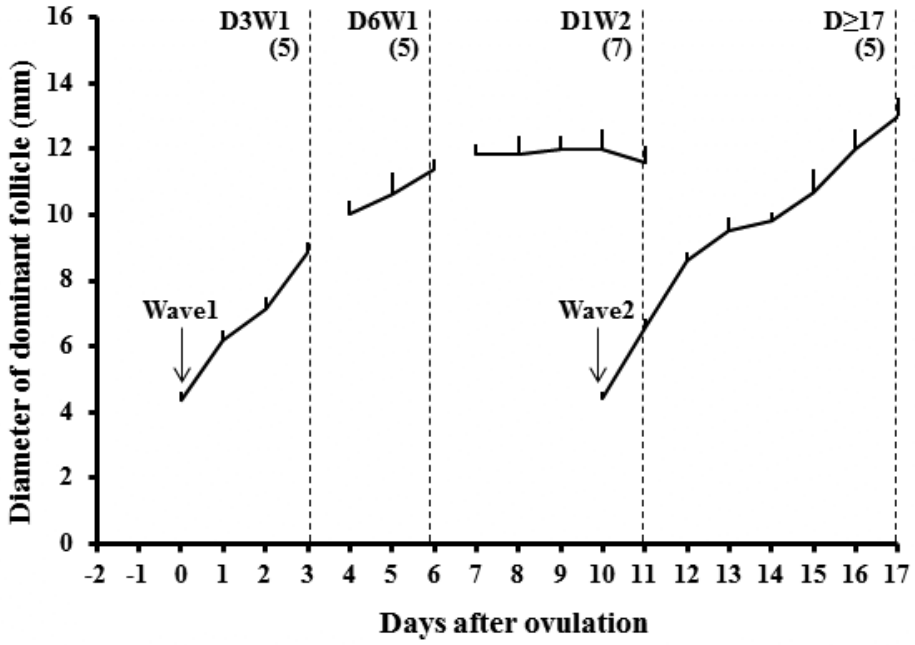

Figure 4.1 Diameter profiles (Mean +SEM, mm) of dominant follicles of Wave 1 (anovulatory) and Wave 2 (ovulatory). Mean days of follicular aspirations on Day 3 of Wave 1 (D3W1), Day 6 of Wave 1 (D6W1), Day 1 of Wave 2 (D1W2) and preovulatory during estrus (Day ≥17) are indicated by dotted vertical lines. Numbers in parentheses show the number of follicles collected for each stage of dominant follicular growth. Day 0 = emergence of wave 1.

The COCs were collected using a modified 5MHz end-fire transvaginal transducer attached to Aloka 500 echocamera as described previously (Brogliatti and Adams 1996). The follicles were aspirated using an 18 gauge, 60 cm long, single-lumen needle with the

flow rate of 30 ml/min (Vacuum pump: Allied Healthcare Products, Inc, St Louis, MO, USA). Follicular contents were collected in 15 ml centrifugation tubes containing 3ml phosphate buffer saline (PBS) with bovine serum albumin (0.2%) as surfactant and sodium heparin (10 IU/ml) as anticoagulant. The COCs were searched under stereozoom microscope and fixed in 1% gluteraldehyde and 0.1M sodium cocodylate buffer (pH 7.4) and stored at 4^0C until further processing for transmission electron microscopy.

4.3.2 Processing of oocytes for transmission electron microscopy

The COCs were stained with 1% Toluidine blue and placed into liquid 1% agarose at 40^0-42^0C (Sigma type II, A 6877) and allowed to cool into blocks at room temperature. The COC-agarose blocks were washed three times with 0.1M sodium cocodylate and post-fixed with fresh 1% osmium tetraoxide (in sodium bicarbonate buffer, pH 7.4) for 1 h at room temperature. The COC-agarose blocks were then dehydrated in 50% ethyl alcohol (5 min) and stained (1 h) with saturated uranyl acetate in 70% ethyl alcohol. Further dehydration was done by sequential treatment of the tissues in 70%, 95%, and 100 % ethyl alcohol (5 min each). The blocks were then washed with propylene oxide (three times, 5 min each). The blocks were incubated in 2:1 and 1:2 (propylene oxide) mixture of epon/araldite embedding media for 30 minutes and two hours, respectively, and were then left overnight in pure epon/araldite embedding media. The COC-agarose blocks were then placed in flat embedding molds to polymerize in embedding medium at 60^0C for 48h. The COCs were sectioned serially using ultramicrotome (Ultratome III, Catalogue # 8801A, LKB, Stockholm, Sweden) at a thickness of 0.5-1 micron. In addition, ultrathin sections (60-80 nm) were obtained at the largest diameter of COC and at the level of the nucleus. Ultrathin sections were overlain by a 75 x 300 mesh copper

grid. Electron micrographs of central, peripheral and perinuclear regions (Figure 4.2) of an oocyte were taken at 3000x primary magnification using a Philips 410LS transmission electron microscope. Negatives were printed on 11 inch x14 inch photographic paper (Kodachrome II RC, Catalogue # 1922970, Eastman Kodak Co., Rochester, NY) to obtain a final magnification of 10,000x.

4.3.3 Analyses of cytoplasmic organelle parameters

Electron micrographs of areas representing peripheral ooplasm (area ooplasm within 10 μm of the oocyte plasma membrane), perinuclear ooplasm (area within 10 μm of the nuclear envelope) and central ooplasm (area excluding peripheral and perinuclear regions) were analyzed. Quantitative analyses were performed by standard stereological methods that involved random placement of a transparent test-grid (Figure 4.2d) over an electron micrograph (Weibel et al., 1966). The distance between each adjacent cross-points on the grid was 1.5 cm and line lengths were 1.5 cm; therefore the area associated with each cross-point was 2.25 cm^2. The surface area density (surface area of organelle per unit volume of cytoplasm; $\mu m^2/\mu m^3$), volume density (volume of organelle per unit volume of cytoplasm; $\mu m^3/\mu m^3$) and numerical density (number of organelle per unit volume of cytoplasm; number/μm^3) were calculated for each organelle (Zoller, 1984; Baddeley et al., 1986). For simplicity, the volume density and numerical density of organelles is presented as percent and number per 1000 μm^3 of oocyte volume.

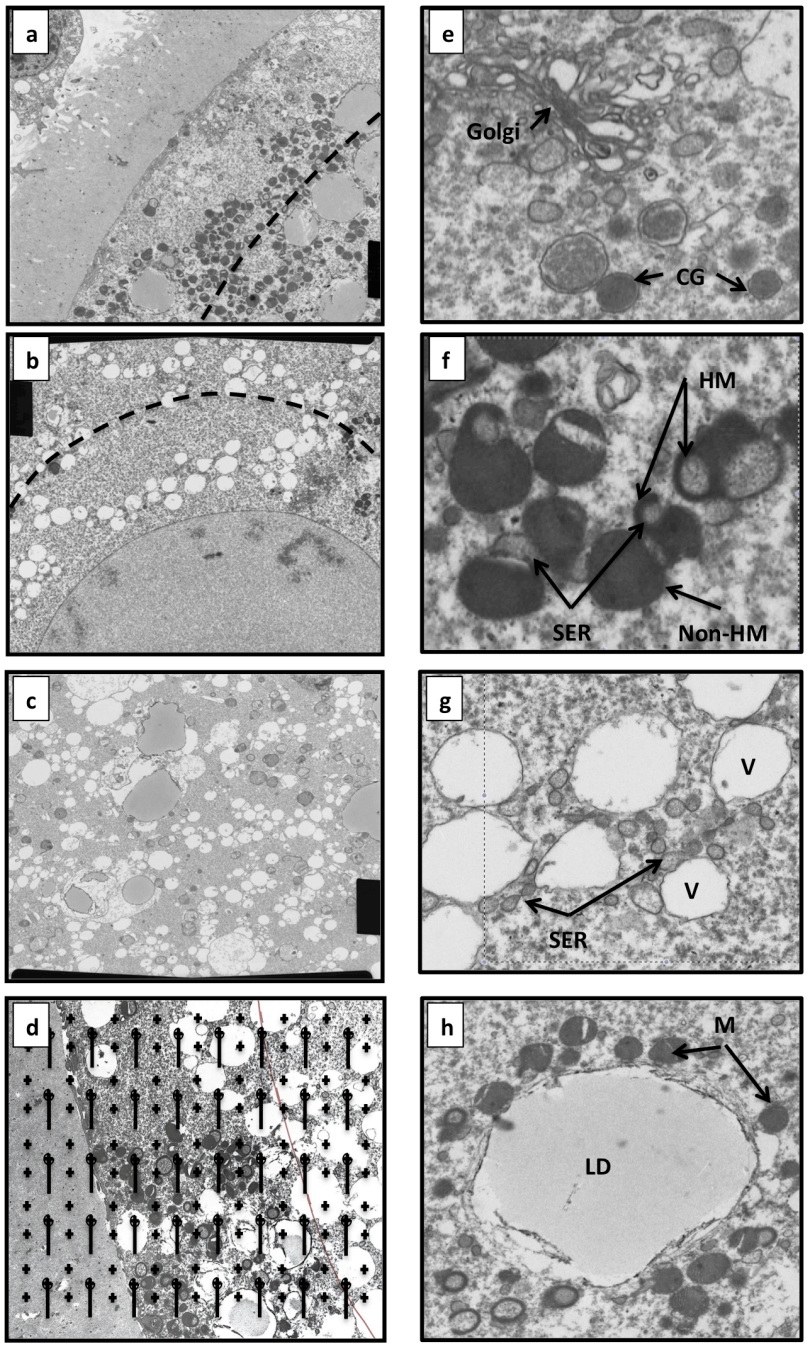

Figure 4.2 (a, b, c, d) Electron micrographs (photographed at a primary magnification of 3000x) representing peripheral (a), perinuclear (b), and central (c) regions of ooplasm as well as the peripheral region overlayed with the transparent grid for stereology (d). (e, f, g, h) Cortical granules (CG), Golgi complex (G), hooded (HM) and non-hooded mitochondria (N-HM), vesicles (V), smooth endoplasmic reticulum (SER), and lipid droplets LD) identified for the quantitative data. Note the close spatial association between mitochondria and SER (f) and mitochondria and lipid droplet (h).

4.3.4 Statistical analyses

All statistical analyses were done using SAS 9.2 (SAS Institute Inc., Cary, NC, USA). Comparisons among stages of dominant follicle growth were made by one-way analysis of variance. When the regions were compared across the stages of follicle growth, two-way analysis of variance was used. Proportional data were transformed to the arcsine and compared among stages by analysis of variance. The least significant difference was used as a post-hoc test. A P-value of 0.05 or lower was considered significant. When significant differences were observed between central and perinuclear regions, data for the central and perinuclear versus peripheral regions were combined to compare with the peripheral region.

4.4 Results

Membrane bound organelles that were examined are shown in Figure 2. Mitochondria exhibited two morphologies, hooded and non-hooded (Figure 4.2f). Both morphologies were closely associated with SER and lipid droplets as clusters. The vesicles coalesced and became larger as the follicles progressed towards regression.

4.4.1 Mitochondria

More than 70% of the mitochondria were located in the peripheral regions of the oocytes from growing, static and preovulatory follicles. However, mitochondria were evenly distributed across the peripheral and central plus perinuclear regions of oocytes from regressing follicles (Figure 4.3a), as each region presented approximately 50% of the total mitochondrial population. Volume of the mitochondrial compartment ranged from 1 to 4 percent of total ooplasmic volume depending on the stage of follicular growth

(Table 4.1). The volume and surface densities of mitochondria increased (P=0.04) in oocytes from regressing follicles compared to oocytes from follicles at other stages (Table 4.1). The mitochondrial numerical density (mitochondria per1000μm^3 volume of ooplasm) was highest (P=0.03) in oocytes from regressing follicles; about 63, 54 and 28% more than in the oocytes from growing, static and preovulatory stage follicles, respectively (Figure 4.4a). The distribution of hooded mitochondria changed across follicular status studied. More (P<0.001) hooded mitochondria were located in the peripheral region of oocytes from growing follicles compared to static, regression phase and preovulatory follicles (95.3±6.3/1000μm^3 vs 69.1±1.2/1000μm^3, 50.7±6.8/1000μm^3 and 76.8±15.2/1000μm^3, respectively). However, there were no changes were detected across follicular stages in hooded mitochondria volume density, surface density and numerical densities (Figure 4.4c).

4.4.2 Mitochondrial relation with lipid droplets and SER profiles

The percent surface area of mitochondria in contact with lipid droplets was less (P=0.04) in the oocytes from growing stage follicles and was not significantly different between other stages (Figure 4.3b). In all regions collectively, the percent surface area of mitochondria in contact with SER profiles did not vary significantly (P=0.42) with the phases of follicle growth (Figure 4.3c).

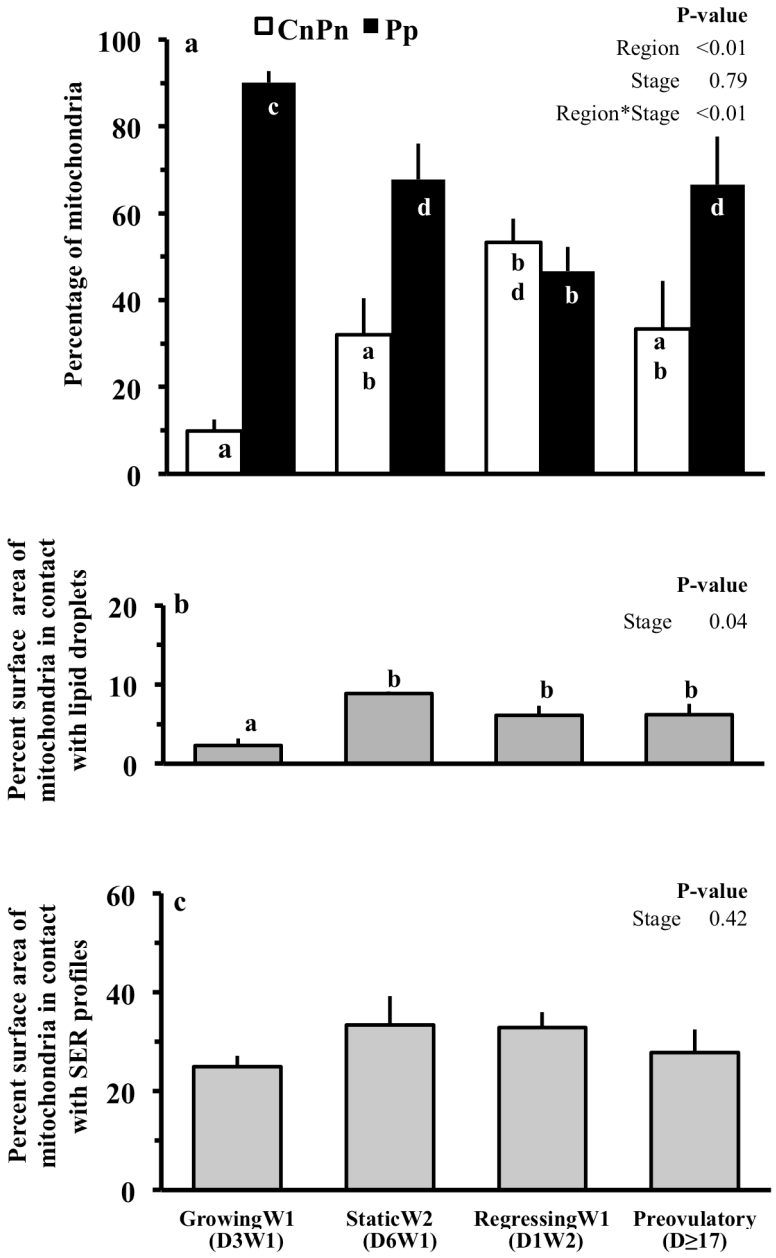

Figure 4.3 Percent distribution of mitochondria in different regions of ooplasm (a), percentage of mitochondrial surface in contact with lipid droplets (b), and smooth endoplasmic reticulum (c) in oocytes collected at different stages of follicular growth and maturation. [ab]Values with no common superscript are different (P<0.05).

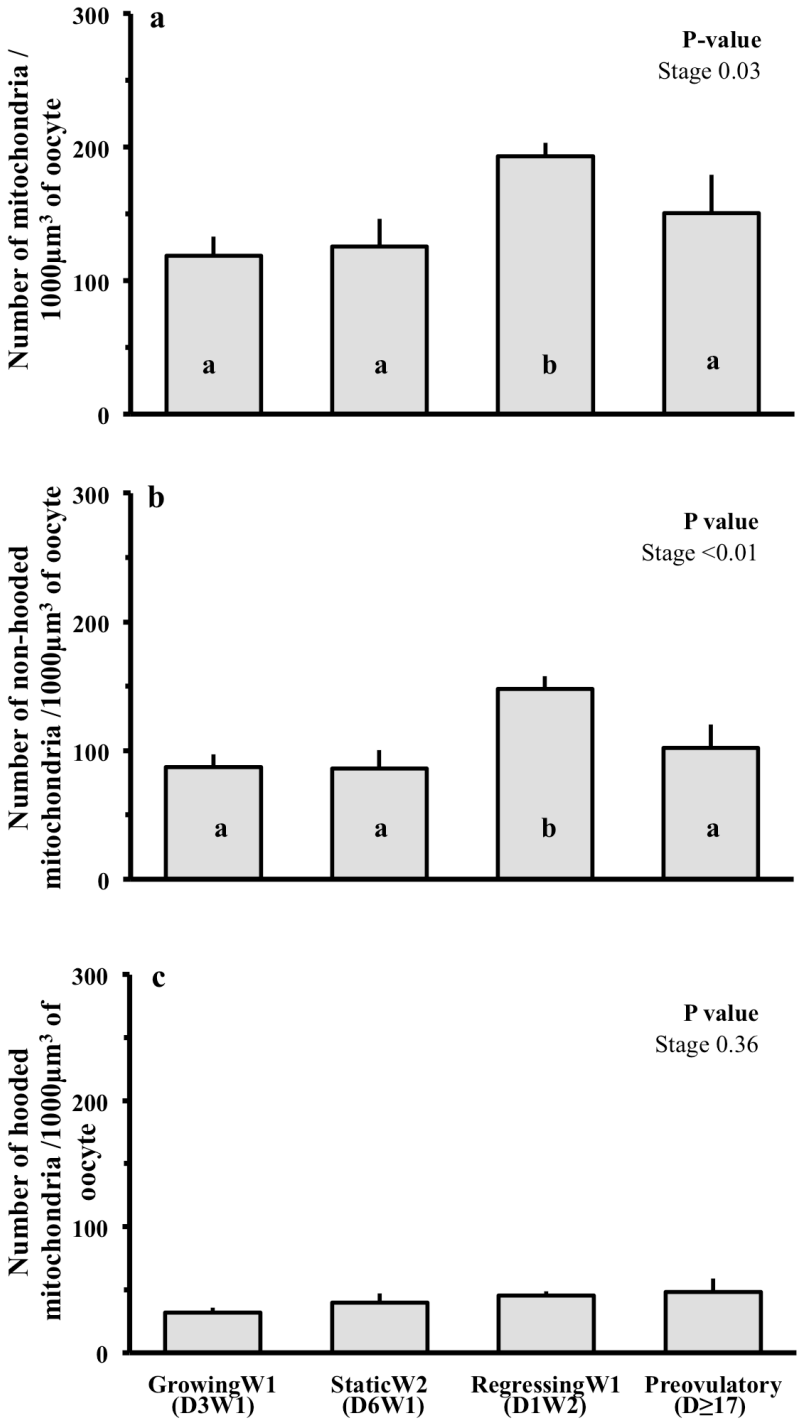

Figure 4.4 Number (Mean + SE) of total (non-hooded and hooded combined) (a), non-hooded (b) and hooded (c) mitochondria per 1000µm^3 of oocyte from follicles at different stages of follicular growth and maturation. The bars with no common letters indicate significant difference (P<0.05).

4.4.3 Lipid droplets

In all regions taken together, lipid droplets accounted for 1% to 5% of ooplasmic volume. The peripheral region of oocytes from growing phase follicles had approximately 5 times more of lipid droplets than the central plus perinuclear regions (region P=0.04, stage P=0.10 and region*stage P=0.01, Figure 4.5). During later stages of follicular development, the number of lipid droplets was not different between peripheral vs. central plus perinuclear regions of the ooplasm. The lipid droplet volume was less ($P<0.01$) in oocytes from growing and preovulatory phase follicles (1.1±0.3% and 1.6±0.2%, respectively), it increased to 2.3±0.5% in the static phase and was highest in oocytes from regressing phase follicles (3.5±0.7%). The surface density of lipid droplets in oocyte tended to differ (P=0.09) with the stage of follicular maturation, but no change was detected in the overall number of lipid droplets (/1000μm^3). The changes in lipid droplet volume, surface and numerical densities in different regions of oocyte from follicles at different phases of follicular development are shown in Figure 4.5.

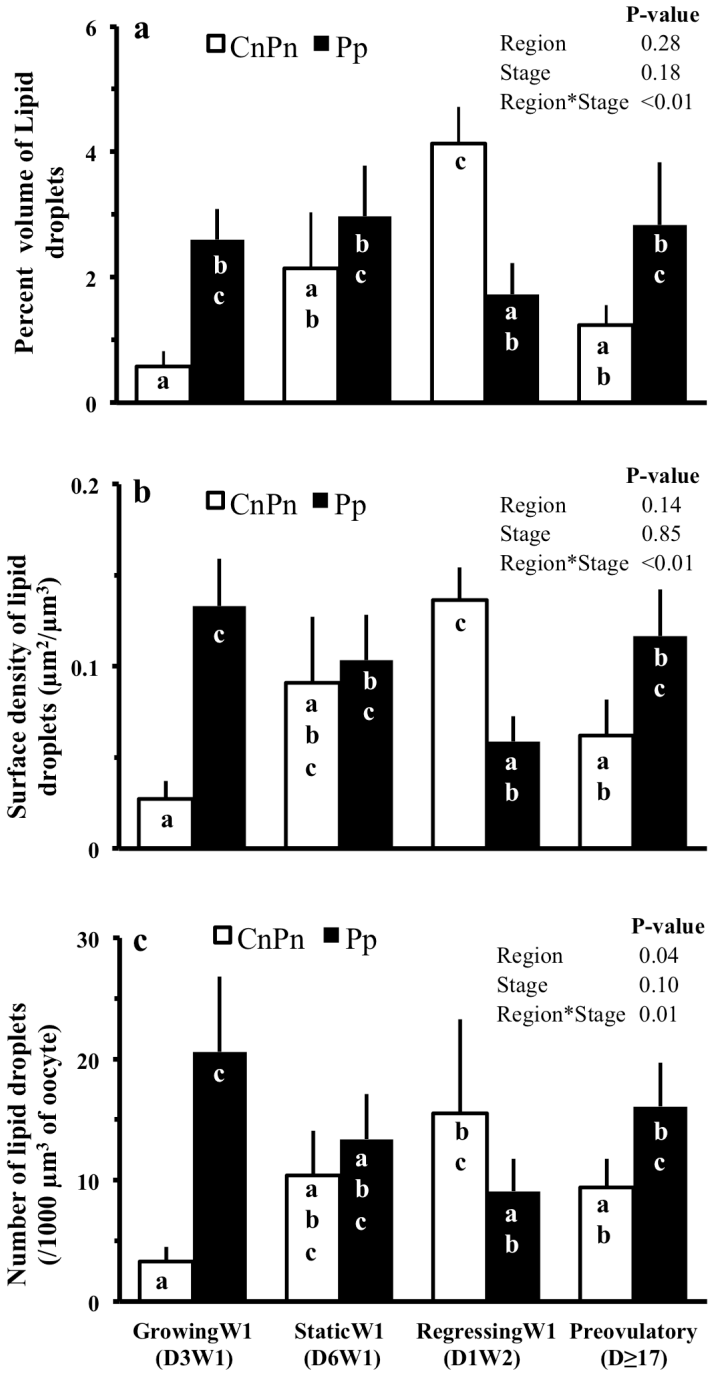

Figure 4.5 Volume (a, percent of oocyte volume), surface density (b, $\mu m^2/\mu m^3$ of oocyte) and number (c, per 1000 μm^3 of oocyte) of lipid droplets. Pp and CnPn represent peripheral and central plus perinuclear regions of oocyte, respectively. The bars with no common letters indicate significant difference ($P<0.05$).

4.4.4 Other organelles

The vesicles were the most abundant structure in the oocyte; their volume ranged from 7 to 31% of ooplasmic volume. However, no significant changes were observed in the volume, surface and numerical densities of the vesicles across different phases of follicular development (Table 4.1). The SER profiles accounted for 2 to 10% of ooplasmic volume (Table 4.1). The volume, surface and numerical densities of SER profiles in oocytes did not change significantly with the phase of follicular development (Table 4.1). There were no significant changes in the number of Golgi complexes when all regions taken together were compared across different phases of follicular maturation. When regions were compared between and within different stages, the peripheral region of oocytes from growing follicle had three times as many Golgi bodies as the perinuclear regions (Figure 4.6a), whereas, the perinuclear region of oocytes from regression phase follicles had twice the number of Golgi bodies than the peripheral region. More than 87% of cortical granules were located in the peripheral region of the oocytes and their distribution did not change significantly with the phase of follicular development (Figure 4.6b). The number of cortical granule did not change across the follicular stages.

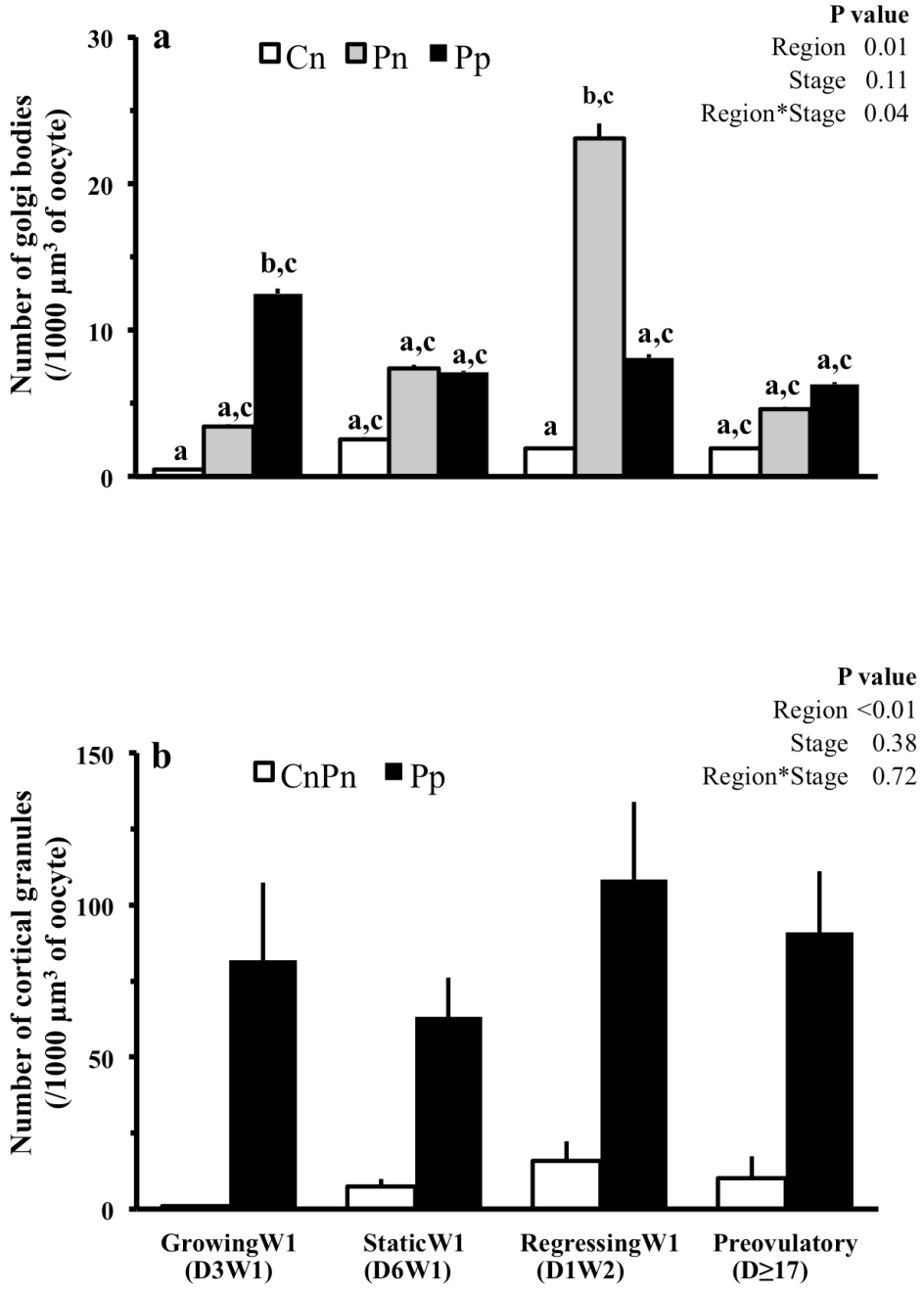

Figure 4.6 Number of Golgi complexes (a) and cortical granules (b) in 1000 µm^3 of oocyte from follicles at different stages of follicular growth and maturation. Cn, Pn, Pp and CnPn represent central, perinuclear, peripheral and central plus perinuclear regions of oocyte, respectively. The bars with no common letters indicate significant difference ($P<0.05$).

Table 4.1 Volume (percent of ooplasm) and surface density (Mean±SEM, $\mu m^2/\mu m^3$ of ooplasm) of mitochondria, SER profiles and vesicles; and number (Mean±SEM, per $1000\mu m^3$ of ooplasm) of SER profiles and vesicles in oocytes at different stages of follicular development.

Organelle	Parameter (P-value)	GrowingW1 (D3W1)	StaticW1 (D6W1)	RegressionW1 (D1W2)	Preovulatory (D≥17)
Mitochondria	Volume (%) (P=0.04)	2.3±0.2[a]	2.6±0.3[a]	3.9±0.5[b]	2.4±0.4[a]
	Surface Density ($\mu m^2/\mu m^3$) (P=0.03)	0.287±0.035[a]	0.299±0.046[a]	0.451±0.039[b]	0.326±0.049[a]
SER profiles	Volume (%) (P=0.87)	3.9±0.2	4.9±0.1	4.7±0.8	4.4±0.4
	Surface Density ($\mu m^2/\mu m^3$) (P=0.34)	0.652±0.065	0.599±0.106	0.780±0.065	0.653±0.055
	Number (per $1000\mu m^3$) (P=0.78)	521.5±87.5	467.3±84.9	670.1±85.4	650.2±40.9
Vesicles	Volume (%) (P=0.42)	20.4±2.9	16.4±1.7	16.2±2.8	21.6±3.2
	Surface Density ($\mu m^2/\mu m^3$) (P=0.84)	0.972±0.126	0.878±0.073	0.884±0.141	1.005±0.083
	Number (/$1000\mu m^3$) (P=0.86)	197.1±33.3	185.8±23.7	254.3±94.4	202.4±9.3

[ab] Values with different superscripts are different (P<0.05). Analyses were done on proportions, not percentages.

4.5 Discussion

The present study is first one in our knowledge to compare the quantitative changes of different organelles in bovine oocytes from dominant follicles at well-defined phase of growth and regression or dominance. Our hypothesis that ooplasmic organelles undergo reorganization during the early stage of dominant follicular growth that determines the

oocyte quality at later stages was partially supported. Mitochondrial numerical density increased and mitochondria translocated from peripheral to an even distribution in the oocytes as the follicles entered regressing phase. Further, the lipid droplets relocated from peripheral to even distribution in static phase of dominant follicle growth and to more central location in regression phase. However, no changes in their numbers were observed.

In cattle, oocyte diameter reaches a plateau by the time antral follicle diameter reaches 3 mm (Fair, 2003). The growth of follicles with size 3-4mm and beyond has been well characterized using transrectal ultrasound. Growth of follicles in bovines occurs in a wave like fashion with two- and three-waves being the most prevalent wave patterns (Savio et al., 1988b; Gibbons et al., 1997b). Each wave starts under the influence of FSH and a group of follicles enter the growth phase (Adams et al., 1992c). The follicles grow with equal pace for next couple of days until one follicle outpaces others to become dominant. At the time of selection, the dominant follicle is around 8.5 mm in size (Savio et al., 1988b; Gibbons et al., 1997b) and attains ovulatory capacity as it acquires LH receptors while other follicles fail to do so (Bao et al., 1997b). In presence of a functional corpus luteum that keep LH secretion at basal levels, dominant follicle continues for another couple of days and then stops growing to enter static phase (Savio et al., 1988b). Three days of static phase ends with the emergence of next wave and dominant follicle of 1^{st} wave undergoes regression. During the ovulatory wave, the LH pulsatility and amplitude gradually increases following luteolysis and the dominant follicle continues its growth phase and culminated in ovulation following LH surge (Rathbone et al., 2001b; Ginther et al., 2012b). As the dominant follicles develop through growing and static to

early regression stages, the ability of oocyte to develop into embryo continues to increase (Lonergan et al., 1994; Hagemann et al., 1999). In order to explain the differences in oocyte competence with variation in size of dominant follicle, previous studies have indicated some changes in cytoplasmic organelles morphology and spatial distribution but failed to test it quantitatively with respect to the definite stages of follicular growth (Assey et al., 1994). Our study fills that gap as COCs were collected at well-defined phases of dominant follicle growth and processed to obtain quantitative data regarding changes in ultrastructural features and distribution pattern of different organelles.

In the present study, major proportion of mitochondrial population remained in peripheral ooplasm of the growing, static and preovulatory phases of dominant follicle growth. Previous reports showed an even distribution of mitochondria in oocytes from preovulatory follicles, which happened ≥19h after LH surge when majority of *in vivo* matured oocytes were at MII stage (Kruip et al., 1983; Assey et al., 1994). As none of the oocytes from preovulatory follicles in our study were at MII stage that might be the reason why we did not observe translocation of mitochondria during preovulatory stage. Interestingly, oocytes from regressing dominant follicles had an even distribution of mitochondria (Figure 4.3a). It has earlier been indicated that oocytes from regressing follicles may display structural features found in preovulatory oocytes collected after the LH surge (Assey et al., 1994). Microtubules facilitates the redistribution of mitochondria across the ooplasm (Van Blerkom, 1991) as colchicine treatment to human oocytes disrupted the spindle formation and normal translocation of mitochondria from periphery to diffused distribution observed *in vitro* maturation (Liu et al., 2010). In mammals, mitochondria use specific kinesin-motors (Nangaku et al., 1994; Tanaka et al., 1998) to

move along the microtubules and an adaptor protein called Milton bound to specific outer mitochondrial membrane protein (known as Miro) assist in the motorized movements (Glater et al., 2006). The redistribution and aggregation of mitochondria in microtubule organizing sites (Van Blerkom, 1991) results in burst of ATP production during oocyte maturation (Yu et al., 2010). Does these organelle translocations in oocyte from regressing follicle indicate maturation like changes as reported in a previous study (Kruip et al., 1983)? In that regards, two out seven oocytes from regressing follicles exhibited undulations of nuclear envelop indicating onset of nuclear maturation. Similar finding was reported elsewhere and raises the question on the need of LH surge for resumption of meiosis. It has been observed that LH induces ROS build up in preovulatory follicle that is required for cumulus cell expansion and ovulation (Shkolnik et al., 2011). Treating preovulatory follicle with antioxidants reduces ROS concentrations and inhibit cumulus cell expansion and ovulation (Shkolnik et al., 2011). Addition of antioxidants during IVM and IVF have been shown to increase blastocyst rates (Combelles et al., 2009). We speculate that regression phase follicles that are undergoing atresia (Singh, 1997) are having increase production of ROS that could simulate maturation changes induce by LH in preovulatory follicle. This might be the reason that oocytes during early regression phase or some degree of atresia are able to yield good quality embryos. We speculate that mitochondria in oocytes from regressing follicles are undergoing oxidative stress. Mitochondria under oxidative stress have been shown to undergo fragmentation due to upregulation of the mitochondrial fission proteins and inhibition of mitochondrial fusion (Parone and Martinou, 2006; Wu et al., 2011). This could also be the reason for an

increase in mitochondria numbers observed in our study in oocytes from regression phase follicles.

The increase in numerical density of mitochondria was due to significant ($P<0.01$) increase in non-hooded mitochondria (Figure 4.4b), as the population of hooded mitochondria did not change with growth and maturation of dominant follicle (Figure 4.4c). No changes in parameters analyzed were observed with regards to hooded mitochondria, which is in contrast to previous study that reported an increase in number of hooded mitochondria (Fair et al., 1997). The specific roles of these mitochondria are yet unknown as two lines of thoughts exists. Some studies propose hooded mitochondria as underdeveloped morphological forms that limit the reactive oxygen species production in oocyte during maturation and embryonic development (Crocco 2011, Van Blerkom 2004). These hoods often encircled SER profiles (Figure 4.2f). Such a close association between mitochondria and SER is crucial for exchange of Ca^{2+} between these two organelles, which is needed for variety of cell signaling and regulation of cell functions (Iino, 2010). More plausible explanation for mitochondria to have these hoods is that such morphology increases the functional surface area as these hoods or extensions involve both outer and inner mitochondrial membranes (Senger and Saacke, 1970).

Lipid droplets store triglycerides that are important source of ATP generation needed for oocyte maturation and further embryonic development (Sturmey et al., 2006). Previously an increase in lipid droplet volume density has been suggested due to increase in so called underdeveloped hooded mitochondria that fail to utilize lipid (Crosier et al., 2000). However, we did not observe any change in the number of hooded mitochondria despite an increase in lipid droplet volume in oocytes as follicles progressed from

growing to regression stage. Close approximations between mitochondria and lipids in oocytes have been reported in cattle (Kruip et al., 1983; Assey et al., 1994) and other species (Cran, 1985). Fluorescence resonance energy transfer analyses of stained mitochondria and lipid droplets in porcine oocytes have shown that these two organelles are located within ≤ 10nm distance to each other (Sturmey et al., 2006). Both these organelles are adequately placed for generation of ATP through β-oxidation of lipids, a process that requires carnitine (Dunning et al., 2010). Recently, it has been shown that inhibiting β-oxidation with etomoxir (carnitine inhibitor) during oocyte maturation or zygote cleavage reduced the blastocyst rate by half (30% vs 60 % in untreated) during IVM and IVF of mouse oocytes (Dunning et al., 2010). The increase in contact between these two organelles at static, regression and preovulatory phases indicate the oocytes in these follicles are more dependent on lipid derived ATP generation to fulfill their energy requirements. Previous report (Kruip et al., 1983) indicated an increase in lipid droplet volume as the follicle grow towards maturation. In the present study, increased lipid content was obvious only when the follicles entered the regression phase. It is not known why atresia leads to an increased lipid droplet volume per unit of ooplasm.

Our findings supported previous observation (Kruip et al., 1983; Assey et al., 1994) that vesicles are the most abundant organelle in the oocytes. However, no change in their size, number and distribution was observed in the oocytes from different phase of growth and maturation. These membrane bound organelles are considered part of SER membrane system and their exact function remains yet to be identified.

Golgi bodies are involved in transport of proteins within a cell and in processing of macromolecules following endocytosis (Rothman, 1994; Allan and Balch, 1999).

Microtubules play an active role in the translocation of these organelles (Racedo et al., 2012). In bovine oocytes, these organelles move from center to the peripheral ooplasm during germinal vesicle breakdown (GVBD) and reverse movement was observed between GVBD and MI stages (Racedo et al., 2012). In present study, Golgi bodies were peripherally located during the growing phase and were centrally located during the regression phase. In the preovulatory follicle, Golgi bodies were evenly distributed (Figure 4.6a), which could be due to none of the oocyte were matured to GVBD in the present study. Also, the difference in observations might occur due to oocyte were matured *in vitro* during the recent study (Racedo et al., 2012) compared to *in vivo* in our study. Some variations in the ultrastructure of oocyte had been reported between the *in vitro* and *in vivo* matured oocytes were compared (Hyttel et al., 1986b).

Cortical granules are Golgi derived organelles and contains recently identified protease, Ovastacin that cleave zona pellucida protein-2 (ZP-2) and thus prevents polyspermy following fertilization (Liu, 2011; Burkart et al., 2012). In present study, the cortical granules were located in the peripheral ooplasm from the beginning of follicular growth. Our observation is in contrast to previous reports where cortical granules were observed to translocate to periphery as the oocytes mature (Kruip et al., 1983; Hyttel et al., 1986b). This discrepancy might be due to difference in the area of ooplasm that was considered as peripheral in our study. Movement of cortical granules is facilitated by microfilaments as treating human oocytes with cytochalasin B inhibited their translocation to cortical region during *in vitro* maturation (Glater et al., 2006).

We conclude that changes in organelle number and distribution pattern occur in a manner specific for phase of follicular growth, maturation and regression. The growing

phase oocytes are characterized by least area of mitochondria in contact with lipid droplets and a peripheral distribution of lipids compared to even in oocytes from other phases. The regression phase oocytes are characterized by an increase in mitochondrial number and even distribution of mitochondria compared to peripheral in other phases of growth and maturation. Moreover, oocytes from regression phase have more lipids content per unit volume of oocyte.

CHAPTER 5

5 EFFECT OF FOLLICULAR AGING ON NUCLEAR MATURATION AND DISTRIBUTION OF LIPID DROPLETS IN BOVINE OOCYTES

Dadarwal D, Honparkhe M, Alce T, Dias FCF, Lessard C and Singh J

Relationship of this study to the dissertation

In my previous studies, I have shown how different hormonal environment affects the dominant follicle development and fertility (Chapter 3) and how organelles behave within the oocytes (oocyte maturation) when follicle develops and matures (Chapter 4). In this study, I examined how the duration of dominant follicle growth during superstimulation protocol affect the oocyte maturation with respect to nuclear maturation and lipid droplet distribution. We hypothesized that longer growth of follicle in protocol with FSH starvation will result in 1) failure of nuclear maturation and 2) accumulation of larger lipid droplets compared to superstimulation with continued FSH support.

5.1 Abstract

Our objective was to study the effect of longer superstimulation protocols on nuclear maturation and distribution of lipid droplets in the ooplasm. We hypothesized that follicular aging after FSH starvation will result in maturation failure with accumulation of larger lipid droplets compared to superstimulation with continued FSH support for short and long durations. Follicular wave was synchronized in Hereford heifers (n=12) during the luteal phase and a progesterone-releasing device (CIDR) was placed into vagina. At 36 h after ablation (expected day of emergence of a new wave, Day 0), heifers were randomly allocated to three groups (n=4 each group). Heifers in short FSH and FSH starvation groups were given 8 im injections of FSH (12-hour intervals) over 4 days, while those in long FSH group were given 14 im injections over 7 days. Two injections of PGF (at 12 hour interval) were given on Day 3 to the short FSH group and on Day 6 to FSH starvation and long FSH groups. In all groups, the CIDR was removed at the second PGF treatment, and LH was given 24 hours later. Cumulus-oocyte-complexes (COC) were collected 18-20 hours after LH treatment by follicular aspiration. Oocytes were fixed and stained for nuclear maturation (Lamin/DAPI) and lipid droplets (Nile Red) and imaged with a Zeiss LSM 710 confocal microscope. Three-dimensional image sets of oocytes were deconvoluted using Autoquant X2 and lipid droplets segmented using Imaris Pro 7.4. Heifers in the long FSH group had a greater proportion of mature oocytes compared to heifers in the short FSH and FSH starvation groups (59/100 vs 5/23, 2/25, respectively; $P<0.01$). The total number, total volume and distribution of lipid droplets within the oocytes were not different across the three groups. Average volume of individual lipid droplets in oocytes was higher in FSH starvation group ($11.5\pm1.5\ 10^{-3}$ pL,

P=0.03) compared to short FSH and long FSH groups (7.2±0.6 10^{-3} and 8.0±0.8 10^{-3} pL). Average surface area of lipid droplets in oocytes was higher in FSH starvation group (20.3±1.5 μm^2 P=0.04) compared to short FSH group (14.6±1.1μm^2) and was not different from long FSH group (17.1±1.1μm^2). In conclusion, both FSH starvation and short FSH treatments yield lesser proportion of mature oocytes compared to long FSH. Further, FSH starvation leads to accumulation of larger lipid droplets in the ooplasm indicating atresia.

Key words: Bovine oocyte, FSH Starvation, lipid droplets, nuclear maturation, superstimulation.

5.2 Introduction

Success of embryo transfer programs depends on optimal superstimulatory response and effects of superstimulatory treatment on oocyte quality. Superstimulatory protocols involve use of exogenous hormones, FSH or eCG, to support growth of small antral follicles leading to multiple ovulations. Initiating superstimulatory protocols at the time of new wave emergence have been shown increase the superstimulatory response (Nasser et al., 1993), but animal-to-animal variation, duration of treatment, and plasma progesterone concentrations during superstimulatory treatment have been related to the ovarian response.

Both duration (Dias et al., 2012a; García Guerra et al., 2012) and levels of progesterone (Jaiswal, 2007) during the superstimulatory treatments have been addressed previously. Superstimulation of beef cattle under subluteal-phase progesterone levels for 4 d increased fertilization rates than luteal progesterone for same duration (Jaiswal, 2007). In the same study, cattle superstimulated for 4 d and given 6d FSH free period (i.e

FSH starvation, 5 d under subluteal-phase levels and 1d under basal progesterone levels) had all follicles loose their ovulation capacity. In a later study, 84 h FSH starvation period (3 d under luteal progesterone levels and 12 h in decreasing progesterone levels) resulted in 60% of the follicles loose their ovulatory capacity (Dias et al., 2012a). This observation is contrary to other reports which indicate a FSH starvation period, although shorter, is necessary for oocyte to acquire developmental competence (Blondin et al., 1997b). A continued FSH support under luteal levels of progesterone for 7 d have been shown to result in a greater ovulatory response compared to 4 d FSH treatment, without affecting oocyte competence (Dias et al., 2012a; García Guerra et al., 2012). Nonetheless, the effects of these superstimulatory treatments on the maturation status of oocytes within the dominant follicles have not been studied so far.

Resumption of meiosis and progression to metaphase II, i.e. nuclear maturation, is one of the measures to assess the optimal stage of oocyte for fertilization. Bovine oocytes arrested at Prophase I in growing antral follicles resume meiosis after removal of oocytes from antral follicles (Edwards, 1965) or after the preovulatory LH surge (Ayalon et al., 1972). The majority of the oocytes reach metaphase II around 19 hours after spontaneous (Kruip et al., 1983; Hyttel et al., 1989c; b) or induced LH surge (Hyttel et al., 1989c; b). The oocytes will remain arrested at metaphase II stage until fertilization in both unstimulated cattle (Hyttel et al., 1989b) and those superstimulated with a 4-day FSH protocol (Hyttel et al., 1989c). In addition to changes observed in the oocyte nucleus, cytoplasmic organelles including lipid droplets redistribute themselves following LH surge (cytoplasmic maturation). Lipid droplets of oocytes contain triglycerides (Ferguson and Leese, 1999; Kim et al., 2001) that act as an important source for ATP generation

through β-oxidation in mitochondria and are considered important for optimal oocyte competence (Dunning et al., 2010). An increased β-oxidation under the influence of cAMP-activated kinase has been indicated as one of the downstream events responsible for resumption of meiosis (Downs et al., 2009). Utilization of lipids during nuclear maturation might be the reason why the triglyceride content of mature oocytes is less than that of the immature oocytes (Ferguson and Leese, 1999; Kim et al., 2001). A previous study done by our group (Dias et al., 2012a) has shown that a large proportion of follicles from FSH starvation fail to ovulate that might have oocytes undergoing degenerative changes due to prolonged growth without FSH or LH support. If that is the case, the oocytes from starvation group will fail to undergo resumption of meiosis and as a result have larger lipid droplets due to non-utilization of triglycerides. In the present study, our objective was to determine the effect of longer superstimulation protocols on nuclear maturation and size and distribution of lipid droplets in the ooplasm. We hypothesized that follicular aging after FSH starvation will result in 1) failure of nuclear maturation and 2) accumulation of larger lipid droplets as compared to superstimulation with continued FSH support.

5.3 Materials and Methods

The study was conducted on postpubertal Hereford heifers (n=12) during the months of July to August. The heifers weighed 294 to 405 kg and were maintained at University of Saskatchewan Goodale Research Farm (52^0N and 106^0W). The heifers were kept on pasture except during the treatment period when they were placed in corrals and fed alfalfa hay and barley silage with free access to fresh water and mineral blocks. The experimental protocol was approved by the University Committee on Animal Care

and Supply and conducted in accordance with the guidelines of the Canadian Council on Animal Care.

5.3.1 Experimental treatments

Heifers were assigned randomly to three treatment groups (n=4), Short FSH treatment, FSH starvation and long FSH groups based on the length of FSH treatment and duration between the last FSH treatment and subsequent LH treatment (Figure 5.1).

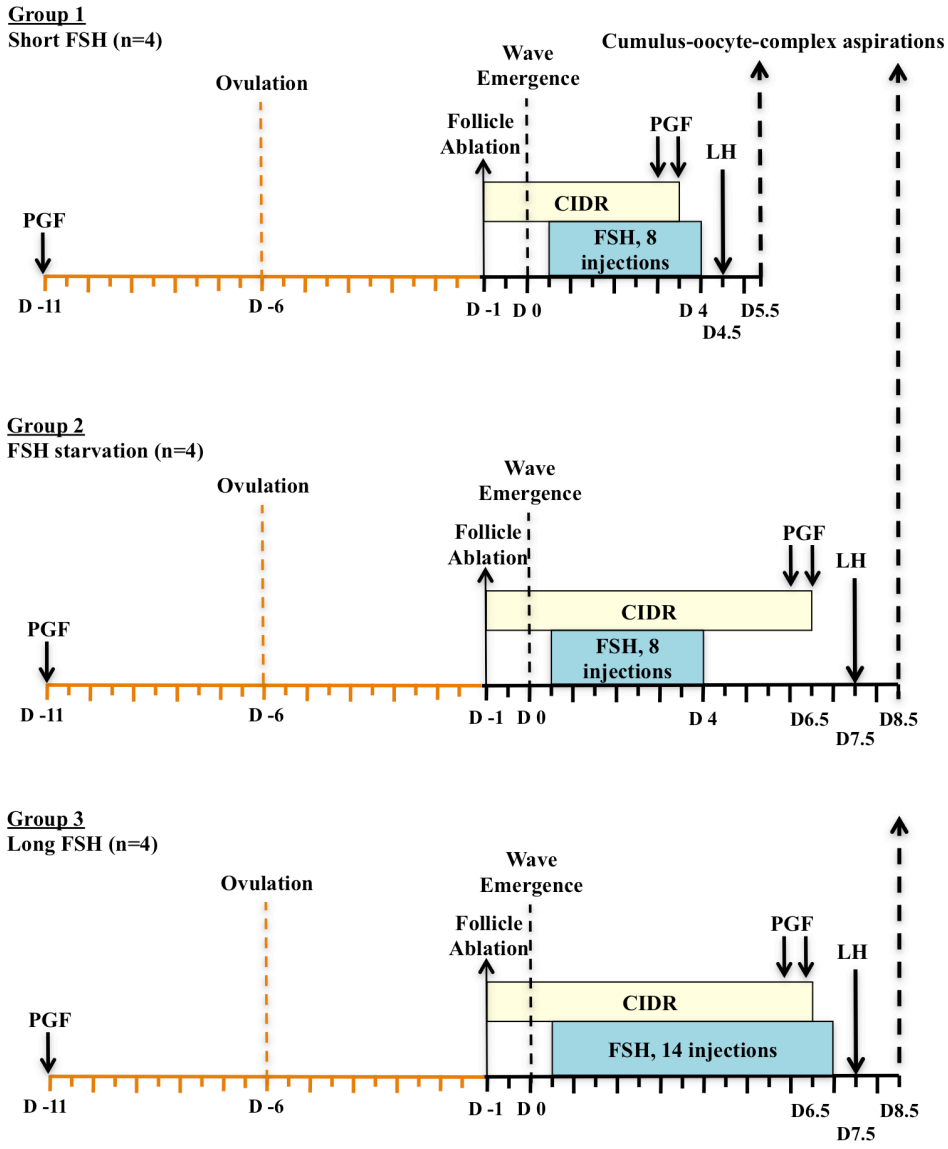

Figure 5.1 Experimental protocols designed to give Short FSH, FSH Starvation and Long FSH superstimulation treatments. in heifers (n=12). CIDR = Controlled Intravaginal Drug Release device for exogenous source of progesteron; PGF = prostaglandin F2α; FSH = Follicular Stimulating Hormone; LH = Lutropin. FSH injections were administered at12 hour intervals.

At the commencement of protocol, heifers were given single luteolytic dose of prostaglandin $F_{2\alpha}$ (PGF, Lutalyse®; Pfizer Canada Inc.) to induce ovulation. Five to eight days later, transvaginal ultrasound-guided ablation of follicles (>5mm) was done to synchronize emergence of a new follicular wave (Bergfelt et al., 1994). On the same day a progesterone-releasing device (1.9 g progesterone; CIDR-B, Bioniche Animal Health, Belleville, Ontario, Canada) was placed into vagina. At 36h after ablation (expected day of emergence of a new wave, Day 0), superstimulation treatment with FSH (Folltropin-V; Bioniche Animal Health, Belleville ON, Canada; each injection equivalent to 25 mg of NIH-FSH-P1) was started. Heifers in short FSH and FSH starvation groups were given 8 im injections of FSH (at 12-hour intervals) over 4 days, while those in long FSH group were given 14 im injections over 7 days. Two luteolytic doses of PGF were given at 12 h interval, on Day 3 to the short FSH group and, on Day 6 to FSH starvation and long FSH groups. In all groups, CIDR was removed at second PGF and pLH (12.5 mg; Lutropin-V, Bioniche Animal Health) was given 24 hours later. Heifers were prepared for follicular aspiration as described previously (Brogliatti and Adams, 1996).

5.3.2 Collection of cumulus-oocyte-complexes

Cumulus-Oocyte-Complexes (COCs) were collected from follicles (>9 mm) 18-20 hours post-LH by transvaginal ultrasound-guided follicular aspiration using a 7.5 MHz linear-array transducer (Aloka SSD-900; Tokyo, Japan) and a custom-made transducer handle. The follicles were aspirated using a 3.75 cm-long disposable ablation needle connected to 115 cm-long silicone tubing (Catalogue # RK-07625-30, Cole Palmer, Montreal, QC, Canada). The tubing was threaded through a rigid metallic tube. The other end of silicone tubing was connected to a 70-μ embryo filter with a modified lid

(Emcon®, Veterinary Concepts, Spring Valley, WI, USA) containing Dulbecco's phosphate buffered saline (dPBS, Catalog # 14040-133. Invitrogen Inc., Burlington, Canada) with surfactant (0.3%, ET Surfactant, Bioniche Animal Health, Belleville, ON, Canada) and sodium heparin (2 IU/ml) as anticoagulant. The COC collection was done under vacuum with the flow rate of 20 to 25 ml/min (Vacuum pump: Allied Healthcare Products, Inc, St Louis, MO, USA). At the end of collection, the needle assembly was flushed with dPBS to get all the aspirated COCs into the filters. The filter lids were removed and rinsed thrice with the dPBS using 20 ml syringe attached to 21G needle. After each rinsing, fluid from filters was drained till 0.25" height of fluid was left. Finally the fluid was replaced with transport media (dPBS plus 5% fetal calf serum) and filters along with the contents were immediately transported in a portable incubator (set at 25^0C) to the laboratory for further processing of COCs. The time from collection of COCs to the time they were put into fixative ranged from 60 to 80 minutes.

5.3.3 Processing of COCs for Nuclear staining

The COCs collected from each animal were searched under stereo-microscope and were categorized as compact and expanded based on the status of cumulus cells. Further, the COCs with >5 layers of cumulus cells and homogenous cytoplasm were classified as Grade 1. Those with <5 intact layers of cumulus cells and slightly heterogeneous cytoplasm were classified as Grade 2. The COCs with intact cumulus layers but distinctly heterogenous cytoplasm were classified as Grade 3. While denuded oocytes and COCs with very light or very dark cytoplasm were classified as Grade 4. In order to manage the large number of COCs Grades 1 and 2 were combined to call 'Good' quality COCs,

while grades 3 and 4 pooled into one group called 'Bad' quality COCs. As a result we had compact 'Good' and 'Bad' and expanded 'Good' and 'Bad' COCs for comparison.

The COCs were then denuded in a droplet of 0.5% hyaluronidase (Catalog # H3884, Sigma Aldrich, St Louis, MO, USA) prepared in Ca^{++} and Mg^{+} free dPBS (Catalog # 14190-144, Invitrogen Inc) by pipetting in-and-out with a narrow-bore glass pipette. Care was taken to remove all cumulus cells. Following denuding, oocytes were incubated for 10 minutes at 37^{0}C in dPBS, supplemented with 5% new-born calf serum (CS; Invitrogen Inc.). Oocytes were fixed in 4% paraformaldehyde solution at room temperature (25^{0}C) for 30 minutes. Fixed oocytes were subjected to immuno-cytochemical staining of nuclear lamin and chromatin (Prentice-Biensch et al., 2012) to detect nuclear envelope and chromatin configurations. All incubations were carried out at room temperature and with gentle shaking. Oocytes were premeabilized by 30-minute incubations in Triton X-100 (0.5%, v/v in DPBS) and then in Tween-20 working solution (BIO-RAD, Hercules, CA, USA, 0.05%, v/v in DPBS). The non-specific binding sites were blocked by incubating oocytes in a blocking buffer (2% BSA in DPBS) for 60 min. Oocytes were then placed in a 1:300 (mouse anti-lamin A/C, Catalog # SC 7292 Santa Cruz Biotechnology, Santa Cruz, CA, USA) for 60 minutes. Next, oocytes were incubated in 1:200 (v/v prepared in blocking buffer) secondary antibody (Alexa 488 labeled anti-mouse IgG, Catalog # A11029, Santa Cruz Biotechnology) for 60 minutes.

Oocytes were placed on a microscope glass slide in a drop of Vectashield Mounting Medium containing DAPI (Catalog# H-1200; Vector Laboratories Inc., Burlingame, CA, USA). In order to prevent rupture of oocytes under glass coverslip pressure, two reinforcement tags (Catalogue # 32202, Avery, Pickering, ON, Canada)

were placed on the microscope slide and oocytes were mounted in the center of these tags. A coverslip with paraffin-vaseline on its all corners was placed on the drop having the oocytes and gently pressed to touch the oocytes slightly. Mounted oocytes were observed under epifluorescence laser microscope (Zeiss Axioskop 5 Carl Zeiss Ltd., Toronto, ON, Canada) for nuclear maturation and classified into immature (GV), intermediate (GVBD and MI) and mature (MII) stages (Prentice-Biensch et al., 2012).

5.3.4 Processing of COCs for Lipid staining

After observation for nuclear maturation, oocytes were recovered by gently removing the glass coverslip from the slides, washed in dPBS and stained for lipid droplets using Nile Red (Genicot et al., 2005). Nile Red (Catalogue # 19123, Sigma Aldrich. Ontario, Canada) was dissolved in anhydrous DMSO (Catalogue # 276855, Sigma) to make a stock solution (1mg/ml) and stored at -20^0C in 10µl aliquots. Oocytes were incubated in Nile Red (5µg/ml in DPBS) at room temperature for 3 hours (under gentle shaking on rocking platform). The oocytes were washed in DPBS (thrice, 5 minutes each) and were mounted in Vectashield Mounting Medium containing DAPI drops in glass bottom petri plates (P50G-0-14-F, Matteck Corporation, Ashland, MA). Oocytes were imaged with Zeiss LSM 710 confocal microscope (63x 1.4 oil objective lens, 2-photon laser, excitation: 790nm, emission: 514-540nm) to obtain 3D image stacks (XYZ: 800x800x350 pixels, voxel size: 0.169x0.169x0.340 microns).

5.3.5 Image processing and segmentation of 3D volume sets

The steps involved in image processing and segmentation of 3D volume sets are shown in Figure 5.2. Oocyte volumetric datasets (LSM format) were converted into 32-

bit format and saved (IDS format) and subjected to blind deconvolution using Autoquant X2 (Media Cybernetics, Rockville, MD, USA). The default setting for theoretical point spread function was used to account for convolution in z-axis except for number of iterations (changed from 10 to 20) and noise level (changed from 200 to 600) with automatic settings. Deconvolved datasets were imported and processed using Imaris Pro 7.4 C1 package containing Imaris Track, Imaris Coloc, Imaris XT, Imaris Cell and Vantage modules (Bitplane AG, Badenerstrasse, Zürich, Switzerland). Italicised terms in the following paragraph indicate the Imaris-specific terminology. Variable size *spots* were created to segment lipid droplets using following filters, *estimated diameter* set to 1.7 μm, *background substraction* and *region of growing* based on *local contrast*. The *minimum threshold* used to identify the *spots* was subjectively selected depending on whether or not *seeds* were put into the intensities representing stained lipid droplet. In order to determine the exact volume of oocyte, a *surface* was created by manually drawing the oocyte plasma membrane boundary at every 5-10 sections along the Z-direction. The filters within Imaris Pro were used to generate quantitative data for statistical comparison. The statistic section within the *spots* was used to get the average lipid droplet volume and surface area volume. The statistic volume within the *surface* was used to obtain the oocyte volume. The number of lipids in <1μm, 1-3μm and >3μm size categories was obtained using the selection of spots by diameter. The surface was used to create a *cell* and the *spots* (i.e. lipid droplets) were imported as its *vesicles*. The filter, *vesicles within x distance from the surface,* was used to detect lipids within the 10μm distance from the surface (peripheral region) and vesicles (lipid droplets) in the remaining region were identified as centrally located. The distribution pattern of lipid

droplets within the ooplasm was identified by creating a MIP-image (maximum intensity projection image) from 10-micron z-stack (30 images) selected around the largest diameter of oocyte. The qualitative distribution pattern was defined based on the location of lipid droplets within the ooplasm and proximity between the lipid droplets into peripheral/central/uniform, and scattered/clustered patterns (Figure 5.3).

Flow chart for segmentation of lipid droplets stained with Nile Red

Step 1 Preliminary Processing in Imaris Pro
- Convert the raw 8 bit image set to 32 bit float.
- Background subtraction based on automatic settings.
- Save the image as .ids format.

Step 2 Processing in Autoquant X2
- Upload .ids image set created as above.
- Use 3-D deconvolution option
- Use blind deconvolution option to use theoretical point spread function.
- Change the iterations to 20 and noise level to 600 and initiate the deconvolution.
- Save the processed file as .lsm format.

Step 3 Final Processing in Imaris Pro
- Upload the above .lsm image set.
- Use *spots* to represent lipid droplets.
- Use *surface* to represent ooplasmic membrane.
- Import the created *surface* as membrane and *spots* as *vesicles* into *cell* module.
- Use *vesicle distance to the surface* filter to select the peripheral and centrally located.

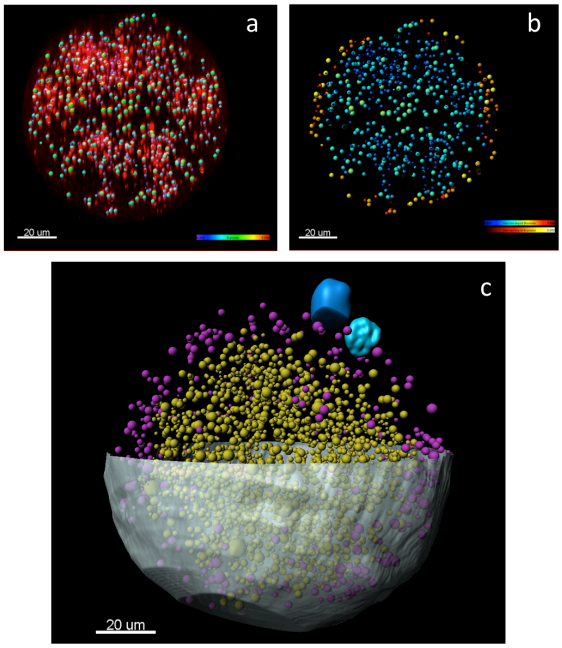

Figure 5.2 Flow chart showing steps involved in identifying lipid droplets of an oocyte stained with Nile Red. a) maximum intensity projection image in X-Z plane of 10 μm stack at the center of an metaphase II oocyte showing *spots* representing lipid droplets (red signal), b) maximum intensity projection image of same oocyte with *variable size spots* to represent lipid droplets of different size in the peripheral and central ooplasm, c) same oocyte with *surface* created to represent the ooplasmic membrane, peripherally (purple) and centrally (yellowish) located *spots*. Note the haploid set of chromosomes (light blue) of oocyte and polar body (dark blue) adjacent that was extruded from the oocyte.

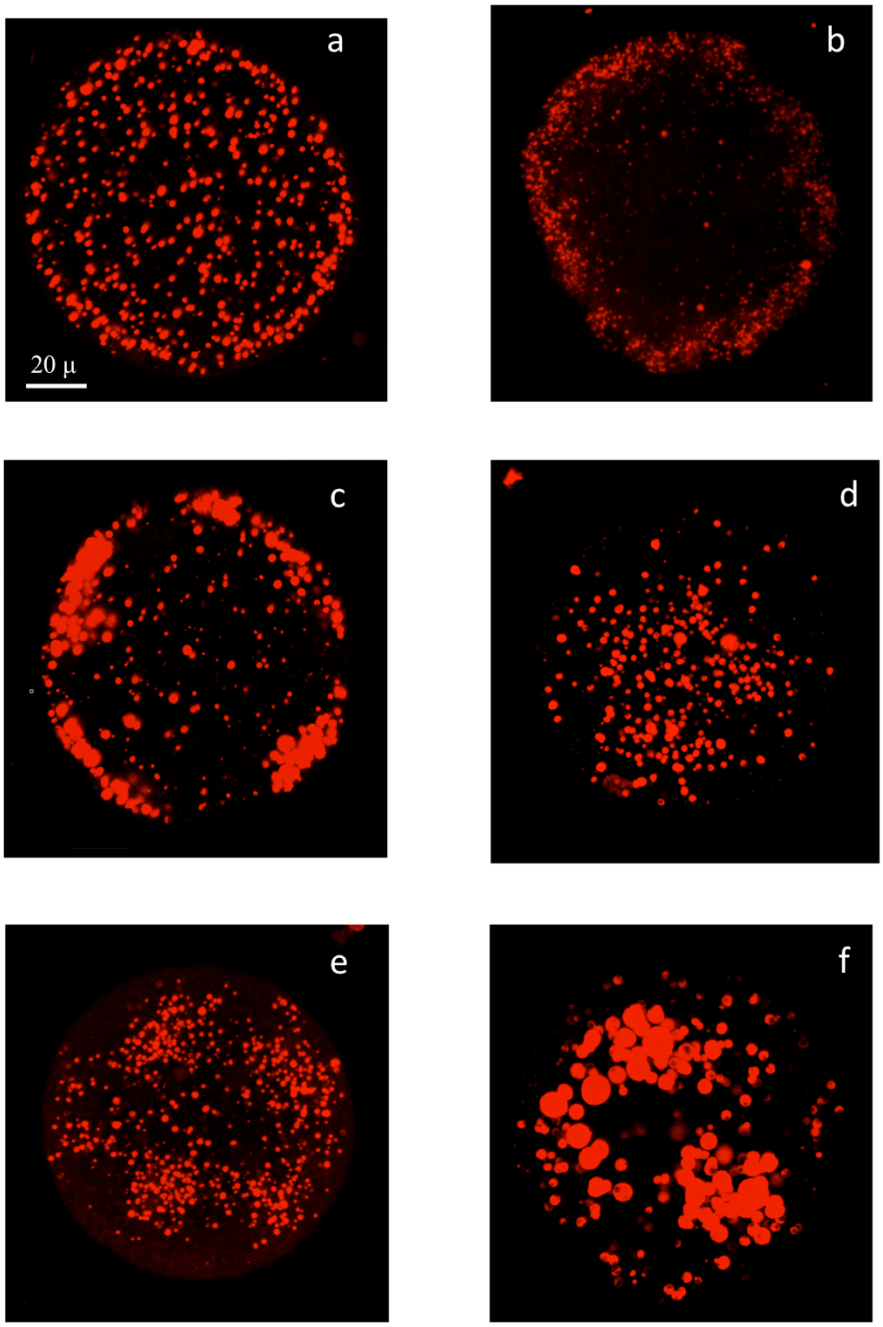

Figure 5.3 Images representative of distribution patterns observed in bovine oocytes, uniformly scattered (a), peripherally scattered (b), peripherally clustered (c), centrally scattered (d) and centrally clustered (e). The images are maximum intensity projection of 10 µm z-stacks around the largest diameter of the oocytes. A major proportion of oocytes from FSH starvation group exhibited larger lipid droplets (f).

5.3.6 Statistical analyses

All statistical analyses were performed using the Statistical Analysis System software package (SAS 9.2; SAS Institute Inc., Cary, NC, USA) and probabilities ≤0.05 were considered significant. The effect of treatment (short FSH, FSH starvation and long FSH) on proportions of grades of COCs, categories of nuclear maturation and distribution pattern of lipids was compared by Fisher's exact test using Proc Frequency procedure. The data for lipid droplet volume, number and surface area were compared by analysis of variance. The data for proportion of lipid droplets within different regions of oocytes from three treatment groups were arcsine transformed and then subjected to analysis of variance for comparisons. The Fischer's least significant difference was taken as post-hoc test if the main effect was significant.

5.4 Results

5.4.1 Follicle numbers and collection efficiency

The total number of follicles 12h after LH administration was highest (P=0.01) in the long FSH group than the short FSH and FSH starvation groups (Table 5.1). The number of follicles in the 6-8 mm category did not differ (P=0.69) between the superstimulation treatments. The number of ≤5 mm follicles was lowest (P=0.04) and number of ≥9 mm follicles was highest (P=0.03) in heifers given long FSH treatment than those given short FSH and FSH starvation treatments. Irrespective of groups, the overall COC collection efficiency (percent COC obtained/follicles aspirated) through transvaginal ultrasound guided-follicular aspiration was 53.7% (159/259; based on n=11) and did not differ across the treatment groups (Table 5.2).

Table 5.2 Mean number (±SE) of follicles in different size categories at 12h after LH administration.

Number of follicles	Short FSH	FSH Starvation	Long FSH
Total follicles	23.8±4.0[a]	23.5±2.8[a]	46.5±5.7[b]
Follicles ≤5 mm	5.3±1.3	4.5±1.3	1.3±0.6
Follicles 6-8mm 12 h post LH	7.0±3.6	9.8±1.9	9.3±1.5
Follicles ≥9mm	11.5±3.6[a]	9.3±1.3[a]	36.0±16.8[b]

[ab] Values with different superscripts are different (P<0.05).

The proportion of morphological Good (Grades 1and 2 combined) or Bad (Grades 3 and 4 combined) quality COCs tended to differ (P=0.06) between the superstimulation treatments (Table 5.2). The short FSH group tended to have more of 'Good' quality oocytes (Grades 1 and 2 combined) and less of 'Bad' quality (Grades 3 and 4) COCs (P=0.06) than the other two groups.

Table 5.1 Proportion of COCs collected to follicles aspirated (percent collection efficiency) and different grades of expanded COCs in different superstimulation.

	Short FSH	FSH Starvation	Long FSH
COCs collected/total follicles aspirated (% efficiency)*	25/65 (38.5%)	25/74 (33.8%)	106/168** (63.1%)
Good quality	19/25 (76.0%)	11/25 (44.0%)	55/106 (51.9%)
Bad quality	6/25 (24.0%)	14/24 (56.0%)	51/106 (48.1%)

[ab] Values with different superscripts are different (P<0.05).
*Analysis done on arcsine transformed data of proportions.
** Proportion based on data from n=3, as data for number of follicles aspirated was missing from one animal.

5.4.1. Nuclear maturation

Two COCs from the short FSH and nine COC from long FSH groups were lost during the processing; therefore data of nuclear maturation status was analyzed from the remaining 23 and 100 oocytes of these groups, respectively. Higher proportions ($P<0.01$) of oocytes reached MII stage in the long FSH group, about six times and 3 times more than FSH starvation and long FSH groups, respectively (Figure 5.4C). The proportion of immature oocytes (at GV stage) in FSH starvation and short FSH groups was about three times and two times more, respectively ($P<0.01$) than the long FSH group (Figure 5.4A). The proportion of oocytes at intermediate stage of nuclear maturation (GVBD and MI) did not differ ($P=0.21$) between the groups (Figure 5.4B).

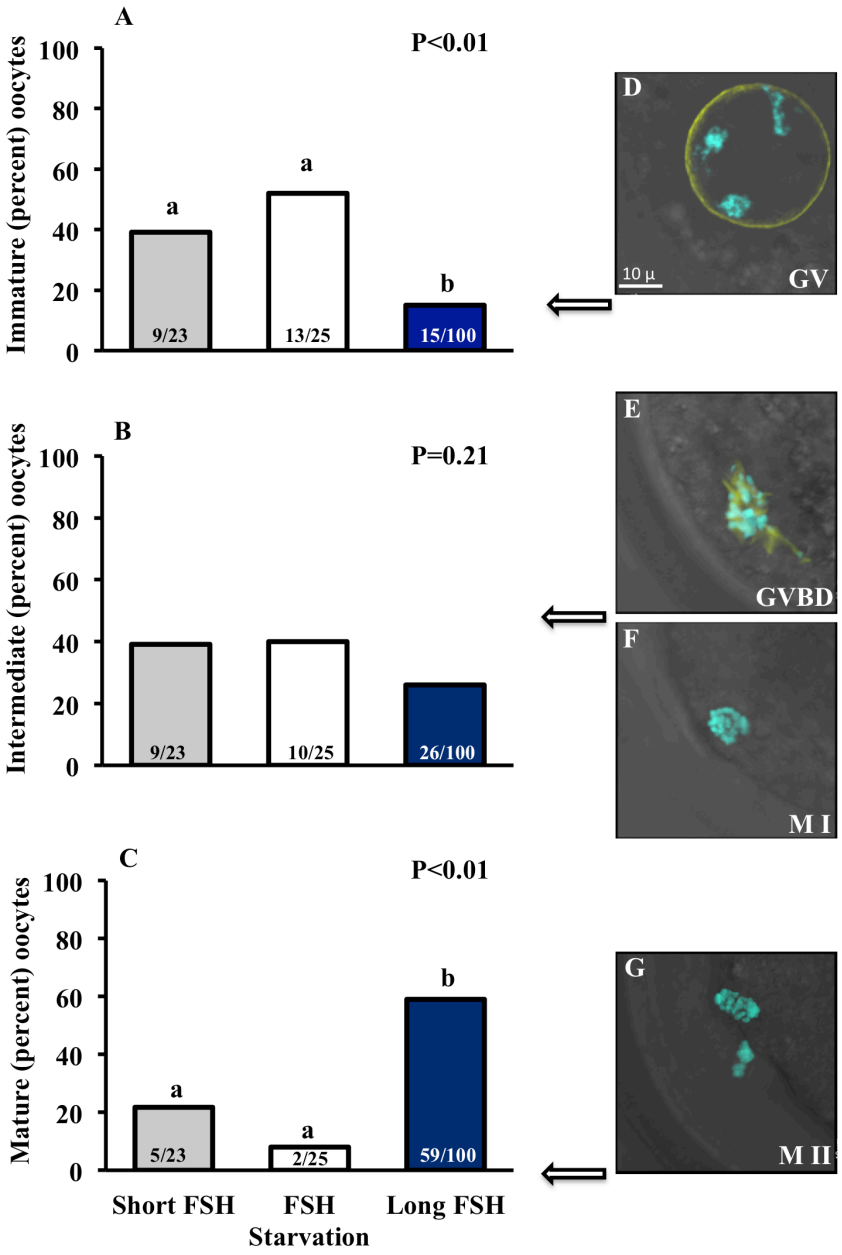

Figure 5.4 Percent rates of immature (A), intermediate (B) and mature (C) oocytes following Short FSH, FSH starvation and Long FSH treatments. Nuclear envelop of oocytes was immunostained with anti-Lamin A/C followed by Alex 488 (pseudo-colored yellowish green to enhance visualization) as secondary. Chromatin material (Aqua color) was stained with DAPI. Immature = Germinal Vesicle (GV, Fig. D); Intermediate = Germinal Vesicle Breakdown (GVBD, Fig. E) and Metaphase I (M I, Fig. F); Mature = Metaphase II (M II, Fig. G). ^{ab} Values with no common superscripts are different (P<0.05). The number of oocytes (belonging to the stage/total) is indicated inside the bars.

5.4.2 Oocyte volume, lipid volume and surface area

Some oocytes were lost during their recovery from slides prepared for anti-Lamin/DAPI staining, as a result 10, 11 and 24 oocytes from short FSH, FSH starvation and long FSH groups, respectively, were processed and analyzed for lipid droplets data. The selected oocytes represent the relative proportion of mature vs immature oocytes across the groups. The average oocyte volume (all groups combined) was 670.4±31.6 pL and did differ within treatments (P=0.15). The lipids represented 3.0 to 3.5% of total oocyte volume and on an average lipid volume was 22.2±1.6 pL (averaged over all treatment). The volume (Figure 5.5b) and surface area of lipids within an oocyte (all lipid droplets combined together) did not differ between the superstimulation protocols. The mean volume of individual lipid droplets was larger (P=0.03) in the starvation group compared to short and long FSH groups (Figure 5.5). The mean surface area of individual droplets was largest in starvation group, significantly more (P=0.04) than the short FSH group but not different from the long FSH group (Figure 5.5).

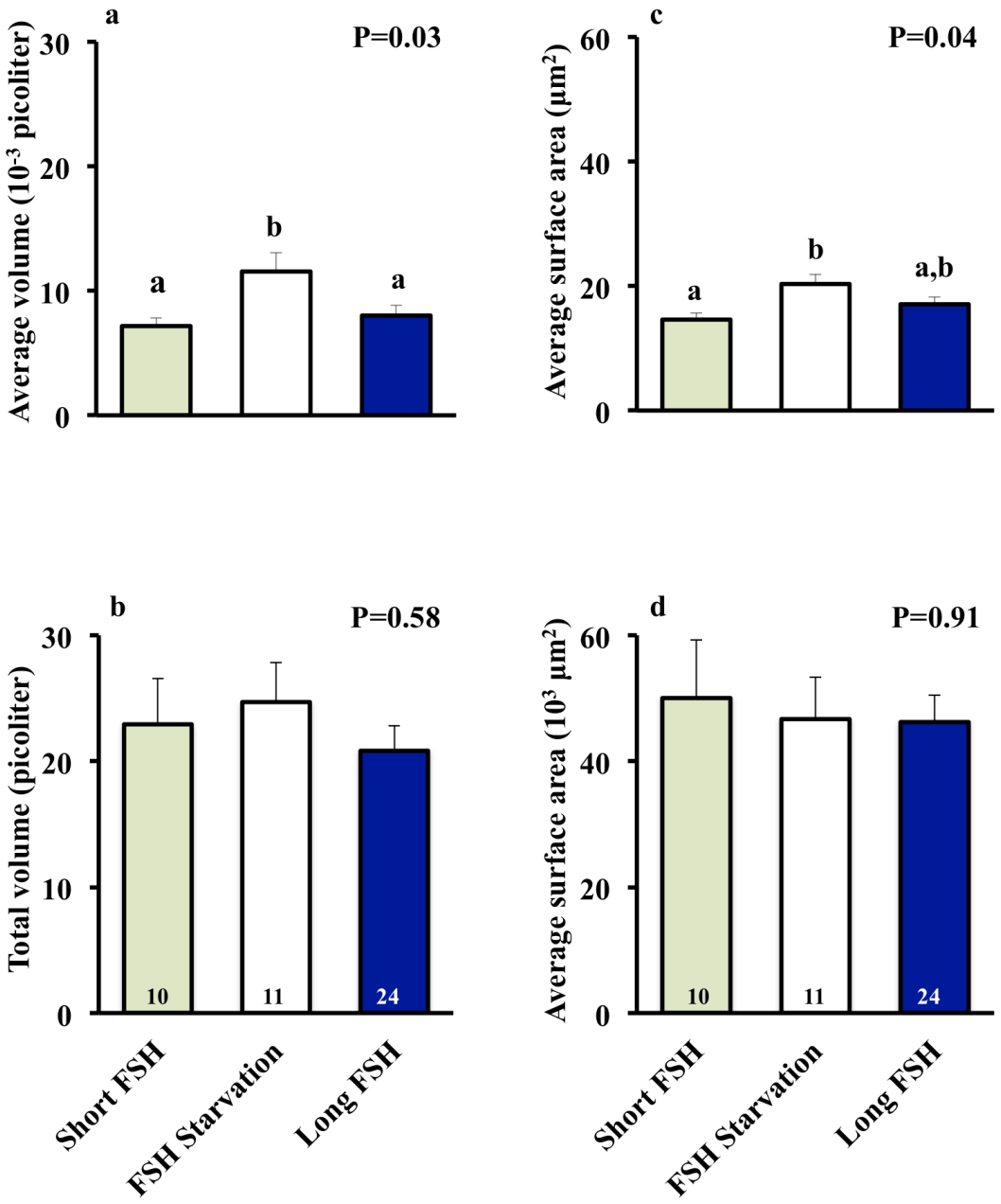

Figure 5.5 Mean (+ SE) volume of individual lipid droplets (10^{-3} picoliter, a), total lipid volume (picoliter, b), surface area of individual lipid droplets (μm^2, c) and total surface area (10^3 μm^2, d) within the oocytes collected following three superstimulatory treatments. Values with no common superscripts are different ($P<0.05$). The number of oocytes is indicated in parentheses.

5.4.3 Lipid droplets number and distribution

Five different types of lipid distribution patterns were observed in the *in vivo* matured bovine oocytes (Figure 5.3). In the long and short FSH groups, 45% (11/24) and 40%(4/10) of the oocytes, respectively, had uniformly scattered distribution of lipid droplets. Only 18% (2/11) oocytes (P=0.33 compared to other groups) from the starvation group showed uniformly scattered distribution and majority had clustered (either peripheral or centrally located) distribution. The effect of three superstimulatory treatments on the lipid droplet number and relative proportion is shown in Table 5.3. The *in vivo* matured oocytes from superstimulated heifers had approximately 3000 lipid droplets (averaged over all treatment groups) and the diameter of lipid droplets ranged between 0.3 to 11.6 μm. About 70% lipid droplets were between 1 and 3μm in diameter. There was a numerical drop in the total lipid droplet number in the FSH starvation group that was not significant (P=0.39) from other groups. The number and proportion of lipid droplets in <1μm, 1-3μm and >3μm size categories was not different between the groups (P=0.53, P=0.35, P=0.62 for numbers and P=0.73, P=0.25, P=0.28 for proportions, respectively). There was a numerical but non-significant increase in the >3μ size lipid droplets in the FSH starvation groups.

Around 47% of total number of lipids droplets were located in the peripheral 10 micron of the ooplasm and did not differ between the three treatments (Table 5.3, P=0.21). Approximately half of the total lipid content was within the peripheral region of ooplasm and did not differ significantly between the groups (10.6±1.5 pL, 11.4±1.4 pL and 9.2 ±1.4 pL, respectively; P=0.58).

Table 5.3 Mean (±SEM) number and relative proportion lipid droplets in oocytes collected following superstimulation protocols.

	Short FSH (n=10)	**FSH Starvation (n=11)**	**Long FSH (n=24)**
Total	3497±616	2451±365	2960±376
<1µm diameter			
Number	439±136	266±125	290±74
Proportion	0.11±0.02	0.12±0.05	0.09±0.01
1-3µm diameter			
Number	2703±499	1744±342	2321±337
Proportion	0.76±0.03	0.67±0.06	0.76±0.03
>3µm diameter			
Number	355±71	441±60	350±61
Proportion	0.13±0.03	0.21±0.03	0.15±0.03
Peripheral	1639±308 (49±4%)	1223±183 (50±3%)	1347±332 (40±4%)
<1µm diameter			
Number	219±74	160±87	145±63
Proportion	0.11±0.03	0.13±0.06	0.10±0.03
1-3µm diameter			
Number	1251±242	848±174	1056±276
Proportion	0.76±0.03	0.66±0.06	0.71±0.04
>3µm diameter			
Number	169±30	215±31	146±24
Proportion	0.13±0.03	0.21±0.03	0.18±0.03
Central	1858±359 (51±4%)	1228±216 (50±3%)	1613±127 (60±4%)
<1µm diameter			
Number	220±71	106±39	145±28
Proportion	0.11±0.03	0.11±0.05	0.09±0.01
1-3µm diameter			
Number	1452±297	896±195	1264±123
Proportion	0.76±0.03	0.67±0.06	0.77±0.03
>3µm diameter			
Number	186±45	226±33	204±42
Proportion	0.13±0.03	0.22±0.03	0.14±0.03

The number of oocytes that were processed for Nile red staining and bioimage informatics is indicated in parentheses under the group headings. [ab] Analyses were done on arcsine transformed proportions.

5.5 Discussion

Present study shows that 84h FSH starvation period following last FSH injection yields more immature oocytes compared to 7-d FSH protocol (simulating 2-wave animal). Moreover, mean volume of individual lipid droplet was larger in the oocytes from starvation group, compared to either 4-d FSH or 7-d FSH treatments. Both these findings indicate that 84 h starvation was too long and resulted in degenerative changes in the oocytes. The hypotheses that FSH starvation will lead to failure of nuclear maturation and accumulation of bigger lipid droplets within the oocytes and, prolonged FSH treatment will produce higher proportion of mature oocytes were supported.

Increase in total number of follicles at 12h after LH administration in 7-d superstimulation protocol (Table 5.1) indicates that longer FSH treatment allowed more time for small antral follicles to enter and continue the growth phase. Does that mean by supplying FSH for longer duration we rescued the follicles from the growing cohort or we added new follicles to the cohort by stretching the period of wave emergence? This aspect is currently being studied in our lab by tracking individual follicles throughout the short and long FSH protocols. The increase in total number of follicles is mainly due to an increase in number of large size follicles (>9mm); the number of medium size (6-8mm) and small (≤ 5mm) follicles were similar in the long FSH group compared to short and starvation groups (Table 5.1). Similar response has been observed in a previous study (Dias et al., 2012a) and in a parallel study (Dias et al, personal communication) from our laboratory. In more recent study, the number of large size follicles at 12 h after LH was similar between the 7 d and 4 d superstimulation protocols (García Guerra et al., 2012). However, by 36 h after LH administration more follicles ovulated with greater

synchronicity in the 7-d group compared to the 4-d group (García Guerra et al., 2012), which is in contrast to a previous observation that number of ovulations did not differ between the long and short superstimulation protocols (Dias et al., 2012a). The difference in observations of two studies could be due to the differences in total dose of FSH used over the entire superstimulation protocols. In stark contrast to the short and long FSH groups, the majority of the follicles in the 84 h starvation group failed to ovulate after exogenous LH administration (Dias et al., 2012a). In regards to that, present study shows that less than 10% oocytes from the starvation group were able to reach the Metaphase II stage at 20 h after LH administration (Figure 5.4C). Moreover, about 50% of the oocytes from the 84h starvation group did not proceed beyond GV stage indicating a failure in resumption of meiosis. During a 5d superstimulation protocol, the oocytes resume meiosis and undergo germinal vesicle breakdown at 9 h after LH surge and reach MII stage by 20 h (Hyttel et al., 1986a). However, the authors did not mention the proportion of oocytes that reach MII at 20 h after LH surge. In the present study, about $1/5^{th}$ of oocytes from the 4-d treatment reached MII by 20 h following LH administration compared to 59% of oocytes from long treatment group (Figure 5.4C). Previously a 4-d FSH protocol resulted in similar percentage of oocytes reaching MII 24 h after LH (Takagi et al., 2001). Our results indicate that a longer superstimulation protocol allows more time for the oocytes to acquire nuclear maturation competence.

The oocytes from FSH starvation group exhibited a numerical increase in lipid volume and numerical decrease in lipid droplet number compared to short and long FSH groups. However, the differences in individual lipid droplet size was more evident as the volume of individual lipid droplets was more in starvation group compared to the oocytes

from other two groups. Previous observations have also indicated that poor quality oocytes have darker and granular ooplasm due to accumulation of lipids (Awasthi et al., 2010). We have recently shown in an ultrastructural study that oocytes from regressing follicles have bigger lipid droplets (Chapter 4). Lipid droplets are dynamic organelles that store triglycerides, (an important source ATP generation through β-oxidation in oocytes in addition to glucose and pyruvate (Dunning et al., 2010)). Similar to adipocytes, oocytes can accumulate more lipid droplets if there is more supply or if there is failure of utilization, as reviewed earlier (Murphy, 2001). We speculate that oocytes from FSH starvation group accumulated more lipids due to failure to utilize lipids as majority of the oocytes from FSH starvation group failed to complete the nuclear maturation. It has been shown that there is reduction in the triglyceride content of the oocyte as it matures (Ferguson and Leese, 1999; Kim et al., 2001). Further, inhibiting the rate-limiting enzyme for β-oxidation i.e. carnitine palmitoyl transferase I (CPT1B) significantly decrease the blastocyst rate in mouse (Dunning et al., 2010). It is worth mentioning here that our knowledge of proteins (adipohilin and perilipin) that are involved in growth and fusion of lipid droplets in oocytes is much less compared to what has been reported in adipocytes and granulosa cells (Murphy, 2001).

With regards to oocyte competence, the long and short treatment groups did not differ when the proportion of good quality embryos were compared (Dias, 2008; Dias et al., 2012a; García Guerra et al., 2012). In a study done parallel to the present study, when the oocytes from long and short superstimulation groups were fertilized *in vitro*, no differences in the cleavage rates, morula plus blastocyst rates on day 7 and blastocyst rates on day 9 after IVF (Dias et al, personal communication) were observed. However, a

significantly lower cleavage rates, morula plus blastocyst rates on day 7 and blastocyst rates on day 9 after IVF were observed in the 84 h FSH starvation group (Dias et al, personal communication). It is clear that 84 h of starvation period exceeds the 48h FSH-free period, mentioned in an earlier report (Blondin et al., 1997b), that is required for oocyte to undergo maturational changes for better oocyte competence. In the present study animal were superstimulated under luteal levels of progesterone and all follicles >3mm were collected after different starvation period, matured, fertilized and cultured *in vitro*. Recent study has shown that a FSH starvation period ranging from 44-68 h is ideal to increase the blastocyst rates while a 92 h starvation resulted in poor blastocyst rates (Nivet et al., 2012). Above mentioned study was done on animal superstimulated during spontaneous luteal phase and oocytes were collected from dominant follicles (size not indicated) and processed for *in vitro* maturation and culture after different periods of FSH period. The study, similar to a previous one (Blondin et al., 1997b), did not compare the competence of *in vivo* matured oocytes and also failed to include groups with continued FSH support where follicle grew for similar period as in the FSH starvation groups. In present study, the starvation period of 84 included a 3 d of luteal levels of progesterone when LH pulses are low and 24 h of decreasing/low progesterone when LH levels and pulses are gradually picking up. In another study from our group (Jaiswal, 2007), where subluteal-phase levels of progesterone were used during the a 4 d FSH treatment and 5 d FSH free period, all follicles lost their ovulation capabilities. Presumably these follicles became persistently dominant due to increased LH pulsatility (Stock and Fortune, 1993; Kinder et al., 1996), oocytes underwent atresia (Savio et al., 1993).

In conclusion, the longer FSH superstimulation increases the superstimulatory response with higher proportion of mature oocytes compared to short FSH treatment. On the other hand, FSH starvation of 84 h results in failure of meiotic resumption and accumulation of large lipid droplets indicating cytoplasmic degenerative changes.

CHAPTER 6

6 EFFECT OF FOLLICULAR AND MATERNAL AGING ON ATP CONTENT AND DISTRIBUTION OF MITOCHONDRIA IN *IN VIVO* MATURED OOCYTES

Dadarwal D, Dias FCF, Adams GP and Singh J

Relationship of this study to the to dissertation

In my previous studies, I have shown that ooplasmic organelle reorganization occurs when follicle develops and matures (Chapter 4) and longer duration of follicular growth without continued gonadotropin support resulted in failed nuclear maturation and altered lipid content in the oocytes (Chapter 5). Previous report and results from Chapter 4 have shown that lipid droplets are in close approximation with mitochondria within the oocyte and this contact changes with stage of follicle development. The contact between mitochondria and lipid droplets within the ooctye is crucial for ATP production though β-oxidation. In this study, I looked into how the duration of dominant follicle growth (follicle age) and age of animal (maternal aging) on mitochondrial population and functionality in the oocytes. We tested the hypotheses that a) *in vivo* matured bovine oocytes obtained from aged follicles (84 h gonadotropin starvation after 4-day FSH treatment) have a decrease in mitochondrial number, an altered distribution and a decrease in cytoplasmic ATP content compared to those obtained at the end of superstimulatory protocol (4-day or 7-day FSH treatment) and b) *in vivo* matured oocytes from old cows have a reduction in number of mitochondria, an altered distribution of mitochondria and a decrease in the ATP content compared to those from young cows.

6.1 Abstract

Our objective was to determine how follicular aging and maternal aging affects the mitochondrial numbers, distribution and ATP content of the *in vivo* matured bovine oocytes. We hypothesized that a) *in vivo* matured bovine oocytes obtained from aged follicles (84 h gonadotropin starvation after 4-day FSH treatment) have decreased mitochondrial number, altered distribution and decreased cytoplasmic ATP content compared to those obtained at the end of a superstimulatory protocol (4-day or 7-day FSH treatment) and b) *in vivo* matured oocytes from old cows have reduced number of mitochondria, altered distribution of mitochondria and decreased the ATP content compared to those from young cows. For follicular aging, Hereford heifers were given prostaglandin $F_{2\alpha}$ (PGF) to induce ovulation. Five days after ovulation (Day -1), a progesterone-releasing device (CIDR) was placed into vagina and transvaginal ultrasound-guided ablation of follicles was done to synchronize emergence of a new follicular wave. At 36 h after ablation (day of new wave emergence, Day 0), heifers in short FSH and FSH starvation groups (n=5 each) were given 8 im injections of FSH (12-hour intervals) over 4 days, while those in long FSH group (n=4) were given 14 im injections over 7 days. Two injections of PGF (at 12 hour interval) were given on Day 4 to the short FSH group and on Day 7 to FSH starvation and long FSH groups. In all groups, CIDR was removed at second PGF and LH was given 24 hours later. One day later, ovaries were removed by colpotomy and COCs were by aspirating follicle ≥ 8mm. For maternal aging, young and old cows (n=7 each) were superstimulated using a protocol similar to short FSH group with few exceptions. No CIDR was inserted and all animals were made sure to be in mid-luteal phase. FSH treatment was started at the time

of expected wave emergence (Day 0) and LH was given 24 hours after last FSH injection COCs were collected 18-20 hours post-LH by follicular aspiration. Oocytes from both follicular and maternal aging were denuded and were either processed for staining with Mitotracker Deep Red FM or for ATP assay. Stained oocytes were imaged with Zeiss LSM 710 confocal microscope. Oocyte volume sets were deconvoluted using Autoquant X2 and mitochondria segmented using Imaris Pro 7.4. Proportion of different grades of COCs was compared using Fischer's exact test and, ATP and mitochondrial data were compared using ANOVA. Within the expanded COCs, the short and long FSH groups had significantly (P=0.02) higher proportion of Grade 1 COCs than the FSH starvation group. The total ATP content of the oocytes from the expanded COCs in the long FSH group tended to be higher (P=0.09) than the short FSH; FSH starvation group was intermediate. The total ATP content did not differ (P=0.49) when the oocytes from compact COCs were compared across groups. Overall the proportion of mitochondrial clusters (P=0.01) was highest and proportion of individual mitochondria was least (P=0.01) in the FSH starvation group compared to short and long FSH groups. Individual mitochondria and mitochondrial clusters in oocytes from Long FSH and FSH starvation groups had twice the relative intensity compared to the short FSH group (P<0.01). *In vivo* matured oocytes derived from old cows were similar in morphological quality to those from young cows but had 30% less intracellular ATP (P=0.01). The individual mitochondria had higher mean number of voxels (P<0.05) in old cows and old cows tended to have more clusters compared to young cows (P=0.06). To conclude FSH starvation of 84 h leads to more poor quality oocytes that have ATP contents similar to short FSH group. Furthermore, organization of mitochondria as intense and bigger

clusters within the oocytes from FSH starvation group might indicate oxidative stress and hence atresia. Maternal aging leads to decrease in cytoplasmic ATP content of *in vivo* mature oocytes despite no differences in mitochondrial population and distribution pattern.

Key words: Bovine, *in vivo* matured oocytes, follicular aging, maternal aging, superstimulation.

6.2 Introduction

Hormonal environment experienced by the follicle during its growth and duration of follicle development affect the oocytes ability to get fertilized and develop into embryo. Growth of follicles (≥4 mmm) in cattle occurs in the form of 2 to 3 waves in an estrous cycle with last wave being ovulatory (Pierson and Ginther, 1984; Pierson and Ginther, 1988; Savio et al., 1988a; Sirois and Fortune, 1988; Knopf et al., 1989; Jaiswal et al., 2009). Each wave each begins with a cohort of 3-4 mm follicles commencing their growth under the influence of FSH (Adams et al., 1992b). During non-ovulatory wave dominant and subordinate follicles undergo ultrasonographically defined phases of growth, static and regression due to a functioning CL that secretes luteal levels of progesterone (Rahe et al., 1980). During ovulatory wave, the dominant follicle grows for 9 days (6 days under luteal and 3 days under basal progesterone) in a 2-wave animal and 6 days in a 3-wave animal (3 days under luteal and 3 days under basal progesterone) before ovulation (Pierson and Ginther, 1988; Savio et al., 1988a; Sirois and Fortune, 1988; Knopf et al., 1989). Although argued, no differences were found in the fertility rates following insemination of animals simulating 2-wave or 3-wave animals in a recently conducted study (Dias et al., 2012b). Superstimulation of animals allows us to

induce dominance of multiple follicles to obtain large number of oocytes to test their *in vivo* or *in vitro* competence. Results from previous experiments have shown that the developmental competence of oocytes after a 7-d protocol is not different than of the oocytes obtained from a 4-d protocol when superstimulation is done under luteal levels of progesterone (Dias et al., 2012a; Dias et al., 2012b; García Guerra et al., 2012). On the other hand, a 4-d FSH treatment followed by 84 h FSH starvation period (total length = 7.5 days) under luteal progesterone environment lead to loss of ovulatory capacity in approximately 60% of the heifers (Dias et al., 2012a). On the same line, similar period of superstimulation followed by 144 h FSH starvation, under subluteal-phase levels of progesterone, resulted in failure of ovulation in all dominant follicles (Jaiswal, 2007). Oocyte competence is also affected by age of cow as about twice the number of oocytes from old cow failed to undergo fertilization compared to those from young cows (Malhi et al., 2007). Results from IVF trials also showed similar results as blastocyst production is reduced with advancing age of donor cow (Iwata et al., 2011; Su et al., 2012). These differences in developmental competence of the oocyte are thought to be due to differences in the nuclear and cytoplasmic maturation that an oocyte undergoes during the growth of a follicle (Chapter 5).

Nuclear maturation has been well-characterized and involves resumption of meiosis and release of polar body at 19-22 h after LH surge (Assey et al., 1994). In aged follicles that experience 84h FSH starvation period, only 8% of the oocytes reached metaphase-II, while about 60% of the oocytes matured from the follicles with similar duration of growth but under continued FSH support (Chapter 5). Cytoplasmic maturation of bovine oocytes involves translocation of organelles (Assey et al., 1994), a process poorly defined

but considered crucial for oocytes to attain developmental competence. In that context, aged follicles with FSH starvation had larger lipid droplets compared to oocytes from 4-d or 7-d superstimulation protocols (Chapter 5). As lipid droplets are closely associated with mitochondria (Sturmey et al., 2006) for ATP synthesis through β-oxidation (Sturmey et al., 2006; Dunning et al., 2010). We could speculate that mitochondrial population; its distribution and ATP content of the oocytes might be affected by the age of follicle and age of cow.

Both mitochondrial number and their distribution pattern have been related to the status of oocyte maturation and subsequent developmental competence (Van Blerkom et al., 1995; Bavister and Squirrell, 2000; Stojkovic et al., 2001; Nagano et al., 2006). The estimated numbers of mitochondria in human oocytes increase about 10 fold from the numbers in primary oocyte to reach around 100,000 in mature oocytes (Jansen and de Boer, 1998). ATP content in oocyte is indicative of mitochondrial function and is closely related to grouping of mitochondria into clusters (Van Blerkom et al., 1995; Wilding et al., 2001). Positive correlations exist between ATP content of mature oocytes and subsequent embryonic development before genomic activation of mouse embryo (Van Blerkom et al., 2003; Zhang et al., 2006). Similarly, good quality bovine oocytes with higher cytoplasmic ATP content have better developmental potential than poor quality oocytes (Stojkovic et al., 2001). With regards to distribution pattern, translocation of mitochondria is affected by the quality of bovine oocyte (Stojkovic et al., 2001), stage of follicle growth (Chapter 4) and culture conditions during *in vitro* maturation (Bavister, 2000). A negative correlation have been shown between mitochondrial population of *in vitro* matured bovine oocytes and advancing age (Iwata et al., 2011). However, the effect

of maternal age on mitochondrial number, distribution and ATP content of *in vivo* matured oocytes is unknown.

Thus our objective was to determine the effect of follicular aging and maternal aging on the mitochondrial numbers, distribution and ATP content of the *in vivo* matured bovine oocytes. We tested the hypotheses that a) *in vivo* matured bovine oocytes obtained from aged follicles (84 h gonadotropin starvation after 4-day FSH treatment) have a decrease in mitochondrial number, an altered distribution and a decrease in cytoplasmic ATP content compared to those obtained at the end of superstimulatory protocol (4-day or 7-day FSH treatment) and b) *in vivo* matured oocytes from old cows have a reduction in number of mitochondria, an altered distribution of mitochondria and a decrease in the ATP content compared to those from young cows.

6.3 Materials and methods

All animals were maintained at the University of Saskatchewan Goodale Research Farm (52^0N and 106^0W), placed in corrals, and fed alfalfa hay and barley silage with free access to fresh water and mineral blocks. The experimental protocol was approved by the University Committee on Animal Care and Supply and conducted in accordance with the guidelines of the Canadian Council on Animal Care.

6.3.1 Follicular aging: experimental design and protocol

The study was conducted on pubertal Hereford heifers (n=14) during the months of August to November. The heifers were between 14 to 20 months of age. Heifers were assigned randomly to three treatment groups as in Chapter 5: Short FSH treatment (n=5), FSH starvation (n=5) and long FSH (n=4) groups based on the length of FSH treatment

and duration between the last FSH treatment and subsequent LH treatment (Figure 5.1). Only exception in the protocol was that animals were ovariectomized by colpotomy at 18-20 h after LH administration, and ovaries were immediately brought to the laboratory for follicular aspirations of follicles >8 mm. Follicular aspiration was done with 18-gauge needle attached to a 6 ml syringe previously rinsed with 5% new born calf serum (CS, Invitrogen Inc., Burlington, ON, Canada) in DPBS (Invitrogen Inc.). All collected COCs were searched under a stereomicroscope and given 3 washings in DPBS plus 5% CS and processed for grading.

6.3.2 Maternal aging: experimental design and protocol

Young (4 to 10 yrs) and old (13 to 22 yrs) Hereford cows (n=7 each) were superstimulated using a 4-day protocol as mentioned in chapter 5 for the short FSH group (Chapter 5), with few exceptions (Figure 6.1). Six days after detected spontaneous ovulation (using ultrasound), all follicles >5mm were ablated to synchronize a new wave emergence. A day later (day of wave emergence, Day 0), FSH treatment was initiated in presence of a CL from previous ovulation. Two injections of PGF (at 12 hour interval) were given on Day 3.5 and LH was given 24 hours later. The animals were prepared for follicular aspiration a day later, as described previously in section 5.3.2 of chapter 5.

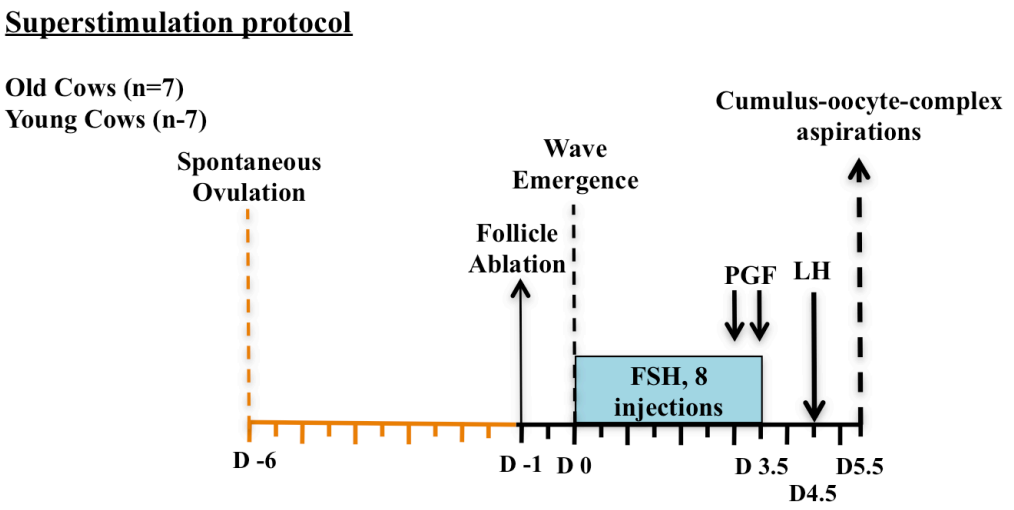

Figure 6.1 Supertimulation protocol applied to mother-daughter pairs (n=7). PGF = prostaglandin F2α; FSH = Follicular Stimulating Hormone; LH = Lutropin. FSH injections were administered at 12 h intervals. Follicles Transvaginal ultrasound guided follicular aspirations was done 18-20 h after LH administration to collect the COCs from the follicles ≥8 mm antral diameter**.**

6.3.3 Grading of COCs

The COCs collected from each animal were categorized as compact and expanded. The COCs were further graded as Grade 1, 2, 3 and 4 as mention previously in chapter 5 (section 5.3.3). The COCs were then denuded in a droplet of hyaluronidase (0.5% in Ca^{2+} and Mg^{2+} free DPBS, Invitrogen Inc). Denuded oocytes were either kept for mitochondrial staining or individually snap frozen in liquid nitrogen for ATP assay.

6.3.4 ATP assay

The total ATP content of the denuded *in vivo* matured oocytes was carried out using Bioluminescent Somatic Cell Assay Kit (Bioluminescent Somatic Cell Assay Kit, FL-ASC) as per manufacturer's guidelines with some modifications. The denuded oocytes meant for ATP assay were stored individually at -80^{0}C in 50 µl of ATP sample buffer

(99.0 mM NaCl, 3.1 mM KCl, 0.35 mM NaH_2PO_4, 21.6 mM Na-lactate, 10.0 mM Hepes, 2.0 mM $CaCl_2$, 1.1 mM $MgCl_2$, 25.0 mM $NaHCO_3$, 1.0 mM Na-pyruvate, 0.1 mg/ml gentamicin, and 6.3 mg/ml BSA) (Stojkovic et al., 2001). Briefly, all reactions were carried out on ice and in darkness. To each tube of sample or standard tube, 50 µl of ice-cold ultrapure water (Nanopure Diamond, Barnstead Intl. Dubuque, Iowa, USA) and 100 µl of FLSAR (Somatic Cell ATP Releasing reagent) were added and contents mixed and tube placed on ice. Subsequently, undiluted ice-cold assay mix was added, contents mixed and readings were taken within 5 seconds. The readings for each sample were taken with a luminometer (20/20n single tube Luminometer, Turner Biosystems) over a 10 second period. A six-point standard curve (40 fmol to 125 pmol) was included at the start and the end of each assay. The ATP content each sample was determined from linear regression equation of the standard curve. Quality control samples were prepared by adding three denuded immature oocytes to sample buffer. After adding 100 µl of FLSAR, neat, 3x diluted and 20x dilutions of quality control were run at least four times in an assay to represent the high, medium and low reference samples for calculation of coefficient of variations. The coefficient of variation for high, medium and low standards were 7.1%, 6.5% and 3.8%, respectively.

6.3.5 Processing of COCs for mitochondrial staining

Denuded oocytes were given 3 washings in 1X Dulbecco's Phosphate Buffered Saline (DPBS; Invitrogen Inc., Burlington, ON, Canada), supplemented with 5% new-born calf serum (CS; Invitrogen Inc.). Following washing, oocytes were incubated in maturation medium TCM-199 (Invitrogen Inc.) for 10 minutes. Oocytes were then incubated in 300 nm MitoTracker Deep Red FM (M22426, Molecular Probes, Invitrogen

Corporation, Grand Island, NY, USA) prepared in TCM-199 for 30 minutes (5% CO_2, 100% humidity, 38.5^0C). The oocytes were washed in DPBS (thrice, 5 minutes each) and immediately fixed in 4% paraformaldehyde solution at room temperature for 1 hour. Fixed oocytes were stored in 1.5 ml centrifugation tubes filled with DPBS and covered with aluminum foil to prevent drying and photobleaching.

Oocytes were mounted in Vectashield Mounting Medium containing DAPI (Vector Laboratories Inc., Burlingame, CA, USA) drops in glass bottom petri plates. Oocytes were imaged with Zeiss LSM 710 confocal microscope (63x 1.4 oil objective lens, He Ne 633 laser, excitation: 645 nm, emission: 665-685 nm) to obtain3D volume sets. Under the confocal microscope, we located the closest point of ooplasm to the cover glass (Z=0 micron) and imaged ooplasm from 20 micron to 40 micron to obtain a 20 micron thick 3D volume set (voxel size: 0.1x0.1x0.2 microns). Images were captured using 0.42 µsec pixel dwell time and with two lines averaging. The gain and offset settings were kept same but the laser power was varied such that few pixels in the focal plane were saturated.

6.3.6 Image processing, segmentation of 3D volume sets and bioimage informatics

Due to a sudden drop in the intensity in last 10 micron of the 3D-volume sets in the pilot trial due to photobleaching, only first 10-micron thickness along the Z-direction of the 3D stack was used for image analyses. We use these z-stacks to identify mitochondria and their clusters in order to obtain quantitative data regarding their number, distribution pattern and activity. The changes in mitochondrial membrane potential were assessed by average intensities (±SE) of Mitotracker DR fluorescence and size of mitochondrial by average number of voxels (±SE) of individual mitochondria and mitochondrial clusters.

Oocyte volume sets were subjected to 3-D deconvolution as mentioned in the section 5.3.5 of chapter 5. Deconvolved images were further processed in Imaris Pro 7.4 C1 package containing Imaris Track, Imaris Coloc, Imaris XT, Imaris Cell and Vantage modules (Bitplane AG, Badenerstrasse, Zürich, Switzerland). Italicized terms in the remainder of the paragraph indicate the Imaris-specific terminology. A *surface* was created manually to represent the oocyte plasma membrane. The *outside of surface* intensities was set to zero in order to mask out the volume that represented ooplasmic volume. The masked out volume was used to create *variable size spots* that represented mitochondrial intensities using following filters; *estimated diameter* set to 1 μm, *background substraction* and *region of growing* based on *local contrast*. The *spots to spots distance* extension of XT module was used to estimate the distance between the centers of the *spots. Spots* within 2-micron distance of each other were identified using the *distmin* filter. Further, these *spots* were filtered based on volume to identify clusters. Thus *spots* or groups of *spots* that were within 2-micron distance to each other and volume $\geq 2\ \mu m^3$ were considered as the clusters. Remaining *spots* were classified as individual mitochondria (Figure 6.2). Both individual mitochondria and clusters combined are termed as total structures in rest of the text. The distribution of mitochondria and clusters in the peripheral (ooplasm within 10μm of distance from the oocyte plasma membrane) and central regions (remaining ooplasm) was identified based on the *distance-transformed channel* created based on the *surface*. The filters within Imaris Pro were used to generate quantitative data for statistical comparison. Following end points were compared; number, average intensity, average number of voxels and proportion of individual mitochondria and clusters within the peripheral and central

regions of ooplasm. A MIP-image (maximum intensity projection image) from 2-micron z-stack (10 images) was used to determine the distribution pattern of mitochondrial intensities within the ooplasm. The pattern was defined based on the location of mitochondria within the ooplasm, proximity between the mitochondria and location of mitochondria around vacuoles into scattered/clustered/peripherally clustered, and perivacuolar/perivacuolar clustered patterns (Figure 6.3).

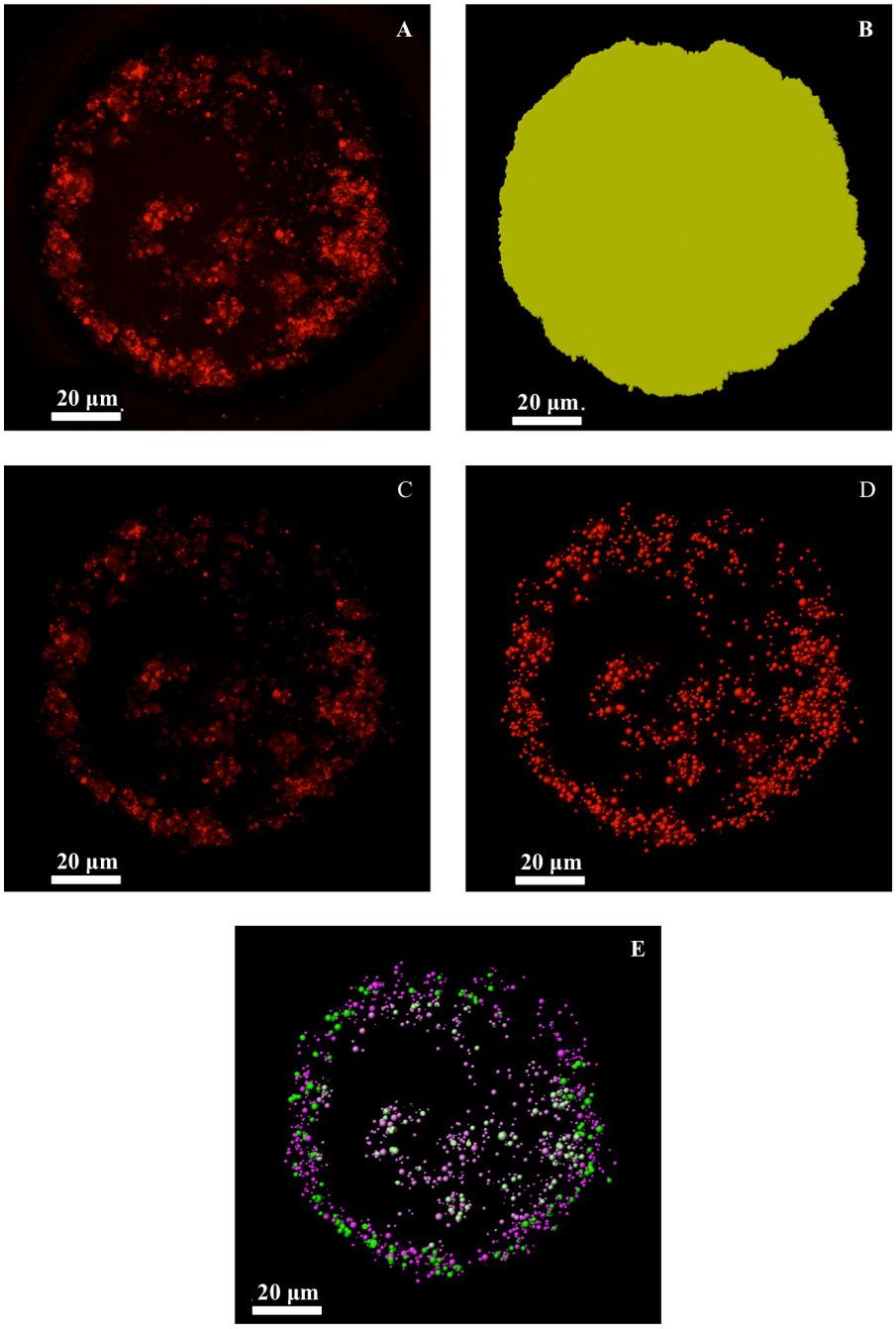

Figure 6.2 Pictures depicting steps of segmentation in Imaris Pro 7.4.2 to identify individual and clustered mitochondria. 3D-deconvolved 10 micron z-stack was imported into Imaris (Maximum intensity projectionA), *surface* was generated to identify ooplasmic membrane (B) and create a *masked channel* with outside set to 0 (C). *Spots* (D) were created using intensities to identify mitochondria. (E) Final segmented image showing peripheral (dark color) and central (light color) localization of individual mitochondria (purple) and mitochondrial (clusters green).

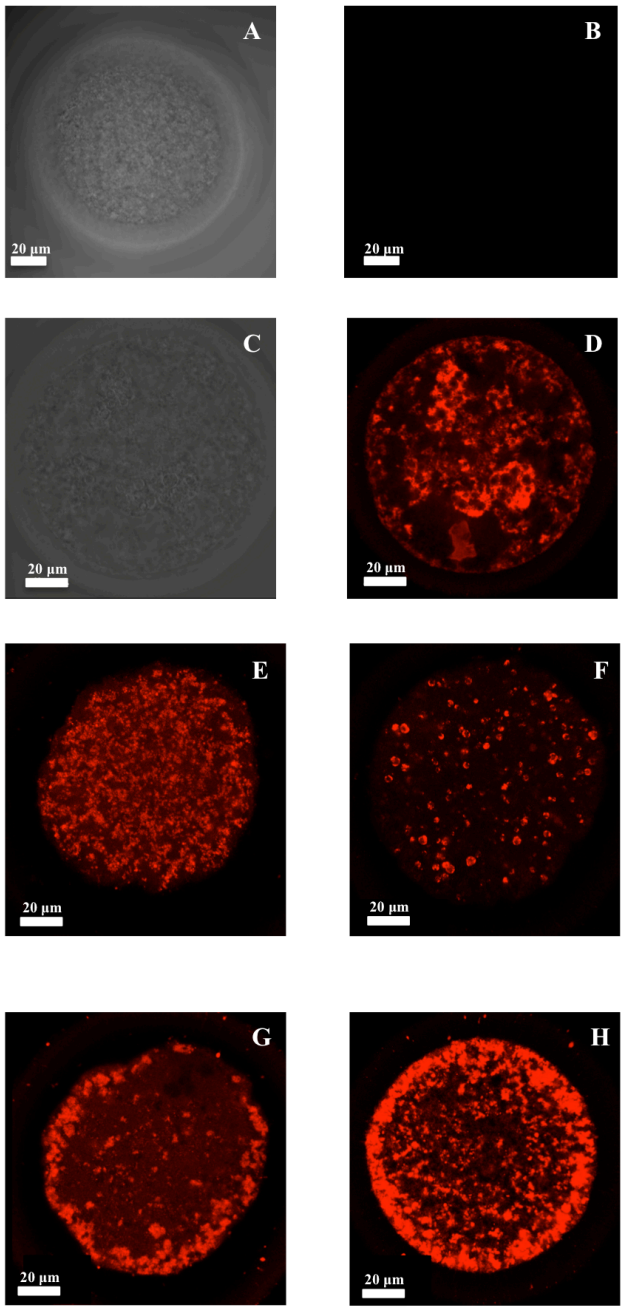

Figure 6.3 Confocal microscopy showing mitochondrial distribution patterns observed in oocytes stained with Mitotracker Deep Red FM (D to H). Unstained negative control oocyte show no mitochondrial staining (A, Transmission light and B, He Ne 633 nm laser). Oocytes showing perivacoular clustered (C, Transmission light and B, He Ne 633 laser), uniformly scattered (E), perivacoular (F), peripherally clustered (G) and uniformly clustered (H) distribution patterns. Confocal images represent maximum intensity projection of 2 micron z-stack

6.3.7 Statistical analyses

All statistical analyses were performed using the Statistical Analysis System software package (SAS 9.2; SAS Institute Inc., Cary, NC, USA) and probabilities ≤0.05 were considered significant. The effect of superstimulatory treatment (short FSH, FSH starvation and long FSH) and age on proportions of grades of COCs and categories of mitochondrial distribution patterns was compared by Fisher's Exact test and Chi-square test using Proc Frequency procedure. The data for mitochondrial number, average intensities and average number of voxels were compared by analysis of variance or t-test. The number of follicles in different size categories was compared with Non-parametric ANOVA using Kruskal Wallis test. The proportion of COCs collected to follicles aspirated and the proportion of mitochondrial numbers within different regions of oocytes were arcsine transformed and then subjected to ANOVA for comparisons. The Fisher's least square difference was used as post-hoc test if the P-vlaue for the main effect was ≤0.05.

6.4 Results

6.4.1 Follicular Aging: collection efficiency and grades

Irrespective of groups, the overall COC yield through transvaginal ultrasound guided-follicular aspiration was 54.1% (164/303) and did not differ (P=0.79) across the treatment groups (Table 6.1). One, 14 and four oocytes from the Short FSH, FSH starvation and Long FSH groups were lost before grading and remaining COCs were used for analyses (Table 6.1). The short FSH group and FSH starvation groups had significantly (P<0.01) more compact COCs compared to the long FSH group. Within the

expanded COCs, the short and long FSH groups had significantly (P=0.02) higher proportion of Grade 1 COCs than the FSH starvation group (table 6.1). While the proportion of expanded Grades 2 and 3 combined did not differ (P=0.35) across the treatments, the proportions of expanded grade 4 were highest in FSH starvation group, intermediate in short FSH group and lowest in the long FSH group (P<0.01).

Table 6.1 Percent collection efficiency and proportion (percent) of different grades of COCs obtained from follicles aspirated at 18-20 h after LH administration. N= number of animals analyzed for each group.

Grades	**Short FSH (n=5)**	**FSH Starvation (n=5)**	**Long FSH (n=4)**
Total COCs collected/Total follicles aspirated (Percent collection efficiency)*	25/51 (49.0%)	85/153 (55.5%)	54/99 (54.5%)
Compact COCs	9/24 (37.5%)[a]	32/71 (45.1%)[a]	0/50 (0%)[b]
Expanded COCs	15/24 (62.5%)[a]	39/71 (54.9%)[a]	50/50 (100±0%)[b]
Expanded Grade 1	6/15 (40.0%)[a]	5/39 (12.8%)[b]	19/50 (38.0)[a]
Expanded Grades 2 + 3	4/15 (26.7%)	16/39 (41.0%)	24/50 (48.0%)
Expanded Grade 4	5/15 (33.3%)[a,b]	18/39 (46.2%)[a]	7/50 (14.0%)[b]

[ab] Values with different superscripts are different (P<0.05).
Grades were compared separately.
*Non-parametric ANOVA using Kruskal Wallis test analysis was done on arcsine transformed proportions of follicles in different groups.

6.4.2 Follicular Aging: total ATP content

A total of 12, 30 and 21 oocytes from the short FSH, FSH starvation and long FSH groups were used for the analyses of ATP content in oocytes. On average, the total ATP content (±SEM) of *in vivo* matured oocyte was 21.2±2.4 pmol and was not different

(P=0.28) across the three superstimulation treatments. The total ATP content did not differ (P=0.49) when the oocytes from compact COCs were compared across the groups (Figure 6.4A). However, the total ATP content of the oocytes from the extended COCs in the long FSH group tended to be more (P=0.09) than the short FSH and not different from the FSH starvation groups (Figure 6.4B).

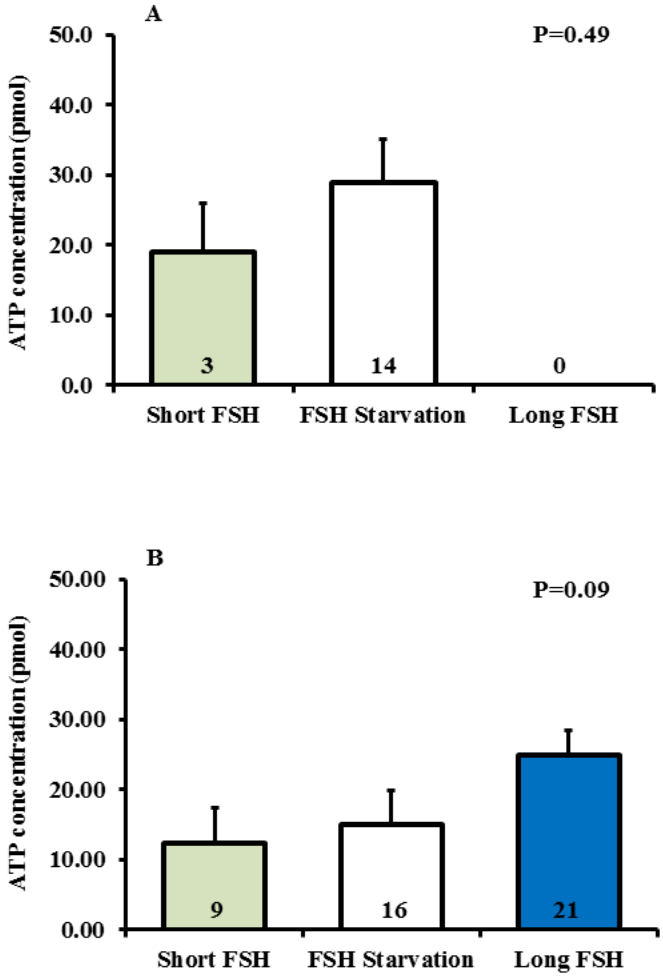

Figure 6.4 Total ATP content (mean±SE) in the oocytes from compact and extended COCs of Short FSH, FSH starvation and Long FSH groups. Both compact and extended COCs included all grades. The Long FSH group had no compact COCs. [ab] Values with different superscripts are different (P<0.05).

6.4.3 Follicular aging: mitochondrial population and distribution pattern

Five patterns of mitochondrial distribution were recognized uniformly scattered, uniformly clustered, peripherally clustered, perivacuolar and perivacuolar clustered (Figure 6.3). The proportion of the oocytes with uniformly scattered distribution ($P<0.01$) was highest in long FSH group compared to other two groups (Table 6.2). While FSH starvation group had highest proportion ($P<0.01$) of oocytes with perivacuolar clustered distribution of mitochondria compared to oocytes from other two groups (Table 6.2). The proportion of other distribution patterns did not differ ($P>0.32$) across the treatment groups.

Table 6.2 Proportion of oocytes from Short FSH, FSH starvation and Long FSH groups different distribution pattern of mitochondria within the ooplasm. N= number of oocytes analyzed for each group.

Distribution Pattern	**Short FSH (n=5)**	**FSH Starvation (n=32)**	**Long FSH (n=20)**
Uniformly Clustered	3/5 (60%)	13/32 (41%)	5/20 (25%)
Peripherally clustered	1/5 (20%)	2/32 (6%)	1/20 (5%)
Uniformly Scattered	1/5 (20%) [a]	1/32 (3%) [a]	10/20 (50%) [b]
Perivacuolar	-	-	3/20 (15%)
Perivacuolar clustered	-	16/32 (50%) [a]	1/20 (5%) [b]

[ab] Values with different superscripts are different ($P<0.05$).

Effects of different superstimulation protocols on the number, proportion and central/peripheral localization of individual mitochondria and clusters are shown in Table 6.3. On an average there were 2143±142 mitochondrial structures (individual mitochondria and mitochondrial clusters combined) per 10-micrometer thickness of the ooplasm irrespective of the superstimulation protocol used and did not differ ($P=0.29$)

across the treatment groups. The mean number of individual mitochondria and mitochondrial clusters did not differ across the treatment groups ($P>0.30$). The long FSH group tended to have higher ($P=0.08$) mean number of individual mitochondria in the peripheral ooplasm compared to FSH starvation group but was not different from the short FSH group. The average number of mitochondrial clusters in the peripheral ooplasm tended to be higher ($P=0.09$) in the FSH starvation group compared to short FSH group but was not different from the long FSH group. However, there were no differences in the mean number of individual mitochondria and mitochondrial clusters when the central region of ooplasm was compared across the three treatments ($P>0.48$). Overall, the proportion of individual mitochondria ($P=0.01$) was the least and that of mitochondrial clusters ($P=0.01$) was the highest in the FSH starvation group compared to short and long FSH groups. The relative proportions of individual mitochondria and clusters in the peripheral and central regions did not differ ($P>0.61$) between the treatments.

Table 6.3 Effect of superstimulatory treatment on the mean (±SEM) number, proportion, and distribution of individual mitochondria and clusters within the oocyte. N= number of oocytes analyzed for each group. Imaged volume of oocyte refers to the 10 micron Z-stack of oocyte that was used for analysis. [ab] Values with different superscripts are different (P<0.05).

Endpoints	**Short FSH (n=5)**	**FSH Starvation (n=32)**	**Long FSH (n=20)**
Total Structures	1997±556	1976±161	2447±277
Individual Mitochondria: Imaged volume			
Average number	1786±501	1662±135	2099±228
Proportion of total structures	0.89±0.03[a]	0.84±0.01[b]	0.87±0.01[a]
Individual Mitochondria: Peripheral region of imaged volume			
Average number	660±145	685±41	864±78
Proportion of total individual mitochondria	0.41±0.04	0.44±0.02	0.45±0.03
Individual Mitochondria: Central region of imaged volume			
Average number	1126±361	977±119	1236±188
Proportion of total individual mitochondria	0.59±0.04	0.56±0.02	0.55±0.03
Mitochondrial clusters: Imaged volume			
Average number	211±70	314±28	347±56
Proportion of total structures	0.11±0.03[a]	0.16±0.01[b]	0.13±0.01[a]
Mitochondrial clusters: Peripheral region of imaged volume			
Average number	79±16	137±8	135±15
Proportion of total clusters	0.46±0.07	0.47±0.03	0.43±0.04
Mitochondrial clusters: Central region of imaged volume			
Average number	132±55	177±24	212±44
Proportion of total clusters	0.54±0.07	0.53±0.03	0.57±0.04

6.4.4 Follicular aging: Mitochondrial activity and size

Both individual mitochondria and clusters in oocytes from Long FSH and FSH starvation groups had twice the relative intensity compared to the short FSH group (Figure 6.5; $P<0.01$). The average volume of individual mitochondria indicated by average number of voxels was biggest (Figure 6.5; $P=0.02$) in the FSH starvation group compared the other two groups. The average volume of clusters was smaller (Figure 6.5; $P=0.02$) in long FSH group than the FSH starvation groups, while average size of clusters in short FSH group was not different from other two groups.

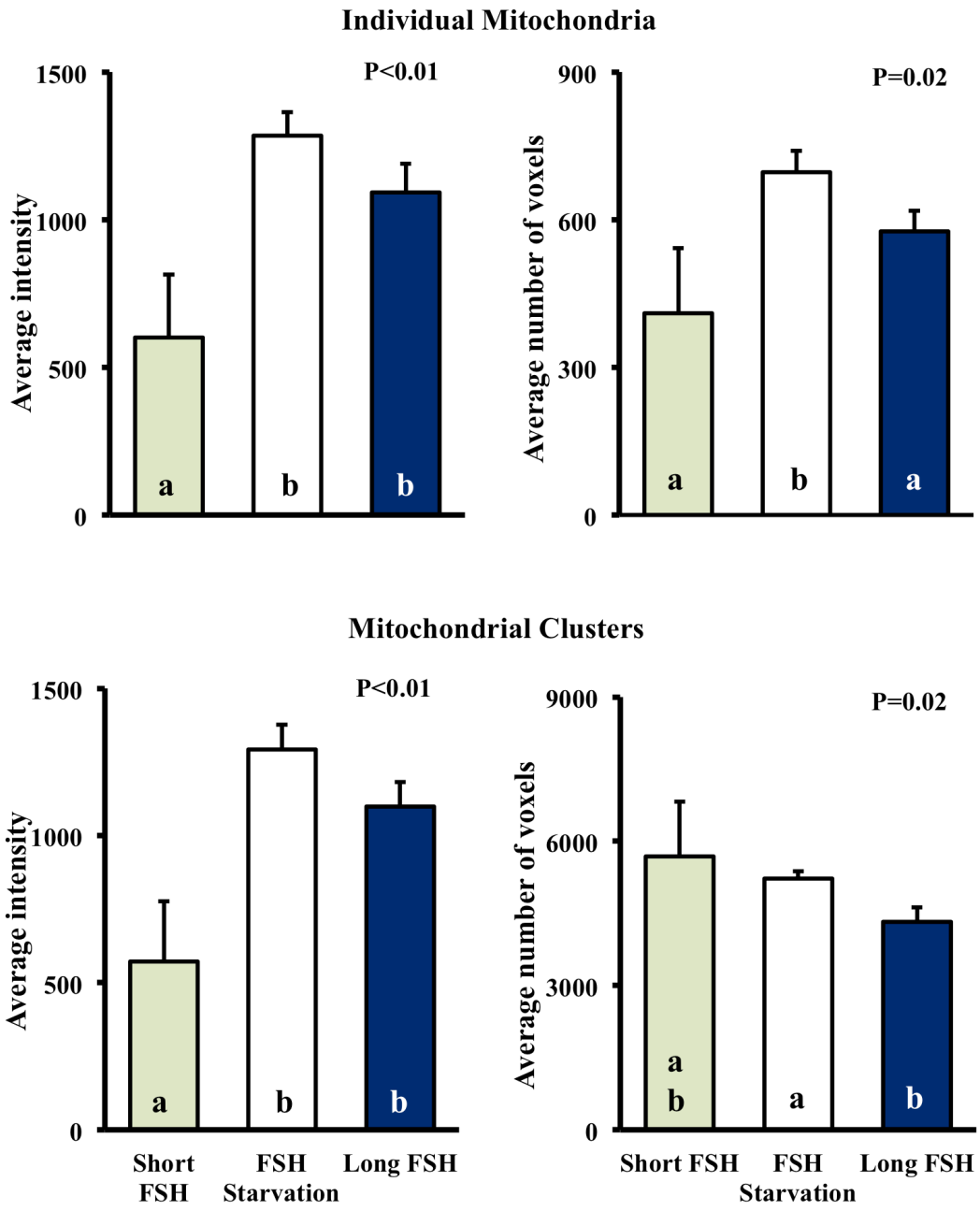

Figure 6.5 Average intensity (±SE) and average number voxels (±SE) in individual mitochondria and clusters in the oocytes from COCs of Short FSH (n=5), FSH starvation (n=30) and Long FSH (n=12) groups. [ab] Values with different superscripts are different (P<0.05).

6.4.5 Maternal Aging: collection efficiency and grades

Two daughters and one mother were removed from further analyses, as they did not yield any COC. The overall COC yield through transvaginal ultrasound guided-follicular aspiration was 49.6% (178/359) and did not differ (P=0.80) across the treatment groups (Table 6.4). Five and three COCs from the young and old cow groups were lost before grading and remaining COCs were used for analyses. The proportion of compact or expanded COCs did not differ (P=0.40) between the young and old cows. Within the expanded COCs, the proportion of different grades did not differ between the groups (P=0.12 for Grade 1, P=0.74 for Grade 2 plus 3, P=0.12 for Grade 4).

Table 6.4 Percent collection efficiency and proportion (percent) of different grades of COCs obtained from follicles aspirated at 18-20 h after LH administration. N= number of animals analyzed for each group.

Grades	**Young Cows (n=6)**	**Old Cows (n=5)**
Total COCs collected/Total follicles aspirated (Percent collection efficiency)*	66/141 (46.8%)	112/218 (51.4%)
Compact COCs	8/61 (13.1%)	8/109 (7.3%)
Expanded COCs	53/61 (86.9%)	101/109 (92.7%)
Expanded Grade 1	25/53 (47.2%)	34/101 (33.7%)
Expanded Grades 2 + 3	23/53 (43.4%)	47/101 (46.5%)
Expanded Grade 4	5/53 (9.4%)	20/101 (19.8%)

* Five and three COCs were lost before grading. * Non-parametric ANOVA using Kruskal Wallis test analysis was done on arcsine transformed proportions of follicles in different groups.

6.4.1 Maternal aging: total ATP content

A total of 28 and 49 oocytes from the young and old cow groups were utilized for the analyses of total ATP in oocytes**.** Irrespective of the grades, the total ATP content in mothers was significantly less in the old cows compared to the young cows (27.4±1.9 pmol vs 35.7±2.2 pmol, P<0.01). The ATP in oocytes from compact COCs did not differ across the two groups Figure 6.6A). The *in vivo* matured oocytes from expanded COCs of superstimulated cows had significantly less (P<0.01) total ATP than the young cows (Figure 6.6B).

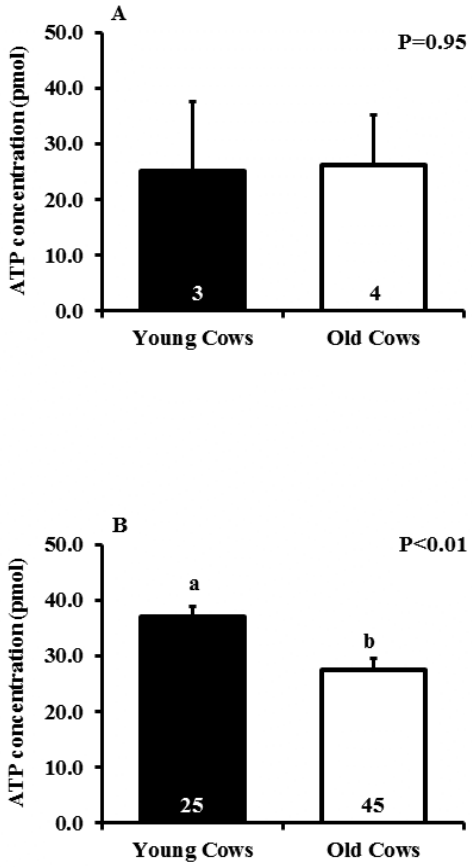

Figure 6.6 Total ATP content (mean±SE) in the oocytes from compact (A) and expanded (B) COCs of mother and daughter groups. Both compact and expanded COCs included all grades. [ab] Values with different superscripts are different (P<0.05).

6.4.6 Maternal aging: mitochondrial population

The proportion of mitochondrial distribution patterns did not differ (P>0.18) between the oocytes from two groups (Table 6.5). A total of nine and 15 oocytes from young and old cows, respectively, did not show detectable fluorescent signal. As a result, 24 and 45 oocytes from young and old cows, respectively, were processed for image analysis. Out of these, 4 and 3 oocytes from the young and old cows were from compact COCs and therefore not used for further analysis. The following quantitative comparison is based on 20 and 42 oocytes from the young and old cow groups, respectively. Comparison of numbers and proportions of individual mitochondria and clusters in the *in vivo* matured oocytes from young and old cows are given in Table 6.6. Combined number of individual mitochondria and clusters were similar (P=0.54) in oocytes from both groups. The number of mitochondria did not differ (P>0.42) between the groups when either imaged ooplasmic volume or peripheral and central regions were compared. The oocytes from older cows tended to higher number (P=0.06) and proportion of clusters (P=0.06) compared to oocytes from younger cows. The number of clusters in the central region of oocytes from old cows was greater than oocytes from young cows (P=0.04). Conversely, number and proportion of clusters in the peripheral region of oocytes from young and old cows were not different (P>0.12).

Table 6.5 Proportion of oocytes from young and old cows with different distribution pattern of mitochondria within the ooplasm. N= number of oocytes analyzed for each group.

Distribution Pattern	**Young Cows (n=20)**	**Old Cows (n=42)**
Uniformly Clustered	-	6/42 (14%)
Peripherally clustered	2/20 (10%)	1/42 (2%)
Uniformly Scattered	2/20 (10%)	2/42 (5%)
Perivacoular	4/20 (20%)	17/42 (41%)
Perivacoular clustered	9/20 (45%)	16/43 (38%)
Uncharacterized*	3/20 (15%)	-

[ab] Values with different superscripts are different ($P<0.05$).
*Some oocytes had distribution pattern that fell in between the identified distribution pattern.

Table 6.6 Mean (±SEM) number and proportion of individual mitochondria and clusters within the oocyte of superstimulated young and old cows. N= number of oocytes analyzed for each group. Imaged volume of oocyte refers to the 10 micron Z-stack of oocyte that was used for analysis.

Endpoints	**Young Cows (N=20)**	**Old Cows (N=42)**
Total Structures	1647±144	1774±126
Individual Mitochondria: Imaged volume		
Average number	1493±135	1572±112
Proportion of total structures	0.90±0.01	0.88±0.01*
Individual Mitochondria: Peripheral region of imaged volume		
Average number	715±48	683±40
Proportion of total individual mitochondria	0.52±0.04	0.46±0.01
Individual Mitochondria: Central region of imaged volume		
Average number	778±109	889±79
Proportion of total individual mitochondria	0.48±0.04	0.54±0.01
Mitochondrial clusters: Imaged volume		
Average number	154±18	202±17*
Proportion of total structures	0.10±0.01	0.12±0.01*
Mitochondrial clusters: Peripheral region of imaged volume		
Average number	85±10	102±9
Proportion of total clusters	0.59±0.04	0.52±0.02
Mitochondrial clusters: Central region of imaged volume		
Average number	69±18 [a]	100±9 [b]
Proportion of total clusters	0.41±0.04	0.48±0.02

[ab] Values with different superscripts are different (P<0.05).

* Values tended to be different between the groups.

6.4.7 Maternal aging: average intensities and voxel numbers of mitochondria

The mean intensities and of individual mitochondria and clusters within the oocytes did not differ with the age of cow (Figure 6.7). The average volume of individual mitochondria indicated by average number of voxels was significantly higher (P=0.05) in old cows compared to young cows (Figure 6.7). However, oocytes from two groups did not differ with regards to the average number of voxels in the clusters (P=0.33).

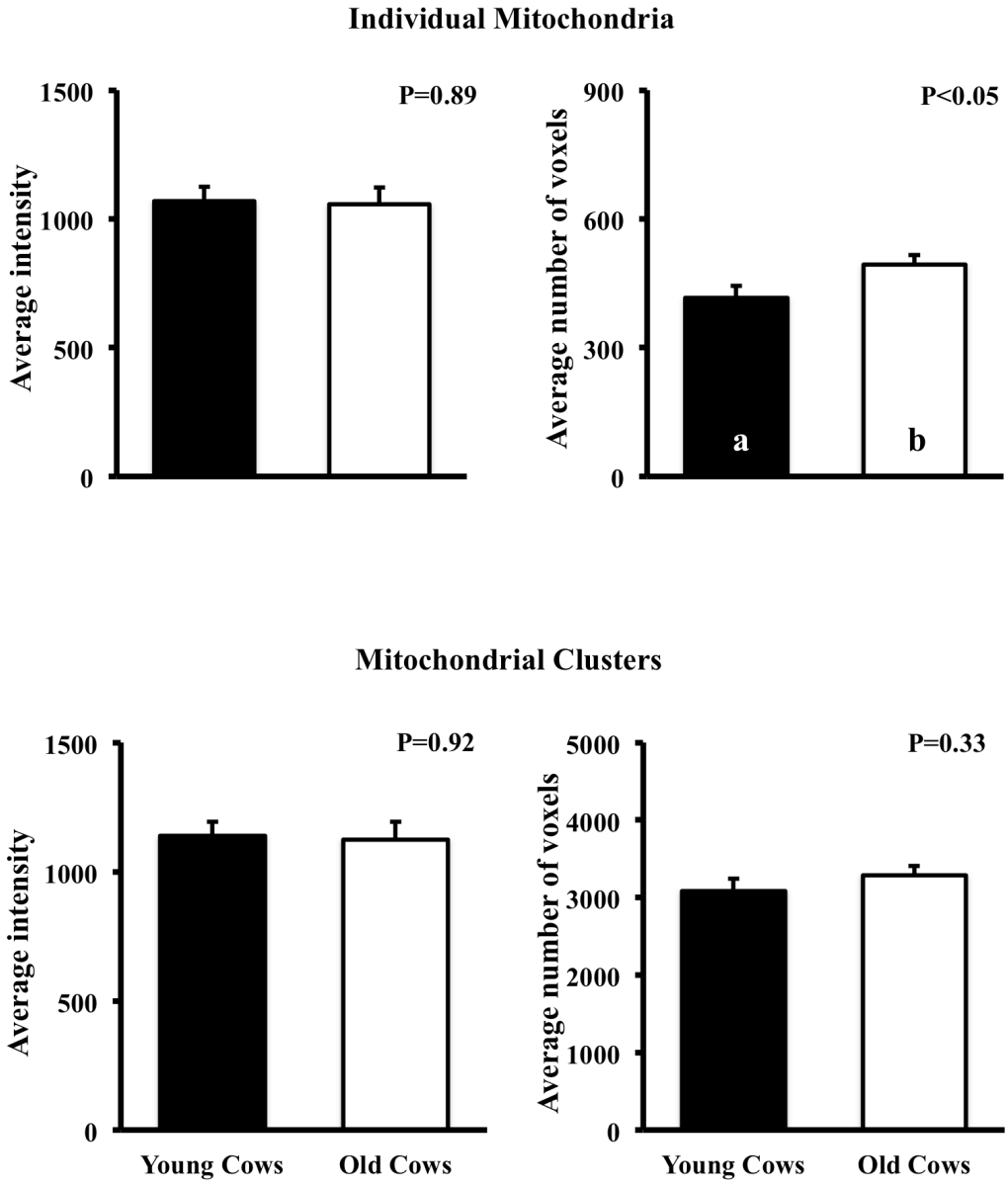

Figure 6.7 Mean intensity (±SE) and mean number of voxels (±SE) in individual mitochondria and clusters in the oocytes from COCs of young (N=20) and old cows (N=42). ab Values with different superscripts are different (P<0.05).

6.5 Discussion

FSH starvation of 84 h negatively affects the quality of *in vivo* matured oocytes that have higher proportion of mitochondrial clusters compared to short and long FSH groups. The ATP content of oocytes is not affected by duration of FSH treatment or FSH starvation. Both longer FSH protocol and FSH starvation result in an increased intensity of both individual and clustered mitochondria compared to short FSH protocol. Maternal aging did not affect the grades of *in vivo* matured oocytes obtained following superstimulation. However, *in vivo* matured oocytes from older cows have less ATP content than the younger cows that could be the reason for poor oocyte competence with advancing age.

Consistent with recent findings from a parallel study (Fernanda et al, unpublished data), an 84 h starvation is detrimental for oocyte quality as higher proportion of lower grade COCs are obtained compared to 4-d and 7-d FSH superstimulation protocols. Further, a major proportion of these oocytes fail to resume meiosis and undergo atresia indicated by accumulation of large lipid droplets (Chapter 5). In that regards, completion of nuclear maturation is not considered vital for acquisition of oocyte competence but is essential for fertilized ovum to proceed beyond 2 cell stage (Eppig, 1996). When *in vivo* matured COCs from starvation group were fertilized and cultured *in vitro*, very few of them cleaved and reached blastocyst stage compared to those from 4-day and 7-day superstimulation protocols (Fernanda et al, unpublished data).

Overall cytoplasmic ATP content of the oocytes from the present study is higher than those reported in previous studies on bovine oocytes (Stojkovic et al., 2001; Nagano et al., 2006). The difference might be due to the maturation status of the oocytes as

oocytes were matured *in vivo* in the present study compared to the *in vitro* matured in the above-cited studies. Poor quality bovine oocytes have been shown to have less ATP stores that at least in part negatively affect their ability to develop into embryos (Stojkovic et al., 2001). However, the notion was not supported in our study as oocytes from FSH starvation group had ATP content similar to short and long FSH groups. It has been shown that oocytes with darker cytoplasm have higher ATP content but poor developmental competence (Nagano et al., 2006). Such oocytes were categorized as Grade 3 (with less darker ooplasm) or 4 (with more darker ooplasm) in our study. FSH starvation group had more of these grades and about half of them had higher ATP content. Other reason for the failure to detect differences in ATP content of oocytes across the treatment groups could be due to less number of oocytes analyzed in the present study.

No differences were found between the oocytes from the three superstimulation groups with regards to the number, proportion and distribution of individual mitochondria. In a parallel study, we have observed that oocytes from FSH starvation are less competent to undergo fertilization and subsequent development. In contrast to our findings, previous reports have observed low mitochondrial numbers were related to poor fertilization rates in pigs (El Shourbagy et al., 2006) and humans (Reynier et al., 2001). However, these studies used mitochondrial DNA copy number as a method to quantify mitochondria. The number of mitochondrial DNA copy per mitochondria in oocyte is a matter of controversy and could result in wide variation in results. Moreover, studies have shown that it is the clustering of mitochondrial that reflects into ATP production (Van Blerkom et al., 1995; Wilding et al., 2001). Interestingly greater proportions of

mitochondrial clusters were present in the starvation group compared to other two groups (Table 6.3), despite our previous observation that majority of oocytes from starvation group fail to undergo nuclear maturation (Chapter 5). Our observation is in contrast to findings of a previous study that reported a decreased mitochondrial cluster formation in oocytes undergoing failure of nuclear maturation (Machatkova et al., 2011). The question remains why the oocytes from the FSH starvation group had bigger mitochondrial clusters than the long FSH group despite showing a tendency to have lower ATP content. A possibility is that these clusters in oocytes from FSH group are indicative of impending apoptosis in oocytes undergoing atresia. It has been shown that mitochondrial clustering occured following over expression of mitochondrial fusion proteins (Huang et al., 2007). These clusters contained the fragmented mitochondria, resulting in mitochondrial dysfunction and cell death (Huang et al., 2007). If mitochondrial clustering in oocytes from FSH group is indicative of mitochondrial dysfunction, then the average mitochondrial intensity should have been lower in the starvation group compared to other groups in the present study. However, individual mitochondria and clusters in oocytes from the starvation group showed higher average intensities similar to oocytes from long FSH groups, indicating the mitochondrial are still functional. For long FSH group, increased mitochondrial activity of oocytes was reflected in numerically higher ATP contents than FSH starvation group. Other reason for increased uptake of Mitotracker Deep Red in oocytes from starvation group could be an increased oxidative stress in these oocytes as carbocyanine-based Mitotracker dyes have been found to show an increased labeling in neurons exposed to hydrogen peroxide (Buckman et al., 2001). Presumably an increase oxidative stress might be the reason why even the individual mitochondria in the

oocytes from starvation group had higher average intensity compared to those from other two groups.

COCs from older cows were not different from young cows as similar proportion of good quality COCs were obtained following 4-day superstimulation (Table 6.4). This observation is similar to as reported previously (Malhi et al., 2007). However, the *in vivo* matured oocytes from older cows had less intracellular ATP than those from young cows, which is contrary to a previous report wherein However, a recent *in vitro* study has reported a higher ATP content in oocytes obtained from older cows compared to those from young cows (Iwata et al., 2011). The aforementioned study, did not mention details of the grades of the COCs that were compared. It has been shown that oocytes from good quality COCs have more ATP content and that reflect in the better developmental competence of these COCs (Stojkovic et al., 2001). Moreover, differences do exist between the ATP content of oocytes obtained from slaughterhouse ovaries and oocytes obtained through ovum pick-up (Tamassia et al., 2004). ATP is needed for energy consuming processes such as cytoplasmic and nuclear maturation and fertilization. In that regards, old cows had similar or higher proportion of metaphase-II oocytes following superstimulation (Malhi, 2007). Furthermore, about two-third of the oocytes from old cows failed to undergo fertilization when oocyte competence were compared between the two groups (Malhi et al., 2007). It is possible that the oocytes from older cows have sufficient ATP to undergo nuclear maturation but not enough to complete fertilization. In that regards, human oocytes have been reported to mature over a wider range of ATP content but oocytes with >2pg/ml have better fertilization and developmental competence (Van Blerkom et al., 1995).

Despite having lower cytoplasmic ATP content, oocytes from older cows tended to have higher number and greater proportion of mitochondria as clusters compared to oocytes from young cows. However, the intensity within these clusters or even the individual mitochondria did not differ between the oocytes from two groups (Figure 6.7). This observation is in contrast to the findings that clustering of mitochondria is related to ATP production in oocytes (Van Blerkom et al., 1995; Wilding et al., 2001). The number and proportion of individual mitochondria in the oocytes did not differ between the two age groups. Previous reports have shown a decline in mitochondria number with advancing age when a different quantification method (mitochondrial DNA) was used in the study (Iwata et al., 2011). There is lack of information on number of mitochondrial DNA copy numbers in each mitochondrion and how that changes with advancing age.

In conclusion, FSH starvation of 84 h leads to more poor quality oocytes that have ATP contents similar to short FSH group. Further, organization of mitochondria as intense and bigger clusters within the oocytes from FSH starvation group might indicate oxidative stress and hence atresia. Maternal aging leads to decrease in cytoplasmic ATP content of *in vivo* mature oocytes despite no differences in mitochondrial population and distribution pattern.

CHAPTER 7

7 GENERAL DISCUSSION

Overall, the aim of studies included in the present thesis was to characterize functional and structural changes in bovine oocytes originating from follicles grown under different hormonal environment and physiological status of animal. First study was conducted to determine effect of hormonal environment during follicle growth on fertility in cattle (Chapter 3). Subsequently, experiment was done on oocytes collected at defined stages of dominant follicle growth of anovulatory wave and at the preovulatory stage of ovulatory wave to describe the alterations in organelle structure and their interrelationships (Chapter 4). In the next study, different superstimulation protocols with or without continued FSH support were used to determine the effect of duration of follicle growth on nuclear maturation and cytoplasmic maturation with respect to modulations in number and distribution of lipid droplets (Chapter 5). In the last experiment (Chapter 6), effects of follicular aging and maternal age on the energy status, and mitochondrial distribution and functioning within the *in vivo* matured oocytes were studied.

During ovulatory wave, the dominant follicle undergoes a continuous growth period until ovulation (Pierson and Ginther, 1988; Savio et al., 1988a; Sirois and Fortune, 1988; Knopf et al., 1989). The initial part of dominant follicle growth (6 days in 2-wave animal and 3 days in 3-wave animals) destined for ovulation occurs in presence of luteal levels of progesterone. While the remaining 2-3 days (known as proestrus) of dominant follicle growth occurs in initially decreasing and then basal levels of progesterone (Peters and Pursley, 2003). Maintaining subluteal-phase levels of progesterone (0.5-1.5 ng/ml)

during dominant follicle growth allowed follicles to reach bigger diameters at ovulation due to increase in LH pulsatility (Bigelow and Fortune, 1998; Jaiswal, 2007). My results (Chapter 3) support the finding that bigger preovulatory follicles result in larger and more functional CLs following ovulation (Robinson et al., 2005; Jaiswal, 2007). Contrary to the effects on follicular and luteal dynamics, the effect of subluteal-phase levels of progesterone on fertility has been a subject of debate. One group of studies has shown that subluteal-phase levels of progesterone during the dominant follicle growth, as seen during 1st wave, decreased the fertility (Savio et al., 1993; Bisinotto et al., 2010; Denicol et al., 2012). However, other groups have shown no adverse effect or advantage of creating subluteal-phase environment on subsequent fertility (Colazo et al., 2004b; Pfeifer et al., 2009; Cerri et al., 2011). My findings in beef cattle support the later group of studies and extend our understanding further. Cattle with luteal progesterone and normal proestrus duration had pregnancy rates similar to those with subluteal-phase levels of progesterone and normal duration of proestrus. However, if cattle with short duration of proestrus are compared, subluteal-phase levels of progesterone improve the fertility when tested against those with luteal levels. Recent experiments have also demonstrated that a longer proestrus period improved fertility rates when luteal-phase levels of progesterone during early part of first wave dominant follicle growth were provided (Bridges et al., 2008; Bridges et al., 2010). These studies and my study indicate that a progesterone-free period (proestrus) during final stages of dominant follicle is necessary for an oocyte to undergo certain changes crucial for attaining developmental competence. This notion is supported by another study, as subluteal-phase level of progesterone during superstimulation resulted in higher proportion of fertilized oocytes

without affecting subsequent development (Jaiswal, 2007). Other aspect that needs to be kept in mind while developing subluteal-phase progesterone-based protocols is the duration for which follicles are allowed to grow. It was observed that prolonged duration of subluteal-phase progesterone lead to untimely maturation of oocyte that adversely affected the pregnancy rates (Savio et al., 1993; Mihm et al., 1999). This attribute needs to be considered while comparing results across the studies. The duration for which subluteal-phase progesterone was maintained in my study is at least 1 day shorter than in previous studies (Bisinotto et al., 2010; Denicol et al., 2012) that demonstrated a negative effect of subluteal-phase progesterone on pregnancy rates.

The effect of subluteal-phase levels on improving fertility can be explained by its effect on the pattern of gonadotropin secretion (discussed above), the oocyte quality, on the sperm, or at the level of uterus. Subluteal-phase levels of progesterone have been shown to increase the estrogenic capacity of follicles due to increase in LH pulses (Bigelow and Fortune, 1998). LH was observed to affect the oocyte maturation process, while elevated estradiol in blood circulation (mainly derived from dominant follicle (Ireland et al., 1979) along with basal levels of progesterone at estrus could also affect oviductal transport of gametes (Mahmood et al., 1998), sperm capacitation (Adeoya-Osiguwa et al., 2003) and fertilization (Binelli et al., 1999). Thus, the level at which subluteal-phase progesterone acts to improve or reduce fertility is yet to be determined.

Studies have shown that *in vivo* matured oocytes performed better in terms blastocyst rates when compared to *in vitro* matured oocytes from a heterogeneous population (3-8mm) of follicles (Dieleman et al., 2002). It has also been shown that follicles >8 mm have better blastocyst rates during IVF than those in the range of 3-7 mm

(Hendriksen et al., 2000). Furthermore, oocytes matured *in vivo* produced higher proportion of hatched blastocysts after IVF in comparison to oocytes that were matured *in vitro,* despite having similar duration of *in vivo* growth (Hendriksen et al., 2000). These findings indicated that oocytes undergo certain cytoplasimc changes during the growth of the follicle before LH surge and completed after LH surge, which influence the subsequent developmental competence. In one study (Chapter 4), we used ultrasound to montor the growth of dominant follicle following its selection to collect oocytes from definite stages of growing, static and regression phases of anovulatory wave 1 and preovulatory stage of ovulatory wave. My study involved use of quantitative evaluation of morphology and distribution pattern of organelles based on stereological principles in order to remove bias that is inherent to qualitative observations.

The growing stage follicles are 9-11 mm in size on Day 3 of 1st wave (day of ovulation = Day 0) and these highly estrogenic follicles are just past the step of dominant follicle selection (Badinga et al., 1992; Singh et al., 1998). My results (Chapter 4) showed that these oocytes have had least surface area of contact between mitochondria and lipid droplets compared to all other stages of follicle development. The functional importance of this finding need to be studied in future studies. It is plausible that this change in mitochondrial contact with lipids is reflective of a gradual shift in dependency of oocyte on lipids for ATP generation as the follicle differentiates from growing phase to other phases. The granulosa cells in growing phase follicle have been shown to arrange in compact layers and display high mitotic activity (Singh, 1997). Specialized granulosa cells (cumulus cells) surrounding oocyte were observed to maintain intimate contact with oocyte through their cell projections (Assey et al., 1994). These cumulus cell projections,

that traverse zona pellucida, have been proposed to allow passage of small molecular weight molecules such as amino acids and nucleotides (including ATP) (Sutton et al., 2003). It is possible that oocyte in growing follicle needs less energy from lipid resources, as contacts of oocyte with surrounding cumulus cells were presumably still intact (Assey et al., 1994). Lipids are least studied organelles especially in bovine oocytes. In mouse, close proximity of mitochondria with lipids is needed for energy (i.e. ATP) production through beta-oxidation in mitochondria, which has been observed to affect oocyte maturation and competence (Dunning et al., 2010). In that regard, total lipid content in bovine oocytes is approximately 10 times more than mouse oocytes (McEvoy et al., 2000) and around 30% of which is triglyceride (McEvoy et al., 2000). I have shown (Figure 7.1) that oocytes from later stages of follicle growth have a greater proportion of mitochondrial surface in contact with lipids compared to the growing stage. Does this observation mean that static and regression phase oocytes start utilizing lipid droplet for ATP production? It needs to be addressed in future studies, especially in the context of my observations that there is an increase in lipid droplet compartment within the oocyte as the follicle proceeds through static phase and enter regression phase.

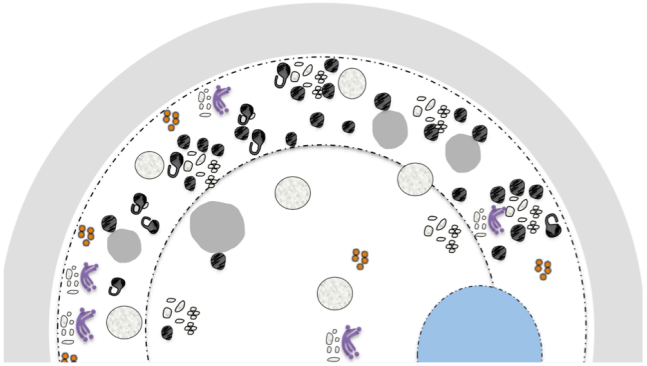

Growing Phase

- Least proportion of mitochondrial surface in contact with lipid droplets
- Mitochondria and lipid droplets more peripherally located

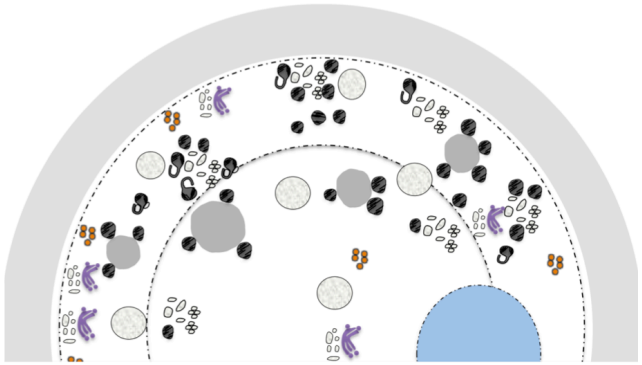

Static and Preovulatory Phases

- Increase in mitochondria+lipid contacts
- Even distribution of lipids
- Peripherally distributed mitochondria

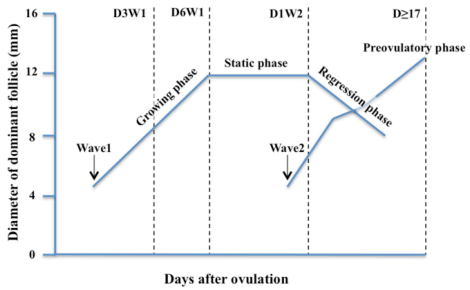

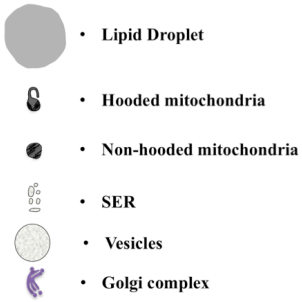

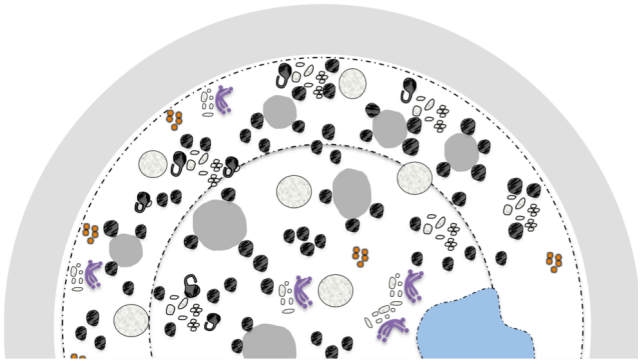

Regression Phase

- Increase in lipid volume
- Even distribution of lipids and mitochondria
- Increase in numerical density of mitochondria
- Golgi complexes move closer to nucleus

Figure 7.1 Schematic presentation of changes in organelle characteristics with development of dominant follicle.

The preovulatory stage oocyte have lipid content similar to growing stage oocyte but less than those from wave 1 static and regression phase follicles (Chapter 4). This finding does not agree to that from other reports where preovulatory stage oocytes had more and bigger lipids compared to those from early stages of follicle growth (Assey et al., 1994; Yang et al., 2010). The first study used qualitative assessment of electron micrographs and preovulatory follicles were aspirated after LH surge. In my study, preovulatory follicles were collected when cows showed signs of estrus. As none of the oocytes in my study showed GVBD (Chapter 4), the collection must have been around LH surge. In general, bovine oocytes enter GVBD 6 hours after preovulatory LH surge (Motlik et al., 1978; Hyttel et al., 1986b). Moreover, accumulation of lipid droplets was reported to occur more prominently in oocytes collected before LH surge compared to oocyte reaching Metaphase II (which happens 19-22h after LH surge) (Kruip et al., 1983; Assey et al., 1994). It is possible that oocyte gradually stores lipid droplets as a source of endogenous energy at nuclear maturation, fertilization and for early embryonic development before genomic activation embryo. Utilization of lipid stores by oocyte undergoing nuclear maturation explained the decline in lipid content of an oocyte as it progressed from GV stage to Metaphase II (Ferguson and Leese, 1999). Furthermore, facilitating ß-oxidation by supplementing carnitine improved blastocyst rates during IVF of mouse oocytes (Dunning et al., 2010).

Recent work on mouse oocytes have shown the presence of perilipin-2 mRNA and its protein during *in vitro* maturation (Yang et al., 2010). Perilipin proteins have been reported to provide the framework for lipid droplet formation, fusion and lipolysis in other cell types (Murphy, 2001). Recently perilipin-5 was observed to facilitate bringing

of lipid droplets in close contact with mitochondria (Wang et al., 2011). Very little information is available on uptake of lipids into mammalian oocytes and proteins involved in fusion and dissociation of lipid droplets. Studying these proteins in future studies can further our understanding of the dynamics of lipid droplet formation and utilization in oocytes.

In my study (Chapter 4), oocytes in regression phase were collected a day after the next wave emerged, which indicates functional loss of dominance. Follicles in regression phase have been characterized by changes in histomorphology of granulosa cells, estradiol content in follicular fluid and follicular wall echogenicity (Singh et al., 1998). Granulosa cells in the wall of these follicles showed an increase in pyknosis and a further decline in mitotic activity compared to follicles in static phase follicles (indicative of atresia) (Singh, 1997). Concomitant to an increase in lipid volume in the oocytes from regression phase follicles observed in my study, an increase in mitochondrial number and relocation of mitochondria from primarily peripheral to evenly spread distribution was noticed (Chapter 4). Mitochondria are needed by cells to produce ATP using variety of substrates; store Ca^{2+} that is exchanged with closely associated SER to control different cell function and release cytochrome c to induce apoptosis (Ramalho-Santos et al., 2009). The population of mitochondrial morphology, hooded mitochondria, that is closely associated with SER did not change and nor did the association between mitochondria and SER (Chapter 4). The increase in mitochondrial population was due to non-hooded mitochondria, which are round in shape with less number of cristae indicating a quiescent morphology characteristic to oocyte. It's intriguing why an oocyte in a follicle that has lost its dominance and started to undergo atresia needs largeer mitochondrial population.

It could mean either the oocyte is going to rely on its own resources for ATP generation or could be an indication of apoptotic signal. Although not observed in oocytes, it has been shown that increased oxidative radicals lead to increased mitochondrial fission (Parone and Martinou, 2006; Wu et al., 2011). This observation warrant further studies to determine the functional status of mitochondria in oocyte from regressing follicle as well as status of oxidative stress experienced by the oocyte.

My findings support a previous study (Assey et al., 1994) in that some oocytes obtained from regressing phase follicle showed signs of nuclear and cytoplasmic maturation similar to preovulatory follicle following LH surge. As LH surge cannot occur during the presence of luteal levels of progesterone, it raises the question whether LH surge is really needed for these maturational changes in the oocyte. In my opinion, LH is a signal higher in the hierarchy that initiates final oocyte maturation. Following LH surge, ROS accumulation in preovulatory follicle have been shown to be crucial for cumulus cell expansion and ovulation (Shkolnik et al., 2011). Inhibition of ROS with ROS scavengers resulted in a drastic decrease in cumulus cell expansion and ovulation rate (Shkolnik et al., 2011). However, a balance between the ROS and their scavengers must be reached. This concept is supported by a previous report that there was an increase in oocyte maturation and embryonic development when different antioxidants were added during IVM and IVF, reviewed earlier (Combelles et al., 2009). During *in vivo* maturation, these antioxidants come from follicular fluid, cumulus cells and from within the oocyte itself (Combelles et al., 2009). During regression phase, I speculate that ROS may develop in absence of LH surge due to loss of dominance and onset of atresia. Moreover, the cytoplasmic contacts of oocyte with surrounding cumulus cells have been

shown to retract in oocytes from regressing follicles (Kruip et al., 1983), as a result the antioxidants from outside might become unavailable. With the limited antioxidants available for the oocyte in the regressing follicle, the oocyte might hold on for sometime before undergoing apoptosis. This might be the reason why the oocytes from follicles with slight degree atresia still have the ability to develop into embryos.

The target of superstimulation protocols is to obtain maximum number of dominant follicles destined for ovulation that will provide good quality embryos following AI. Over last eight decades, FSH or PMSG-based protocols have been designed and modified in several ways. Marked progress have been made in terms of initiating these protocols at will during an estrous cycle of cattle by synchronizing the time of wave emergence (Nasser et al., 1993). However, the number of transferable number embryos generated by these protocols has remained at 5-6 embryos per animal (Mapletoft et al., 2002; Tríbulo et al., 2012). My study (Chapter 5) and other ones from my supervisor's lab (Dias et al., 2012a; García Guerra et al., 2012) have shown that prolonging the duration of FSH treatment by 3 days increased the number of follicles available for ovulation. In the longer (7-d) superstimulation protocol, an increased synchrony of ovulation was observed but the number of ovulations did not differ when compared to a shorter FSH (4-d) protocol (Dias et al., 2012a; García Guerra et al., 2012). Increasing number of dominant follicles can be useful, particularly in situations where *in vitro* production of embryos is derived from oocytes obtained by ovum-pick-up. For production of embryos through IVF, quality of oocyte is of utmost importance. On comparing the quality of *in vivo* matured oocytes, 3 times more MII stage oocytes were obtained in the 7-d protocol than the 4-d protocol (Chapter 5). It has been shown previously that majority of the oocytes

reach MII stage around 19-20 h after LH surge (Hyttel et al., 1989c), which correspond to the time when I collected the *in vivo* matured oocytes. Morphologically, the quality of oocytes was similar between the 7-d and 4-d treatment groups (Chapter 6), corroborating the findings of a parallel study by our laboratory (Dias et al unpublished data, personal communication). In that regard, cytoplasmic maturation of oocytes was compared between these two groups with respect to lipid droplets (Chapter 5) and mitochondria (Chapter 6). I applied a newer approach to generate quantitative data regarding these two organelles. Three-dimensional image sets were obtained using multiphoton confocal microscope. For lipid droplets stained with Nile Red, it was possible to image the entire oocyte, however, for mitochondria photobleaching hindered our approach. Once the 3-D image sets were obtained, Autoquant X2 was used to correct for the distortion of image in Z-direction (i.e., deconvolution). Next, I developed a segmentation protocol in Imaris Pro7.4.2 to identify lipid droplets (Chapter 5, Appendix A) and mitochondria (Chapter 6) in order to obtain quantitative data for these organelles. The number, distribution and size of lipid droplets did not differ between the oocytes from 4-d and 7-d protocols (Chapter 5). The mean number and proportion of individual mitochondria and mitochondrial clusters did not differ when different regions of oocyte were compared between the two groups (Chapter 6). However, an increase in mean intensity of individual mitochondria or clusters was observed in the 7-d protocol compared to 4-d protocol. This observation indicated that mitochondria in oocytes from 7-d protocol were more active. An increase in functionality of mitochondria in oocytes of 7-d protocol group was also shown by the tendency of these oocytes to have higher ATP content than oocytes from 4-day protocol. Positive relations between ATP content and oocyte maturation rates and subsequent

embryo development have been shown in bovine (Stojkovic et al., 2001; Nagano et al., 2006) and human oocytes (Van Blerkom et al., 1995). However, developmental competence of the oocytes did not differ between the 7-d and 4-d treatment group when fertilization was done either *in vivo* (Dias et al., 2012a) or *in vitro* (Dias et al unpublished data, personal communication).

Some studies have demonstrated that a certain duration of FSH-free period during FSH-based superstimulation protocols is obligatory for the bovine oocytes to attain achieve competence (Blondin et al., 1997b; Sirard et al., 1999; Jaiswal, 2007; Nivet et al., 2012). I used an 84 h gap between the last FSH and LH injections. It seems that this period might be too long as about 60% of the follicles lost their ability to ovulate (Dias et al., 2012a). Moreover, preovulatory follicles from this group had highest proportion of bad quality oocytes compared to 4-d and 7-d superstimulation protocols (Chapter 6). The poor quality of FSH starved oocytes was also reflected in their nuclear maturation and cytoplasmic maturation status. Less than $1/10^{th}$ of the oocytes from the starvation group reached MII after induced LH surge. Further, around 50% of oocytes from the starvation group did not proceed to GVDB, which reportedly happened at 9-12 h after LH surge *in vivo* (Hyttel et al., 1986a)., indicating failure of mechanisms that are responsible for resumption of meiosis in oocyte. There is an increasing evidence that stored lipids are utilized by oocyte for ATP generation needed during nuclear maturation (Downs et al., 2009; Dunning et al., 2010). Failure of nuclear maturation in oocytes that were starved for 84 h might have lead to accumulation of bigger lipid droplets in the ooplasm of these oocytes (Chapter 5). Strangely enough, a higher proportion of mitochondria were organized in clusters in oocytes that had higher mean intensity compared to those from 4-

d protocol, but had mitochondrial intensity similar to the oocytes from 7-d protocol. Both these observations indicated that oocytes from FSH starvation group had more active mitochondria. However, the ATP content of FSH starvation group was numerically less than 7-d protocol. It is not clear why even the individual mitochondria were more intense in oocytes from FSH starvation group despite previous reports that ATP production was highly correlated with mitochondrial redistribution and clustering (Van Blerkom et al., 1995; Wilding et al., 2001). I speculate that mitochondria and clusters in FSH starved oocytes might have shown intense staining with Mitotracker Deep Red due to an increased oxidative stress. The rationale behind my assumption is that accumulation of cabocyanine based Mitotracker dyes have been shown to occur in neurons exposed to increased concentrations of hydrogen peroxide (Buckman et al., 2001). Taken together, FSH starvation for 84h resulted in a reduction of quality of oocytes. A recent study has shown a reduced *in vitro* developmental competence of oocytes when 92 h FSH starvation was applied (Nivet et al., 2012), whereas, it was noted that a short FSH starvation period in the range of 48-60 h was better for the oocyte to reach developmental competence. It will be worth testing the protocols of above study with respect to the competence of *in vivo* matured oocytes. Moreover, this study and a previous one from the same group (Blondin et al., 1997b), did not have groups with continued FSH support to match the period of growth in different starvation groups. This issue needs to be addressed in future studies as that would be the true test of whether or not FSH starvation is crucial for an oocyte to gain developmental competence. It will be interesting to study if the follicles during the starvation periods are growing or become static. In either case, we will be selecting for the follicles that are able to maintain good health despite limited

availability of LH under luteal levels of progesterone. In addition to duration of FSH starvation, the progesterone levels during the superstimulation have been shown to plays a significant role in attainment of oocyte's developmental competence. A short superstimulation (4-d) in a subluteal-phase progesterone milieu was shown to increase the fertilization rates but the developmental competence was similar when compared to 4-d protocol under luteal levels of progesterone (Jaiswal, 2007). Further, a very long FSH starvation (144 h) in subluteal-phase progesterone environment in that study resulted in ovulation failure in all follicles (Jaiswal, 2007). As a result, the competence of oocytes from follicles of prolonged starvation group was not tested.

In addition to the above-explained factors, it has been shown that there is a decline in fertility with advancing age in women (Schwartz and Mayaux, 1982; Chandra et al., 2005). Due to legal and ethical issues of studying human oocytes, I used a bovine model that has been validated for studying effect of old age on fertility (Malhi, 2007). I have shown that *in vivo* matured oocytes from old cows have lesser ATP content than those from young cows (Chapter 6). ATP is generated in oocytes from either a carbohydrate or lipid source and it is needed for energy dependent process of nuclear maturation, fertilization and early embryonic development (Sutton-McDowall et al., 2012). In that regard, the nuclear maturation rates were not different between the oocytes from old and young cows (Malhi et al., 2007), which is supported by results from my study. However, differences in fertilization rates were noticed in other studies as old cows have had more number of unfertilized oocytes compared to young cows (Malhi et al., 2007; Iwata et al., 2011). When I examined the mitochondria, I found no differences in the total number, distribution and intensities of individual mitochondria and clusters (Chapter 6). This

observation was unexpected, as previous studies have indicated a reduction in mitochondrial number with old age (Iwata et al., 2011). The difference could arise due to the difference in methods that were used to quantify mitochondrial numbers. My results show a tendency towards more number of mitochondrial clusters in oocytes of old cows. However, this finding was not related with increased activity of mitochondria and higher ATP content of oocytes as observed in other studies (Van Blerkom et al., 1995; Wilding et al., 2001). Further studies are needed to determine as to why the differences in ATP content exist between the oocytes from old vs young cows despite no differences in mitochondrial numbers and activity.

CHAPTER 8

8 GENERAL CONCLUSIONS

8.1 Progesterone concentration and length of proestrus during dominant follicle growth

a. Shorter duration of proestrus during a fixed-time AI protocol in cattle resulted in a smaller preovulatory follicle, smaller and less functional CL with lower progesterone secretion, and lower fertility.
b. Subluteal-phase progesterone milieu during ovulatory follicle growth induced follicles to grow to a larger size resulting in larger CL and higher pregnancy rates following fixed-time AI.

We concluded that subluteal-phase progesterone concentrations compensated for a shorter proestrus period with regards to pregnancy rate.

8.2 Oocyte ultrastructure with respect to changes dominant follicle growth, regression and maturation

a. Growing phase oocytes are characterized by
    - least area of mitochondria in contact with lipid droplets
    - a peripheral distribution of lipids compared to even distribution in oocytes from other phases
b. Regression phase oocytes are characterized by
    - increase in mitochondrial number
    - even distribution of mitochondria compared to peripheral distribution in

oocytes from other phases

- have more lipids content per unit volume of oocyte.

We conclude that changes in organelle number and distribution pattern occur in a manner specific for phase of follicular growth, maturation and regression.

8.3 Follicular aging: nuclear maturation, lipid droplets, mitochondrial number and distribution and ATP content

a. Long FSH protocol increases the superstimulatory response with higher proportion of oocytes completing nuclear maturation.
b. FSH starvation for 84 h decreased the quality of oocytes, resulted in failure of meiotic resumption and accumulation of large lipid droplets indicating atresia.
c. Long FSH treatment tended to increase the ATP content of oocytes compared to short FSH group.
d. ATP content of oocytes between the Long FSH and FSH starvation groups was similar.
e. Oocytes from FSH starvation group had bigger clusters than other groups and intensity similar to Long FSH group.

8.4 Maternal aging: ATP content and mitochondrial number and distribution.

a. Maternally aged *in vivo* matured oocytes had less ATP content than those from young cows.
b. Mitochondrial population and distribution pattern did not differ between the two

age groups.

The basic information about the cellular changes within the oocyte during follicle development has been lacking till date. My studies clearly describe how the stage of follicle development, hormonal environment and age of animal affect the oocyte morphology. The morphological nature of my studies does limit a direct outcome in clinical sense, however, my findings provide crucial evidence to target functionality of different organelles especially mitochondria and lipid droplets in future studies on oocyte with reference to its developmental competence.

CHAPTER 9

9 BIBLIOGRAPHY

Adams, G., Matteri, R., Ginther, O., 1992a. Effect of progesterone on ovarian follicles, emergence of follicular waves and circulating follicle-stimulating hormone in heifers. J Reprod Fertil 96, 627-640.

Adams, G.P., Jaiswal, R., Singh, J., Malhi, P., 2008. Progress in understanding ovarian follicular dynamics in cattle. Theriogenology 69, 72-152.

Adams, G.P., Matteri, R., Kastelic, J., Ko, J., Ginther, O., 1992b. Association between surges of follicle-stimulating hormone and the emergence of follicular waves in heifers. Journal of reproduction and fertility 94, 177-265.

Adams, G.P., Matteri, R.L., Kastelic, J.P., Ko, J.C., Ginther, O.J., 1992c. Association between surges of follicle-stimulating hormone and the emergence of follicular waves in heifers. Journal of reproduction and fertility 94, 177-188.

Adams, G.P., Singh, J., Baerwald, A.R., 2012. Large animal models for the study of ovarian follicular dynamics in women. Theriogenology 78, 1733-1748.

Adeoya-Osiguwa, S.A., Markoulaki, S., Pocock, V., Milligan, S.R., Fraser, L.R., 2003. 17beta-Estradiol and environmental estrogens significantly affect mammalian sperm function. Hum Reprod 18, 100-107.

Ajduk, A., Ma≈Çagocki, A., Maleszewski, M., 2008. Cytoplasmic maturation of mammalian oocytes: development of a mechanism responsible for sperm-induced Ca2+ oscillations. Reproductive biology 8, 3-25.

Aksglaede, L., Juul, A., Leffers, H., Skakkebaek, N.E., Andersson, A.M., 2006. The sensitivity of the child to sex steroids: possible impact of exogenous estrogens. Human reproduction update 12, 341-349.

Allan, B., Balch, W., 1999. Protein sorting by directed maturation of Golgi compartments. Science (New York, N.Y.) 285, 63-69.

Ambruosi, B., Lacalandra, G., Iorga, A., De Santis, T., Mugnier, S., Matarrese, R., Goudet, G., Dell'aquila, M., 2009. Cytoplasmic lipid droplets and mitochondrial distribution in equine oocytes: Implications on oocyte maturation, fertilization and developmental competence after ICSI. Theriogenology 71, 1093-1197.

Assey, R.J., Hyttel, P., Greve, T., Purwantara, B., 1994. Oocyte morphology in dominant and subordinate follicles. Mol Reprod Dev 37, 335-344.

Austin, E., Mihm, M., Ryan, M., Williams, D., Roche, J., 1999. Effect of duration of dominance of the ovulatory follicle on onset of estrus and fertility in heifers. Journal of animal science 77, 2219-2245.

Austin, E.J., Mihm, M., Evans, A.C., Knight, P.G., Ireland, J.L., Ireland, J.J., Roche, J.F., 2001. Alterations in intrafollicular regulatory factors and apoptosis during selection of follicles in the first follicular wave of the bovine estrous cycle. Biology of reproduction 64, 839-848.

Awasthi, H., Saravia, F., Rodriguez-Martinez, H., Bage, R., 2010. Do cytoplasmic lipid droplets accumulate in immature oocytes from over-conditioned repeat breeder dairy heifers? Reproduction in domestic animals = Zuchthygiene 45, e194-198.

Ayalon, D., Tsafriri, A., Lindner, H.R., Cordova, T., Harell, A., 1972. Serum gonadotrophin levels in pro-oestrous rats in relation to the resumption of meiosis by the oocytes. Journal of reproduction and fertility 31, 51-58.

Baddeley, A.J., Gundersen, H.J., Cruz-Orive, L.M., 1986. Estimation of surface area from vertical sections. J Microsc 142, 259-276.

Badinga, L., Driancourt, M.A., Savio, J.D., Wolfenson, D., Drost, M., De La Sota, R.L., Thatcher, W.W., 1992. Endocrine and ovarian responses associated with the first-wave dominant follicle in cattle. Biology of reproduction 47, 871-883.

Baenziger, J., Green, E., 1988. Pituitary glycoprotein hormone oligosaccharides: structure, synthesis and function of the asparagine-linked oligosaccharides on lutropin, follitropin and thyrotropin. Biochimica et biophysica acta 947, 287-593.

Baerwald, A.R., Adams, G.P., Pierson, R.A., 2003. Characterization of ovarian follicular wave dynamics in women. Biology of reproduction 69, 1023-1031.

Baerwald, A.R., Adams, G.P., Pierson, R.A., 2012. Ovarian antral folliculogenesis during the human menstrual cycle: a review. Human reproduction update 18, 73-91.

Bao, B., Garverick, H., Smith, G., Smith, M., Salfen, B., Youngquist, R., 1997a. Changes in messenger ribonucleic acid encoding luteinizing hormone receptor, cytochrome P450-side chain cleavage, and aromatase are associated with recruitment and selection of bovine ovarian follicles. Biology of reproduction 56, 1158-1226.

Bao, B., Garverick, H.A., Smith, G.W., Smith, M.F., Salfen, B.E., Youngquist, R.S., 1997b. Changes in messenger ribonucleic acid encoding luteinizing hormone receptor, cytochrome P450-side chain cleavage, and aromatase are associated with recruitment and selection of bovine ovarian follicles. Biology of reproduction 56, 1158-1168.

Barcelo-Fimbres, M., Seidel, G.E., Jr., 2011. Cross-validation of techniques for measuring lipid content of bovine oocytes and blastocysts. Theriogenology 75, 434-444.

Barritt, J., Cohen, J., Brenner, C., 2000. Mitochondrial DNA point mutation in human oocytes is associated with maternal age. Reprod Biomed Online 1, 96-196.

Baruselli, P., Reis, E., Marques, M., Nasser, L., Bo, G., 2004. The use of hormonal treatments to improve reproductive performance of anestrous beef cattle in tropical climates. Anim Reprod Sci 82-83, 479-486.

Bavister, B.D., 2000. Interactions between embryos and the culture milieu. Theriogenology 53, 619-626.

Bavister, B.D., Squirrell, J.M., 2000. Mitochondrial distribution and function in oocytes and early embryos. Hum Reprod 15 Suppl 2, 189-198.

Bentov, Y., Yavorska, T., Esfandiari, N., Jurisicova, A., Casper, R.F., 2011. The contribution of mitochondrial function to reproductive aging. J Assist Reprod Genet 28, 773-783.

Bergfelt, D., Kulick, L., Kot, K., Ginther, O., 2000. Follicular and hormonal response to experimental suppression of FSH during follicle deviation in cattle. Theriogenology 54, 1191-1397.

Bergfelt, D.R., Bo, G.A., Mapletoft, R.J., Adams, G.P., 1997. Superovulatory response following ablation-induced follicular wave emergence at random stages of the oestrous cycle in cattle. Anim Reprod Sci 49, 1-12.

Bergfelt, D.R., Lightfoot, K.C., Adams, G.P., 1994. Ovarian synchronization following ultrasound-guided transvaginal follicle ablation in heifers. Theriogenology 42, 895-907.

Bigelow, K.L., Fortune, J.E., 1998. Characteristics of prolonged dominant versus control follicles: follicle cell numbers, steroidogenic capabilities, and messenger ribonucleic acid for steroidogenic enzymes. Biology of reproduction 58, 1241-1249.

Biggs, D.S., 2010. 3D deconvolution microscopy. Curr Protoc Cytom Chapter 12, Unit 12 19 11-20.

Binelli, M., Hampton, J., Buhi, W.C., Thatcher, W.W., 1999. Persistent dominant follicle alters pattern of oviductal secretory proteins from cows at estrus. Biology of reproduction 61, 127-134.

Bisinotto, R.S., Chebel, R.C., Santos, J.E., 2010. Follicular wave of the ovulatory follicle and not cyclic status influences fertility of dairy cows. Journal of dairy science 93, 3578-3587.

Blondin, P., Coenen, K., Guilbault, L., Sirard, M., 1997a. In vitro production of bovine embryos: developmental competence is acquired before maturation. Theriogenology 47, 1061-1136.

Blondin, P., Guilbault, L., Sirard, M., 1997b. The time interval between FSH-P administration and slaughter can influence the developmental competence of beef heifer oocytes. Theriogenology 48, 803-816.

Blondin, P., Sirard, M.A., 1995. Oocyte and follicular morphology as determining characteristics for developmental competence in bovine oocytes. Mol Reprod Dev 41, 54-62.

Bo, G.A., Adams, G.P., Pierson, R.A., Caccia, M., Tribulo, H., Mapletoft., R.J., 1994. Follicular wave dynamics after estradiol-17ß treatment of heifers with or without a progestagen implant. Theriogenology 41, 1555-1569.

Bo, G.A., Peres, L.C., Cutaia, L.E., Pincinato, D., Baruselli, P.S., Mapletoft, R.J., 2011. Treatments for the synchronisation of bovine recipients for fixed-time embryo transfer and improvement of pregnancy rates. Reproduction, fertility, and development 24, 272-277.

Bousquet, D., Milovanov, C., Bell, J.C., Durocher, J., Smith, L.C., 1995. Nuclear and cytoplasmic maturation of oocytes aspirated from large follicles in superovulated heifers. Theriogenology.

Bridges, G.A., Helser, L.A., Grum, D.E., Mussard, M.L., Gasser, C.L., Day, M.L., 2008. Decreasing the interval between GnRH and PGF2alpha from 7 to 5 days and lengthening proestrus increases timed-AI pregnancy rates in beef cows. Theriogenology 69, 843-851.

Bridges, G.A., Mussard, M.L., Burke, C.R., Day, M.L., 2010. Influence of the length of proestrus on fertility and endocrine function in female cattle. Anim Reprod Sci 117, 208-215.

Brogliatti, G.M., Adams, G.P., 1996. Ultrasound-guided transvaginal oocyte collection in prepubertal calves. Theriogenology 45, 1163-1176.

Buckman, J.F., Hernandez, H., Kress, G.J., Votyakova, T.V., Pal, S., Reynolds, I.J., 2001. MitoTracker labeling in primary neuronal and astrocytic cultures: influence of mitochondrial membrane potential and oxidants. J Neurosci Methods 104, 165-176.

Burkart, A., Xiong, B., Baibakov, B., Jim√©nez-Movilla, M., Dean, J., 2012. Ovastacin, a cortical granule protease, cleaves ZP2 in the zona pellucida to prevent polyspermy. The Journal of cell biology 197, 37-81.

Bush, P.G., Wokosin, D.L., Hall, A.C., 2007. Two-versus one photon excitation laser scanning microscopy: critical importance of excitation wavelength. Front Biosci 12, 2646-2657.

Cerri, R., Chebel, R., Rivera, F., Narciso, C., Oliveira, R., Thatcher, W., Santos, J., 2011. Concentration of progesterone during the development of the ovulatory follicle: I. Ovarian and embryonic responses. Journal of dairy science 94, 3342-3393.

Chandra, A., Martinez, G.M., Mosher, W.D., Abma, J.C., Jones, J., 2005. Fertility, family planning, and reproductive health of U.S. women: data from the 2002 National Survey of Family Growth. Vital Health Stat 23, 1-160.

Chazotte, B., 2009. Labeling mitochondria with fluorescent dyes for imaging. Cold Spring Harb Protoc 2009, pdb prot4948.

Chazotte, B., 2011. Labeling mitochondria with TMRM or TMRE. Cold Spring Harb Protoc 2011, 895-897.

Chen, L.B., 1989. Fluorescent labeling of mitochondria. Methods Cell Biol 29, 103-123.

Chohan, K.R., Hunter, A.G., 2003. Meiotic competence of bovine fetal oocytes following in vitro maturation. Animal reproduction science 76, 43-51.

Colazo, M., Kastelic, J., Martinez, M., Whittaker, P., Wilde, R., Ambrose, J., 2004a. Fertility following fixed-time AI in CIDRtreated beef heifers given GnRH or estradiol cypionate and fed diets supplemented with flax seed or sunflower seed. Theriogenology 61, 1115-1124.

Colazo, M.G., Kastelic, J.P., Whittaker, P.R., Gavaga, Q.A., Wilde, R., Mapletoft, R.J., 2004b. Fertility in beef cattle given a new or previously used CIDR insert and estradiol, with or without progesterone. Animal reproduction science 81, 25-34.

Cole, R.W., Jinadasa, T., Brown, C.M., 2011. Measuring and interpreting point spread functions to determine confocal microscope resolution and ensure quality control. Nat Protoc 6, 1929-1941.

Combelles, C.M., Gupta, S., Agarwal, A., 2009. Could oxidative stress influence the in-vitro maturation of oocytes? Reprod Biomed Online 18, 864-880.

Connors, S.A., Kanatsu-Shinohara, M., Schultz, R.M., Kopf, G.S., 1998. Involvement of the cytoskeleton in the movement of cortical granules during oocyte maturation, and cortical granule anchoring in mouse eggs. Dev Biol 200, 103-115.

Conti, M., Hsieh, M., Zamah, A.M., Oh, J.S., 2012. Novel signaling mechanisms in the ovary during oocyte maturation and ovulation. Mol Cell Endocrinol 356, 65-73.

Cran, D.G., 1985. Qualitative and quantitative structural changes during pig oocyte maturation. Journal of reproduction and fertility 74, 237-245.

Crosier, A.E., Farin, P.W., Dykstra, M.J., Alexander, J.E., Farin, C.E., 2000. Ultrastructural morphometry of bovine compact morulae produced in vivo or in vitro. Biol Reprod 62, 1459-1465.

Croteau, D., Bohr, V., 1997. Repair of oxidative damage to nuclear and mitochondrial DNA in mammalian cells. J Biol Chem 272, 25409-25421.

Cui, M.S., Fan, Y.P., Wu, Y., Hao, Z.D., Liu, S., Chen, X.J., Zeng, S.M., 2009. Porcine cumulus cell influences ooplasmic mitochondria-lipid distributions, GSH-ATP contents and calcium release pattern after electro-activation. Theriogenology 71, 412-421.

de Bruin, J., Dorland, M., Spek, E., Posthuma, G., van Haaften, M., Looman, C., te Velde, E., 2004. Age-related changes in the ultrastructure of the resting follicle pool in human ovaries. Biology of reproduction 70, 419-424.

de Loos, F., van Vliet, C., van Maurik, P., Kruip, T.A., 1989. Morphology of immature bovine oocytes. Gamete Research 24, 197-204.

Denicol, A.C., Lopes, G., Jr., Mendonca, L.G., Rivera, F.A., Guagnini, F., Perez, R.V., Lima, J.R., Bruno, R.G., Santos, J.E., Chebel, R.C., 2012. Low progesterone concentration during the development of the first follicular wave reduces pregnancy per insemination of lactating dairy cows. Journal of dairy science 95, 1794-1806.

Dey, S.R., Deb, G.K., Ha, A.N., Lee, J.I., Bang, J.I., Lee, K.L., Kong, I.K., 2012. Coculturing denuded oocytes during the in vitro maturation of bovine cumulus oocyte complexes exerts a synergistic effect on embryo development. Theriogenology 77, 1064-1077.

Dias, F.C., 2008. Effect of progesterone on GnRH-mediated LH release, oocyte quality and fertility in cattle., Veterinary Biomedical Sciences, University of Saskatchewan, Saskatoon p. 88.

Dias, F.C., Costa, E., Adams, G.P., Mapletoft, R.J., Kastelic, J.P., Dochi, O., Singh, J., 2012a. Effect of duration of growing phase of ovulatory follicles on oocyte competence in superstimulated cattle. Reprod Fertil Dev.

Dias, F.C., Mapletoft, R.J., Kastelic, J.P., Adams, G.P., Colazo, M.G., Stover, B.C., Dochi, O., Singh, J., 2012b. Effect of length of progesterone exposure during ovulatory wave development on pregnancy rate. Theriogenology 77, 437-444.

Dieleman, S.J., Hendriksen, P.J., Viuff, D., Thomsen, P.D., Hyttel, P., Knijn, H.M., Wrenzycki, C., Kruip, T.A., Niemann, H., Gadella, B.M., Bevers, M.M., Vos, P.L., 2002. Effects of in vivo prematuration and in vivo final maturation on developmental capacity and quality of pre-implantation embryos. Theriogenology 57, 5-20.

Dong, C.Y., Koenig, K., So, P., 2003. Characterizing point spread functions of two-photon fluorescence microscopy in turbid medium. J Biomed Opt 8, 450-459.

Downs, S.M., Mosey, J.L., Klinger, J., 2009. Fatty acid oxidation and meiotic resumption in mouse oocytes. Molecular reproduction and development 76, 844-853.

Dufourny, L., Caraty, A., Clarke, I.J., Robinson, J.E., Skinner, D.C., 2005a. Progesterone-receptive beta-endorphin and dynorphin B neurons in the arcuate nucleus

project to regions of high gonadotropin-releasing hormone neuron density in the ovine preoptic area. Neuroendocrinology 81, 139-149.

Dufourny, L., Caraty, A., Clarke, I.J., Robinson, J.E., Skinner, D.C., 2005b. Progesterone-receptive dopaminergic and neuropeptide Y neurons project from the arcuate nucleus to gonadotropin-releasing hormone-rich regions of the ovine preoptic area. Neuroendocrinology 82, 21-31.

Dunning, K.R., Cashman, K., Russell, D.L., Thompson, J.G., Norman, R.J., Robker, R.L., 2010. Beta-oxidation is essential for mouse oocyte developmental competence and early embryo development. Biol Reprod 83, 909-918.

Dunning, K.R., Robker, R.L., 2012. Promoting lipid utilization with l-carnitine to improve oocyte quality. Animal reproduction science 134, 69-75.

Edwards, R.G., 1965. Maturation in vitro of mouse, sheep, cow, pig, rhesus monkey and human ovarian oocytes. Nature 208, 349-351.

Ehrenberg, B., Montana, V., Wei, M.D., Wuskell, J.P., Loew, L.M., 1988. Membrane potential can be determined in individual cells from the nernstian distribution of cationic dyes. Biophys J 53, 785-794.

Eichenlaub-Ritter, U., Vogt, E., Yin, H., Gosden, R., 2004. Spindles, mitochondria and redox potential in ageing oocytes. Reprod Biomed Online 8, 45-103.

Eichenlaub-Ritter, U., Wieczorek, M., Luke, S., Seidel, T., 2011. Age related changes in mitochondrial function and new approaches to study redox regulation in mammalian oocytes in response to age or maturation conditions. Mitochondrion 11, 783-796.

El Shourbagy, S.H., Spikings, E.C., Freitas, M., St John, J.C., 2006. Mitochondria directly influence fertilisation outcome in the pig. Reproduction 131, 233-245.

Eppig, J., 1996. Coordination of nuclear and cytoplasmic oocyte maturation in eutherian mammals. Reproduction, fertility, and development 8, 485-494.

Erickson, B., 1966. Development and senescence of the postnatal bovine ovary. Journal of animal science 25, 800-805.

Fair, T., 2003. Follicular oocyte growth and acquisition of developmental competence. Anim Reprod Sci 78, 203-216.

Fair, T., Hulshof, S.C., Hyttel, P., Greve, T., Boland, M., 1997. Oocyte ultrastructure in bovine primordial to early tertiary follicles. Anatomy and embryology 195, 327-336.

Fair, T., Hyttel, P., Greve, T., 1995. Bovine oocyte diameter in relation to maturational competence and transcriptional activity. Molecular reproduction and development 42, 437-442.

Ferguson, E., Leese, H., 2006. A potential role for triglyceride as an energy source during bovine oocyte maturation and early embryo development. Molecular reproduction and development 73, 1195-1396.

Ferguson, E.M., Leese, H.J., 1999. Triglyceride content of bovine oocytes and early embryos. Journal of reproduction and fertility 116, 373-378.

Ferreira, E.M., Vireque, A.A., Adona, P.R., Meirelles, F.V., Ferriani, R.A., Navarro, P.A., 2009. Cytoplasmic maturation of bovine oocytes: structural and biochemical modifications and acquisition of developmental competence. Theriogenology 71, 836-848.

Forde, N., Beltman, M.E., Lonergan, P., Diskin, M., Roche, J.F., Crowe, M.A., 2011. Oestrous cycles in Bos taurus cattle. Animal reproduction science 124, 163-169.

Fortune, J.E., Willis, E.L., Bridges, P.J., Yang, C.S., 2009. The periovulatory period in cattle: progesterone, prostaglandins, oxytocin and ADAMTS proteases. Anim Reprod 6, 60-71.

Fowler, S.D., Mayer, E.P., Greenspan, P., 1985. Foam cells and atherogenesis. Ann N Y Acad Sci 454, 79-90.

Führer, F., Mayr, B., Schellander, K., Kalat, M., Schleger, W., 1989. Maturation competence and chromatin behaviour in growing and fully grown cattle oocytes. Zentralblatt für Veterinärmedizin. Reihe A. 36, 285-376.

Funston, R.N., Martin, J.L., Larson, D.M., Roberts, A.J., 2012. Physiology and Endocrinology Symposium: Nutritional aspects of developing replacement heifers. Journal of animal science 90, 1166-1171.

García Guerra, A., Tribulo, A., Yapura, J., Singh, J., Mapletoft, R., 2012. Lengthening the superstimulatory treatment protocol increases ovarian response and number of transferable embryos in beef cows. Theriogenology 78, 353-413.

Ge, H., Tollner, T.L., Hu, Z., Da, M., Li, X., Guan, H., Shan, D., Lu, J., Huang, C., Dong, Q., 2012. Impaired mitochondrial function in murine oocytes is associated with controlled ovarian hyperstimulation and in vitro maturation. Reproduction, fertility, and development 24, 945-952.

Genicot, G., Leroy, J.L., Soom, A.V., Donnay, I., 2005. The use of a fluorescent dye, Nile red, to evaluate the lipid content of single mammalian oocytes. Theriogenology 63, 1181-1194.

Gentile, L., Monti, M., Sebastiano, V., Merico, V., Nicolai, R., Calvani, M., Garagna, S., Redi, C.A., Zuccotti, M., 2004. Single-cell quantitative RT-PCR analysis of Cpt1b and Cpt2 gene expression in mouse antral oocytes and in preimplantation embryos. Cytogenet Genome Res 105, 215-221.

Gibbons, J., Wiltbank, M., Ginther, O., 1997a. Functional interrelationships between follicles greater than 4 mm and the follicle-stimulating hormone surge in heifers. Biology of reproduction 57, 1066-1073.

Gibbons, J.R., Wiltbank, M.C., Ginther, O.J., 1997b. Functional interrelationships between follicles greater than 4 mm and the follicle-stimulating hormone surge in heifers. Biology of reproduction 57, 1066-1073.

Ginther, O., Bergfelt, D., Kulick, L., Kot, K., 1999. Selection of the dominant follicle in cattle: establishment of follicle deviation in less than 8 hours through depression of FSH concentrations. Theriogenology 52, 1079-1172.

Ginther, O., Khan, F., Hannan, M., Rodriguez, M., Pugliesi, G., Beg, M., 2012a. Role of LH in luteolysis and growth of the ovulatory follicle and estradiol regulation of LH secretion in heifers. Theriogenology 77, 1442-1494.

Ginther, O.J., Bergfelt, D.R., Kulick, L.J., Kot, K., 2000a. Selection of the dominant follicle in cattle: role of estradiol. Biology of reproduction 63, 383-389.

Ginther, O.J., Bergfelt, D.R., Kulick, L.J., Kot, K., 2000b. Selection of the dominant follicle in cattle: role of two-way functional coupling between follicle-stimulating hormone and the follicles. Biology of reproduction 62, 920-927.

Ginther, O.J., Khan, F.A., Hannan, M.A., Rodriguez, M.B., Pugliesi, G., Beg, M.A., 2012b. Role of LH in luteolysis and growth of the ovulatory follicle and estradiol regulation of LH secretion in heifers. Theriogenology 77, 1442-1452.

Ginther, O.J., Knopf, L., Kastelic, J.P., 1989. Temporal associations among ovarian events in cattle during oestrous cycles with two and three follicular waves. Journal of reproduction and fertility 87, 223-230.

Glater, E.E., Megeath, L.J., Stowers, R.S., Schwarz, T.L., 2006. Axonal transport of mitochondria requires milton to recruit kinesin heavy chain and is light chain independent. J Cell Biol 173, 545-557.

Greenspan, P., Fowler, S.D., 1985. Spectrofluorometric studies of the lipid probe, nile red. J Lipid Res 26, 781-789.

Greenspan, P., Mayer, E.P., Fowler, S.D., 1985. Nile red: a selective fluorescent stain for intracellular lipid droplets. The Journal of cell biology 100, 965-973.

Hagemann, L.J., Beaumont, S.E., Berg, M., Donnison, M.J., Ledgard, A., Peterson, A.J., Schurmann, A., Tervit, H.R., 1999. Development during single IVP of bovine

oocytes from dissected follicles: interactive effects of estrous cycle stage, follicle size and atresia. Mol Reprod Dev 53, 451-458.

Hamatani, T., Falco, G., Carter, M., Akutsu, H., Stagg, C., Sharov, A., Dudekula, D., VanBuren, V., Ko, M., 2004. Age-associated alteration of gene expression patterns in mouse oocytes. Hum Mol Genet 13, 2263-2341.

He, C.L., Damiani, P., Parys, J.B., Fissore, R.A., 1997. Calcium, calcium release receptors, and meiotic resumption in bovine oocytes. Biology of reproduction 57, 1245-1255.

Hendriksen, P.J., Vos, P.L., Steenweg, W.N., Bevers, M.M., Dieleman, S.J., 2000. Bovine follicular development and its effect on the in vitro competence of oocytes. Theriogenology 53, 11-20.

Hsieh, M., Zamah, A., Conti, M., 2009. Epidermal growth factor-like growth factors in the follicular fluid: role in oocyte development and maturation. Seminars in reproductive medicine 27, 52-113.

Huang, P., Yu, T., Yoon, Y., 2007. Mitochondrial clustering induced by overexpression of the mitochondrial fusion protein Mfn2 causes mitochondrial dysfunction and cell death. European journal of cell biology 86, 289-591.

Hyttel, P., Callesen, H., Greve, T., 1986a. Ultrastructural features of preovulatory oocyte maturation in superovulated cattle. Journal of reproduction and fertility 76, 645-656.

Hyttel, P., Callesen, H., Greve, T., 1989a. A comparative ultrastructural study of in vivo versus in vitro fertilization of bovine oocytes. Anatomy and embryology 179, 435-442.

Hyttel, P., Greve, T., Callesen, H., 1989b. Ultrastructural aspects of oocyte maturation and fertilization in cattle. J Reprod Fertil Suppl 38, 35-47.

Hyttel, P., Greve, T., Callesen, H., 1989c. Ultrastructure of oocyte maturation and fertilization in superovulated cattle. Prog Clin Biol Res 296, 287-297.

Hyttel, P., Xu, K.P., Smith, S., Callesen, H., Greve, T., 1987. Ultrastructure of the final nuclear maturation of bovine oocytes in vitro. Anat Embryol (Berl) 176, 35-40.

Hyttel, P., Xu, K.P., Smith, S., Greve, T., 1986b. Ultrastructure of in-vitro oocyte maturation in cattle. J Reprod Fertil 78, 615-625.

Iino, M., 2010. Spatiotemporal dynamics of Ca 2+ signaling and its physiological roles. Proceedings of the Japan Academy.

Ireland, J.J., Coulson, P.B., Murphree, R.L., 1979. Follicular development during four stages of the estrous cycle of beef cattle. Journal of animal science 49, 1261-1269.

Ireland, J.J., Roche, J.F., 1982. Effect of progesterone on basal LH and episodic LH and FSH secretion in heifers. J Reprod Fertil 64, 295-302.

Iwata, H., Goto, H., Tanaka, H., Sakaguchi, Y., Kimura, K., Kuwayama, T., Monji, Y., 2011. Effect of maternal age on mitochondrial DNA copy number, ATP content and IVF outcome of bovine oocytes. Reproduction, fertility, and development 23, 424-456.

Jaiswal, R.S., 2007. Regulation of follicular wave patterns in cattle [PhD dissertation]. Veterinary Biomedical Sciences, University of Saskatchewan, Saskatoon (SK).

Jaiswal, R.S., Singh, J., Adams, G.P., 2004. Developmental pattern of small antral follicles in the bovine ovary. Biology of reproduction 71, 1244-1251.

Jaiswal, R.S., Singh, J., Marshall, L., Adams, G.P., 2009. Repeatability of 2-wave and 3-wave patterns of ovarian follicular development during the bovine estrous cycle. Theriogenology 72, 81-90.

Jansen, R.P., de Boer, K., 1998. The bottleneck: mitochondrial imperatives in oogenesis and ovarian follicular fate. Mol Cell Endocrinol 145, 81-88.

Jeong, W., Cho, S., Lee, H., Deb, G., Lee, Y., Kwon, T., Kong, I., 2009. Effect of cytoplasmic lipid content on in vitro developmental efficiency of bovine IVP embryos. Theriogenology 72, 584-593.

Kaneko, H., Nakanishi, Y., Taya, K., Kishi, H., Watanabe, G., Sasamoto, S., Hasegawa, Y., 1993. Evidence that inhibin is an important factor in the regulation of FSH secretion during the mid-luteal phase in cows. The Journal of endocrinology 136, 35-76.

Kaneko, H., Noguchi, J., Kikuchi, K., Todoroki, J., Hasegawa, Y., 2002. Alterations in peripheral concentrations of inhibin A in cattle studied using a time-resolved immunofluorometric assay: relationship with estradiol and follicle-stimulating hormone in various reproductive conditions. Biology of reproduction 67, 38-45.

Kaneko, H., Taya, K., Watanabe, G., Noguchi, J., Kikuchi, K., Shimada, A., Hasegawa, Y., 1997. Inhibin is involved in the suppression of FSH secretion in the growth phase of the dominant follicle during the early luteal phase in cows. Domest Anim Endocrinol 14, 263-334.

Kanka, J., Nemcova, L., Toralova, T., Vodickova-Kepkova, K., Vodicka, P., Jeseta, M., Machatkova, M., 2012. Association of the transcription profile of bovine oocytes and embryos with developmental potential. Animal reproduction science 134, 29-35.

Kasimanickam, R., Collins, J., Wuenschell, J., Currin, J., Hall, J., Whittier, D., 2006. Effect of timing of prostaglandin administration, controlled internal drug release removal and gonadotropin releasing hormone administration on pregnancy rate in fixedtime AI protocols in crossbred Angus cows. Theriogenology 66, 166-172.

Kawashima, I., Liu, Z., Mullany, L., Mihara, T., Richards, J., Shimada, M., 2012. EGF-Like Factors Induce Expansion of the Cumulus Cell-Oocyte Complexes by Activating Calpain-Mediated Cell Movement. Endocrinology.

Kim, J.Y., Kinoshita, M., Ohnishi, M., Fukui, Y., 2001. Lipid and fatty acid analysis of fresh and frozen-thawed immature and in vitro matured bovine oocytes. Reproduction 122, 131-138.

Kim, N.H., Cho, S.K., Choi, S.H., Kim, E.Y., Park, S.P., Lim, J.H., 2000. The distribution and requirements of microtubules and microfilaments in bovine oocytes during in vitro maturation. Zygote 8, 25-32.

Kinder, J.E., Kojima, F.N., Bergfeld, E.G.M., Wehrman, M.E., Fike, K.E., 1996. Progestin and estrogen regulation of pulsatile LH release and development of persistent ovarian follicles in cattle. J Anim Sci 74, 1424-1440.

Kirshner, H., Aguet, F., Sage, D., Unser, M., 2012. 3-D PSF fitting for fluorescence microscopy: implementation and localization application. J Microsc.

Knopf, L., Kastelic, J.P., Schallenberger, E., Ginther, O.J., 1989. Ovarian follicular dynamics in heifers: test of two-wave hypothesis by ultrasonically monitoring individual follicles. Domest Anim Endocrinol 6, 111-119.

Ko, J., Kastelic, J., Del Campo, M., Ginther, O., 1991. Effects of a dominant follicle on ovarian follicular dynamics during the oestrous cycle in heifers. Journal of reproduction and fertility 91, 511-520.

Kruip, T.A.M., Cran, D.G., van Beneden, T.H., Dieleman, S.J., 1983. Structural changes in bovine oocytes during final maturation in vivo. Gamete Research 8, 29-47.

Lamb, G.C., Stevenson, J.S., Kesler, D.J., Garverick, H.A., Brown, D.R., Salfen, B.E., 2001. Inclusion of an intravaginal progesterone insert plus GnRH and prostaglandin F2alpha for ovulation control in postpartum suckled beef cows. J Anim Sci 79, 2253-2259.

Laster, D.B., 1972. Disappearance and uptake of (125 I)FSH in the rat, rabbit, ewe and cow. Journal of reproduction and fertility 30, 407-415.

Liu, M., 2011. The biology and dynamics of mammalian cortical granules. Reproductive biology and endocrinology : RB&E 9, 149.

Liu, S., Li, Y., Feng, H.L., Yan, J.H., Li, M., Ma, S.Y., Chen, Z.J., 2010. Dynamic modulation of cytoskeleton during in vitro maturation in human oocytes. Am J Obstet Gynecol 203, 151 e151-157.

Liu, Y., Sui, H.S., Wang, H.L., Yuan, J.H., Luo, M.J., Xia, P., Tan, J.H., 2006. Germinal vesicle chromatin configurations of bovine oocytes. Microsc Res Tech 69, 799-807.

Lonergan, P., 2011. Influence of progesterone on oocyte quality and embryo development in cows. Theriogenology 76, 1594-1601.

Lonergan, P., Monaghan, P., Rizos, D., Boland, M.P., Gordon, I., 1994. Effect of follicle size on bovine oocyte quality and developmental competence following maturation, fertilization, and culture in vitro. Mol Reprod Dev 37, 48-53.

Looney, C.R., Boutte, B.W., Archbald, L.F., Godke, R.A., 1981. Comparison of once daily and twice daily FSH injections for superovulating beef cattle. Theriogenology 15, 13-22.

Lucy, M.C., Billings, H.J., Butler, W.R., Ehnis, L.R., Fields, M.J., Kesler, D.J., Kinder, J.E., Mattos, R.C., Short, R.E., Thatcher, W.W., Wettemann, R.P., Yelich, J.V., Hafs, H.D., 2001. Efficacy of an intravaginal progesterone insert and an injection of PGF2alpha for synchronizing estrus and shortening the interval to pregnancy in postpartum beef cows, peripubertal beef heifers, and dairy heifers. J Anim Sci 79, 982-995.

Luo, W., Gumen, A., Haughian, J.M., Wiltbank, M.C., 2011. The role of luteinizing hormone in regulating gene expression during selection of a dominant follicle in cattle. Biology of reproduction 84, 369-378.

Lussier, J.G., Matton, P., Dufour, J.J., 1987. Growth rates of follicles in the ovary of the cow. Journal of reproduction and fertility 81, 301-307.

Machaca, K., 2007. Ca2+ signaling differentiation during oocyte maturation. Journal of cellular physiology 213, 331-371.

Machatkova, M., Jeseta, M., Hulinska, P., Knitlova, D., Nemcova, L., Kanka, J., 2011. Characteristics of Bovine Oocytes with Different Meiotic Competence in Terms of Their Mitochondrial Status and Expression of Nuclear-Encoded Factors. Reproduction in domestic animals = Zuchthygiene.

Machatkova, M., Jeseta, M., Hulinska, P., Knitlova, D., Nemcova, L., Kanka, J., 2012. Characteristics of bovine oocytes with different meiotic competence in terms of their mitochondrial status and expression of nuclear-encoded factors. Reproduction in domestic animals = Zuchthygiene 47, 806-814.

Macmillan, K.L., 2010. Recent advances in the synchronization of estrus and ovulation in dairy cows. J Reprod Dev 56 Suppl, S42-47.

Mahmood, T., Saridogan, E., Smutna, S., Habib, A.M., Djahanbakhch, O., 1998. The effect of ovarian steroids on epithelial ciliary beat frequency in the human Fallopian tube. Hum Reprod 13, 2991-2994.

Malhi, P., 2007. A bovine model to study reproductive aging, Veterinary Biomedical Sciences, University of Saskatchewan, Saskatoon.

Malhi, P., Adams, G., Mapletoft, R., Singh, J., 2007. Oocyte developmental competence in a bovine model of reproductive aging. Reproduction (Cambridge, England) 134, 233-242.

Malhi, P., Adams, G., Singh, J., 2005. Bovine model for the study of reproductive aging in women: follicular, luteal, and endocrine characteristics. Biology of reproduction 73, 45-98.

Mapletoft, R., Steward, K., Adams, G., 2002. Recent advances in the superovulation in cattle. Reprod Nutr Dev 42, 601-612.

Mapletoft, R.J., Bo, G.A., 2011. The evolution of improved and simplified superovulation protocols in cattle. Reproduction, fertility, and development 24, 278-283.

Mapletoft, R.J., Martinez, M.F., Colazo, M.G., Kastelic, J.P., 2003. The use of controlled internal drug release devices for the regulation of bovine reproduction. J Anim Sci 81, E28-E36.

Marchesan, D., Rutberg, M., Andersson, L., Asp, L., Larsson, T., Borén, J., Johansson, B., Olofsson, S.-O., 2003. A phospholipase D-dependent process forms lipid droplets containing caveolin, adipocyte differentiation-related protein, and vimentin in a cell-free system. J Biol Chem 278, 27293-27593.

Marei, W.F., Wathes, D.C., Fouladi-Nashta, A.A., 2012. Differential effects of linoleic and alpha-linolenic fatty acids on spatial and temporal mitochondrial distribution and activity in bovine oocytes. Reproduction, fertility, and development 24, 679-690.

Martin, S., Parton, R., 2006. Lipid droplets: a unified view of a dynamic organelle. Nature reviews. Molecular cell biology 7, 373-381.

Martinez, M., Kastelic, J., Adams, G., Cook, B., Olson, W., Mapletoft, R., 2002. The use of progestins in regimens for fixed-time artificial insemination in beef cattle. Theriogenology 57, 1049-1059.

Martinez, M., Kastelic, J., Adams, G., Mapletoft, R., 2001. The use of GnRH or estradiol to facilitate fixed-time insemination in an MGA-based synchronization regimen in beef cattle. Anim Reprod Sci 67, 221-229.

Martinez, M.F., Adams, G.P., Kastelic, J.P., Bergfelt, D.R., Mapletoft, R.J., 2000. Induction of follicular wave emergence for estrus synchronization and artificial insemination in heifers. Theriogenology 54, 757-769.

Martinez, M.F., Kastelic, J.P., Mapletoft, R.J., 2004. The use of estradiol and/or GnRH in a two-dose PGF protocol for breeding management of beef heifers. Theriogenology 62, 363-372.

May-Panloup, P., Vignon, X., Chrétien, M.-F., Heyman, Y., Tamassia, M., Malthièry, Y., Reynier, P., 2005. Increase of mitochondrial DNA content and transcripts

in early bovine embryogenesis associated with upregulation of mtTFA and NRF1 transcription factors. Reproductive biology and endocrinology : RB&E 3, 65.

McEvoy, T.G., Coull, G.D., Broadbent, P.J., Hutchinson, J.S., Speake, B.K., 2000. Fatty acid composition of lipids in immature cattle, pig and sheep oocytes with intact zona pellucida. Journal of reproduction and fertility 118, 163-170.

McKeegan, P.J., Sturmey, R.G., 2011. The role of fatty acids in oocyte and early embryo development. Reproduction, fertility, and development 24, 59-67.

Mehlmann, L., 2005. Oocyte-specific expression of Gpr3 is required for the maintenance of meiotic arrest in mouse oocytes. Dev Biol 288, 397-801.

Meireles, S.I., Esteves, G.H., Hirata, R., Jr., Peri, S., Devarajan, K., Slifker, M., Mosier, S.L., Peng, J., Vadhanam, M.V., Hurst, H.E., Neves, E.J., Reis, L.F., Gairola, C.G., Gupta, R.C., Clapper, M.L., 2010. Early changes in gene expression induced by tobacco smoke: Evidence for the importance of estrogen within lung tissue. Cancer Prev Res (Phila) 3, 707-717.

Mihm, M., Crowe, M.A., Knight, P.G., Austin, E.J., 2002. Follicle wave growth in cattle. Reprod Domest Anim 37, 191-200.

Mihm, M., Curran, N., Hyttel, P., Knight, P.G., Boland, M.P., Roche, J.F., 1999. Effect of dominant follicle persistence on follicular fluid oestradiol and inhibin and on oocyte maturation in beef heifers. J Reprod Fertil 116, 293-304.

Minksy, M., 1961. Microsopy apparatus, In: Office, U.S.P. (Ed.), United States.

Motlik, J., Koefoed-Johnsen, H.H., Fulka, J., 1978. Breakdown of the germinal vesicle in bovine oocytes cultivated in vitro. J Exp Zool 205, 377-383.

Munro, R.K., 1987. Concentrations of plasma progesterone in cows after treatment with 3 types of progesterone pessaries. Aust Vet J 64, 385-386.

Murphy, D.J., 2001. The biogenesis and functions of lipid bodies in animals, plants and microorganisms. Prog Lipid Res 40, 325-438.

Mussard, M.L., Burke, C.R., Behlke, E.J., Gasser, C.L., Day, M.L., 2007. Influence of premature induction of a luteinizing hormone surge with gonadotropin-releasing hormone on ovulation, luteal function, and fertility in cattle. J Anim Sci 85, 937-943.

Nagano, M., Katagiri, S., Takahashi, Y., 2006. ATP content and maturational/developmental ability of bovine oocytes with various cytoplasmic morphologies. Zygote (Cambridge, England) 14, 299-603.

Nangaku, M., Sato-Yoshitake, R., Okada, Y., Noda, Y., Takemura, R., Yamazaki, H., Hirokawa, N., 1994. KIF1B, a novel microtubule plus end-directed monomeric motor protein for transport of mitochondria. Cell 79, 1209-1220.

Nasser, L.F., Adams, G.P., Bo, G.A., Mapletoft, R.J., 1993. Ovarian superstimulatory response relative to follicular wave emergence in heifers. Theriogenology 40, 713-724.

Nivet, A.L., Bunel, A., Labrecque, R., Belanger, J., Vigneault, C., Blondin, P., Sirard, M.A., 2012. FSH withdrawal improves developmental competence of oocytes in the bovine model. Reproduction 143, 165-171.

Norris, R., Freudzon, M., Mehlmann, L., Cowan, A., Simon, A., Paul, D., Lampe, P., Jaffe, L., 2008. Luteinizing hormone causes MAP kinase-dependent phosphorylation and closure of connexin 43 gap junctions in mouse ovarian follicles: one of two paths to meiotic resumption. Development (Cambridge, England) 135, 3229-3267.

Norris, R., Ratzan, W., Freudzon, M., Mehlmann, L., Krall, J., Movsesian, M., Wang, H., Ke, H., Nikolaev, V., Jaffe, L., 2009. Cyclic GMP from the surrounding somatic cells regulates cyclic AMP and meiosis in the mouse oocyte. Development (Cambridge, England) 136, 1869-1947.

Olofsson, S.-O., Boström, P., Andersson, L., Rutberg, M., Perman, J., Borén, J., 2009. Lipid droplets as dynamic organelles connecting storage and efflux of lipids. Biochimica et biophysica acta 1791, 448-506.

Ost, A., Ortegren, U., Gustavsson, J., Nystrom, F., Strålfors, P., 2005. Triacylglycerol is synthesized in a specific subclass of caveolae in primary adipocytes. J Biol Chem 280, 5-13.

Palma, G.A., Arganaraz, M.E., Barrera, A.D., Rodler, D., Mutto, A.A., Sinowatz, F., 2012. Biology and biotechnology of follicle development. ScientificWorldJournal 2012, 938138.

Pape-Zambito, D.A., Roberts, R.F., Kensinger, R.S., 2010. Estrone and 17beta-estradiol concentrations in pasteurized-homogenized milk and commercial dairy products. Journal of dairy science 93, 2533-2540.

Parone, P., Martinou, J.-C., 2006. Mitochondrial fission and apoptosis: an ongoing trial. Biochimica et biophysica acta 1763, 522-552.

Patterson, D.J., Perry, R.C., Kiracofe, G.H., Bellows, R.A., Staigmiller, R.B., Corah, L.R., 1992. Management considerations in heifer development and puberty. Journal of animal science 70, 4018-4035.

Perry, G.A., 2012. Physiology and Endocrinology Symposium: Harnessing basic knowledge of factors controlling puberty to improve synchronization of estrus and fertility in heifers. Journal of animal science 90, 1172-1182.

Perry, G.A., M. F. Smith, M. C. Lucy, J. A. Green, T. E. Parks, M. D. MacNeil, Roberts, A.J., Geary., T.W., 2005. Relationship between follicle size at insemination and pregnancy success. Proc. Natl. Acad. Sci. USA 102, 5268-5273.

Perry, S.W., Norman, J.P., Barbieri, J., Brown, E.B., Gelbard, H.A., 2011. Mitochondrial membrane potential probes and the proton gradient: a practical usage guide. Biotechniques 50, 98-115.

Peters, M.W., Pursley, J.R., 2003. Timing of final GnRH of the Ovsynch protocol affects ovulatory follicle size, subsequent luteal function, and fertility in dairy cows. Theriogenology 60, 1197-1204.

Pfeifer, L.F., Mapletoft, R.J., Kastelic, J.P., Small, J.A., Adams, G.P., Dionello, N.J., Singh, J., 2009. Effects of low versus physiologic plasma progesterone concentrations on ovarian follicular development and fertility in beef cattle. Theriogenology 72, 1237-1250.

Pierson, R.A., Ginther, O.J., 1984. Ultrasonography of the bovine ovary. Theriogenology 21, 495-504.

Pierson, R.A., Ginther, O.J., 1988. Ultrasonic imaging of the ovaries and uterus in cattle. Theriogenology 29, 21-37.

Pincus, G., Enzmann, E.V., 1935. The Comparative Behavior of Mammalian Eggs in Vivo and in Vitro : I. The Activation of Ovarian Eggs. J Exp Med 62, 665-675.

Poot, M., Zhang, Y.Z., Kramer, J.A., Wells, K.S., Jones, L.J., Hanzel, D.K., Lugade, A.G., Singer, V.L., Haugland, R.P., 1996. Analysis of mitochondrial morphology and function with novel fixable fluorescent stains. J Histochem Cytochem 44, 1363-1372.

Prentice-Biensch, J.R., Singh, J., Mapletoft, R.J., Anzar, M., 2012. Vitrification of immature bovine cumulus-oocyte complexes: effects of cryoprotectants, the vitrification procedure and warming time on cleavage and embryo development. Reproductive biology and endocrinology : RB&E 10, 73.

Pursley, J.R., Mee, M.O., Wiltbank, M.C., 1995. Synchronization of ovulation in dairy cows using PGF2alpha and GnRH. Theriogenology 44, 915-923.

Racedo, S., Rawe, V., Niemann, H., 2012. Dynamic changes of the Golgi apparatus during bovine in vitro oocyte maturation. Reproduction (Cambridge, England) 143, 439-486.

Rahe, C., Owens, R., Fleeger, J., Newton, H., Harms, P., 1980. Pattern of plasma luteinizing hormone in the cyclic cow: dependence upon the period of the cycle. Endocrinology 107, 498-1001.

Ramalho-Santos, J.o., Varum, S., Amaral, S., Mota, P., Sousa, A., Amaral, A., 2009. Mitochondrial functionality in reproduction: from gonads and gametes to embryos and embryonic stem cells. Human reproduction update 15, 553-625.

Rathbone, M., Kinder, J., Fike, K., Kojima, F., Clopton, D., Ogle, C., Bunt, C., 2001a. Recent advances in bovine reproductive endocrinology and physiology and their impact on drug delivery system design for the control of the estrous cycle in cattle. Adv Drug Deliv Rev 50, 277-320.

Rathbone, M.J., Kinder, J.E., Fike, K., Kojima, F., Clopton, D., Ogle, C.R., Bunt, C.R., 2001b. Recent advances in bovine reproductive endocrinology and physiology and their impact on drug delivery system design for the control of the estrous cycle in cattle. Adv Drug Deliv Rev 50, 277-320.

Reames, P.S., Hatler, T.B., Hayes, S.H., Ray, D.L., Silvia, W.J., 2011. Differential regulation of estrous behavior and luteinizing hormone secretion by estradiol-17beta in ovariectomized dairy cows. Theriogenology 75, 233-240.

Reis, A.M., Mills, W.K., Ramachandran, I., Friedberg, E.C., Thompson, D., Queimado, L., 2012. Targeted detection of in vivo endogenous DNA base damage reveals preferential base excision repair in the transcribed strand. Nucleic Acids Res 40, 206-219.

Revah, I., Butler, W., 1996. Prolonged dominance of follicles and reduced viability of bovine oocytes. Journal of reproduction and fertility 106, 39-86.

Reynier, P., May-Panloup, P., Chretien, M.F., Morgan, C.J., Jean, M., Savagner, F., Barriere, P., Malthiery, Y., 2001. Mitochondrial DNA content affects the fertilizability of human oocytes. Mol Hum Reprod 7, 425-429.

Rivera, F.A., Mendonca, L.G., Lopes, G., Jr., Santos, J.E., Perez, R.V., Amstalden, M., Correa-Calderon, A., Chebel, R.C., 2011. Reduced progesterone concentration during growth of the first follicular wave affects embryo quality but has no effect on embryo survival post transfer in lactating dairy cows. Reproduction 141, 333-342.

Robenek, H., Hofnagel, O., Buers, I., Robenek, M., Troyer, D., Severs, N., 2006. Adipophilin-enriched domains in the ER membrane are sites of lipid droplet biogenesis. J Cell Sci 119, 4215-4239.

Robinson, R.S., Hammond, A.J., Hunter, M.G., Mann, G.E., 2005. The induction of a delayed post-ovulatory progesterone rise in dairy cows: a novel model. Domest Anim Endocrinol 28, 285-295.

Roche, J., Mihm, M., 1997. Physiology and practice of induction and control of oestrus in cattle. The bovine Practitioner, 4-14.

Roelofs, J., Lopez-Gatius, F., Hunter, R.H., van Eerdenburg, F.J., Hanzen, C., 2010. When is a cow in estrus? Clinical and practical aspects. Theriogenology 74, 327-344.

Romek, M., Gajda, B., Krzysztofowicz, E., Kepczynski, M., Smorag, Z., 2011. New technique to quantify the lipid composition of lipid droplets in porcine oocytes and pre-implantation embryos using Nile Red fluorescent probe. Theriogenology 75, 42-54.

Rothman, J., 1994. Mechanisms of intracellular protein transport. Nature 372, 55-118.

Santos, J.E., Narciso, C.D., Rivera, F., Thatcher, W.W., Chebel, R.C., 2010. Effect of reducing the period of follicle dominance in a timed artificial insemination protocol on reproduction of dairy cows. Journal of dairy science 93, 2976-2988.

Sato, M., Sato, K., 2012. Maternal inheritance of mitochondrial DNA: Degradation of paternal mitochondria by allogeneic organelle autophagy, allophagy. Autophagy 8.

Savio, J., Keenan, L., Boland, M., Roche, J., 1988a. Pattern of growth of dominant follicles during the oestrous cycle of heifers. Journal of reproduction and fertility 83, 663-734.

Savio, J.D., Keenan, L., Boland, M.P., Roche, J.F., 1988b. Pattern of growth of dominant follicles during the oestrous cycle of heifers. Journal of reproduction and fertility 83, 663-671.

Savio, J.D., Thatcher, W.W., Morris, G.R., Entwistle, K., Drost, M., Mattiacci, M.R., 1993. Effects of induction of low plasma progesterone concentrations with a progesterone-releasing intravaginal device on follicular turnover and fertility in cattle. Journal of reproduction and fertility 98, 77-84.

Scarpulla, R.C., 2008. Transcriptional paradigms in mammalian mitochondrial biogenesis and function. Physiol Rev 88, 611-638.

Schafer, D.J., Bader, J.F., Meyer, J.P., Haden, J.K., Ellersieck, M.R., Lucy, M.C., Smith, M.F., Patterson, D.J., 2007. Comparison of progestin-based protocols to synchronize estrus and ovulation before fixed-time artificial insemination in postpartum beef cows. J Anim Sci 85, 1940-1945.

Schwartz, D., Mayaux, M.J., 1982. Female fecundity as a function of age: results of artificial insemination in 2193 nulliparous women with azoospermic husbands. Federation CECOS. N Engl J Med 306, 404-406.

Senger, P.L., Saacke, R.G., 1970. Unusual mitochondria of the bovine oocyte. J Cell Biol 46, 405-408.

Shahiduzzaman, A.K., Beg, M.A., Palhao, M.P., Siddiqui, M.A., Shamsuddin, M., Ginther, O.J., 2010. Stimulation of the largest subordinate follicle by intrafollicular treatment with insulin-like growth factor 1 is associated with inhibition of the dominant follicle in heifers. Theriogenology 74, 194-201.

Shkolnik, K., Tadmor, A., Ben-Dor, S., Nevo, N., Galiani, D., Dekel, N., 2011. Reactive oxygen species are indispensable in ovulation. Proceedings of the National Academy of Sciences of the United States of America 108, 1462-1469.

Siddiqui, M.A., Ferreira, J.C., Gastal, E.L., Beg, M.A., Cooper, D.A., Ginther, O.J., 2010. Temporal relationships of the LH surge and ovulation to echotexture and power Doppler signals of blood flow in the wall of the preovulatory follicle in heifers. Reproduction, fertility, and development 22, 1110-1117.

Singh, J., 1997. Bovine ovary: morphologic and biochemical kinetics, Veterinary Biomedical Sciences, University of Saskatchewan, Saskatoon

Singh, J., Pierson, R.A., Adams, G.P., 1998. Ultrasound image attributes of bovine ovarian follicles and endocrine and functional correlates. Journal of reproduction and fertility 112, 19-29.

Siqueira, L., Barreta, M., Gasperin, B., Bohrer, R., Santos, J., Buratini, J.J., Oliveira, J., Gonçalves, P., 2012. Angiotensin II, progesterone, and prostaglandins are sequential steps in the pathway to bovine oocyte nuclear maturation. Theriogenology 77, 1779-1866.

Sirard, M., 2001. Resumption of meiosis: mechanism involved in meiotic progression and its relation with developmental competence. Theriogenology 55, 1241-1295.

Sirard, M., Picard, L., Dery, M., Coenen, K., Blondin, P., 1999. The time interval between FSH administration and ovarian aspiration influences the development of cattle oocytes. Theriogenology 51, 699-1407.

Sirois, J., Fortune, J., 1988. Ovarian follicular dynamics during the estrous cycle in heifers monitored by real-time ultrasonography. Biology of reproduction 39, 308-325.

Skinner, D., Evans, N., Delaleu, B., Goodman, R., Bouchard, P., Caraty, A., 1998. The negative feedback actions of progesterone on gonadotropin-releasing hormone secretion are transduced by the classical progesterone receptor. Proceedings of the National Academy of Sciences of the United States of America 95, 10978-11061.

Somfai, T., Kaneda, M., Akagi, S., Watanabe, S., Haraguchi, S., Mizutani, E., Dang-Nguyen, T.Q., Geshi, M., Kikuchi, K., Nagai, T., 2011. Enhancement of lipid metabolism with L-carnitine during in vitro maturation improves nuclear maturation and cleavage ability of follicular porcine oocytes. Reproduction, fertility, and development 23, 912-920.

St John, J.C., 2012. Transmission, inheritance and replication of mitochondrial DNA in mammals: implications for reproductive processes and infertility. Cell Tissue Res 349, 795-808.

St John, J.C., Facucho-Oliveira, J., Jiang, Y., Kelly, R., Salah, R., 2010. Mitochondrial DNA transmission, replication and inheritance: a journey from the gamete through the embryo and into offspring and embryonic stem cells. Human reproduction update 16, 488-509.

Steuerwald, N., Bermúdez, M., Wells, D., Munné, S., Cohen, J., 2007. Maternal age-related differential global expression profiles observed in human oocytes. Reprod Biomed Online 14, 700-708.

Stock, A.E., Fortune, J.E., 1993. Ovarian follicular dominance in cattle: relationship between prolonged growth of the ovulatory follicle and endocrine parameters. Endocrinology 132, 1108-1114.

Stojkovic, M., Machado, S., Stojkovic, P., Zakhartchenko, V., Hutzler, P., Gonçalves, P., Wolf, E., 2001. Mitochondrial distribution and adenosine triphosphate content of bovine oocytes before and after in vitro maturation: correlation with morphological criteria and developmental capacity after in vitro fertilization and culture. Biology of reproduction 64, 904-913.

Stuart, J., Brown, M., 2006. Mitochondrial DNA maintenance and bioenergetics. Biochimica et biophysica acta 1757, 79-168.

Sturmey, R.G., O'Toole, P.J., Leese, H.J., 2006. Fluorescence resonance energy transfer analysis of mitochondrial:lipid association in the porcine oocyte. Reproduction 132, 829-837.

Su, L., Yang, S., He, X., Li, X., Ma, J., Wang, Y., Presicce, G., Ji, W., 2012. Effect of donor age on the developmental competence of bovine oocytes retrieved by ovum pick up. Reproduction in domestic animals = Zuchthygiene 47, 184-193.

Su, Y.Q., Sugiura, K., Li, Q., Wigglesworth, K., Matzuk, M.M., Eppig, J.J., 2010. Mouse oocytes enable LH-induced maturation of the cumulus-oocyte complex via promoting EGF receptor-dependent signaling. Mol Endocrinol 24, 1230-1239.

Sun, Q.Y., Wu, G.M., Lai, L., Park, K.W., Cabot, R., Cheong, H.T., Day, B.N., Prather, R.S., Schatten, H., 2001. Translocation of active mitochondria during pig oocyte maturation, fertilization and early embryo development in vitro. Reproduction 122, 155-163.

Sutton, M.L., Gilchrist, R.B., Thompson, J.G., 2003. Effects of in-vivo and in-vitro environments on the metabolism of the cumulus-oocyte complex and its influence on oocyte developmental capacity. Human reproduction update 9, 35-48.

Sutton-McDowall, M., Feil, D., Robker, R., Thompson, J., Dunning, K., 2012. Utilization of endogenous fatty acid stores for energy production in bovine preimplantation embryos. Theriogenology 77, 1632-1673.

Takagi, M., Kim, I.H., Izadyar, F., Hyttel, P., Bevers, M.M., Dieleman, S.J., Hendriksen, P.J., Vos, P.L., 2001. Impaired final follicular maturation in heifers after superovulation with recombinant human FSH. Reproduction 121, 941-951.

Tamassia, M., Nuttinck, F., May-Panloup, P., Reynier, P., Heyman, Y., Charpigny, G., Stojkovic, M., Hiendleder, S., Renard, J.P., Chastant-Maillard, S., 2004. In vitro embryo production efficiency in cattle and its association with oocyte adenosine triphosphate content, quantity of mitochondrial DNA, and mitochondrial DNA haplogroup. Biology of reproduction 71, 697-1401.

Tanaka, Y., Kanai, Y., Okada, Y., Nonaka, S., Takeda, S., Harada, A., Hirokawa, N., 1998. Targeted disruption of mouse conventional kinesin heavy chain, kif5B, results in abnormal perinuclear clustering of mitochondria. Cell 93, 1147-1158.

Tarazona, A., Rodríguez, J., Restrepo, L., Olivera-Angel, M., 2006. Mitochondrial activity, distribution and segregation in bovine oocytes and in embryos produced in vitro. Reproduction in domestic animals = Zuchthygiene 41, 5-16.

Tarin, J.J., Gomez-Piquer, V., Pertusa, J.F., Hermenegildo, C., Cano, A., 2004. Association of female aging with decreased parthenogenetic activation, raised MPF, and MAPKs activities and reduced levels of glutathione S-transferases activity and thiols in mouse oocytes. Molecular reproduction and development 69, 402-410.

Tatone, C., 2008. Oocyte senescence: a firm link to age-related female subfertility. Gynecological endocrinology : the official journal of the International Society of Gynecological Endocrinology 24, 59-122.

Törnell, J., Billig, H., Hillensjö, T., 1990. Resumption of rat oocyte meiosis is paralleled by a decrease in guanosine 3',5'-cyclic monophosphate (cGMP) and is inhibited by microinjection of cGMP. Acta physiologica Scandinavica 139, 511-518.

Tríbulo, A., Rogan, D., Tríbulo, H., Tríbulo, R., Mapletoft, R.J., Bó, G.A., 2012. Superovulation of beef cattle with a split-single intramuscular administration of Folltropin-V in two concentrations of hyaluronan. Theriogenology 77, 1679-1764.

Vailes, L.D., Washburn, S.P., Britt, J.H., 1992. Effects of various steroid milieus or physiological states on sexual behavior of Holstein cows. Journal of animal science 70, 2094-2103.

Valentini, L., Iorga, A., De Santis, T., Ambruosi, B., Reynaud, K., Chastant-Maillard, S., Guaricci, A., Caira, M., Dell'Aquila, M., 2010. Mitochondrial distribution patterns in canine oocytes as related to the reproductive cycle stage. Animal reproduction science 117, 166-243.

Van Blerkom, J., 1991. Microtubule mediation of cytoplasmic and nuclear maturation during the early stages of resumed meiosis in cultured mouse oocytes. Proc Natl Acad Sci U S A 88, 5031-5035.

Van Blerkom, J., 2011. Mitochondrial function in the human oocyte and embryo and their role in developmental competence. Mitochondrion 11, 797-813.

Van Blerkom, J., Davis, P., Alexander, S., 2003. Inner mitochondrial membrane potential (DeltaPsim), cytoplasmic ATP content and free Ca2+ levels in metaphase II mouse oocytes. Human reproduction (Oxford, England) 18, 2429-2469.

Van Blerkom, J., Davis, P., Lee, J., 1995. ATP content of human oocytes and developmental potential and outcome after in-vitro fertilization and embryo transfer. Human reproduction (Oxford, England) 10, 415-439.

van de Leemput, E.E., Vos, P.L., Zeinstra, E.C., Bevers, M.M., van der Weijden, G.C., Dieleman, S.J., 1999. Improved in vitro embryo development using in vivo matured oocytes from heifers superovulated with a controlled preovulatory LH surge. Theriogenology 52, 335-349.

van der Voort, H.T., Strasters, K.C., 1995. Restoration of confocal images for quantitative image analysis. J Microsc 178, 165-181.

Wai, T., Ao, A., Zhang, X., Cyr, D., Dufort, D., Shoubridge, E.A., 2010. The role of mitochondrial DNA copy number in mammalian fertility. Biology of reproduction 83, 52-62.

Walsh, J.H., Mantovani, R., Duby, R.T., Overstrom, E.W., Dobrinsky, J.R., Enright, W.J., Roche, J.F., Boland, M.P., 1993. The effects of once or twice daily injections of pFSH on superovulatory response in heifers. Theriogenology 40, 313-321.

Walsh, S.W., Williams, E.J., Evans, A.C., 2011. A review of the causes of poor fertility in high milk producing dairy cows. Animal reproduction science 123, 127-138.

Wang, H., Sreenevasan, U., Hu, H., Saladino, A., Polster, B.M., Lund, L.M., Gong, D.W., Stanley, W.C., Sztalryd, C., 2011. Perilipin 5, a lipid droplet-associated protein, provides physical and metabolic linkage to mitochondria. J Lipid Res 52, 2159-2168.

Wassarman, P., Josefowicz, W., 1978. Oocyte development in the mouse: an ultrastructural comparison of oocytes isolated at various stages of growth and meiotic competence. Journal of morphology 156, 209-244.

Weibel, E.R., Kistler, G.S., Scherle, W.F., 1966. Practical stereological methods for morphometric cytology. The Journal of cell biology 30, 23-38.

White, F.J., Wettemann, R.P., Looper, M.L., Prado, T.M., Morgan, G.L., 2002. Seasonal effects on estrous behavior and time of ovulation in nonlactating beef cows. Journal of animal science 80, 3053-3059.

Wilding, M., Dale, B., Marino, M., di Matteo, L., Alviggi, C., Pisaturo, M., Lombardi, L., De Placido, G., 2001. Mitochondrial aggregation patterns and activity in

human oocytes and preimplantation embryos. Human reproduction (Oxford, England) 16, 909-926.

Wiltbank, M.C., Sartori, R., Herlihy, M.M., Vasconcelos, J.L., Nascimento, A.B., Souza, A.H., Ayres, H., Cunha, A.P., Keskin, A., Guenther, J.N., Gumen, A., 2011. Managing the dominant follicle in lactating dairy cows. Theriogenology 76, 1568-1582.

Wu, S., Zhou, F., Zhang, Z., Xing, D., 2011. Mitochondrial oxidative stress causes mitochondrial fragmentation via differential modulation of mitochondrial fission-fusion proteins. The FEBS journal 278, 941-995.

Xu, Z., Garverick, H.A., Smith, G.W., Smith, M.F., Hamilton, S.A., Youngquist, R.S., 1995. Expression of follicle-stimulating hormone and luteinizing hormone receptor messenger ribonucleic acids in bovine follicles during the first follicular wave. Biology of reproduction 53, 951-957.

Yamamoto, T., Iwata, H., Goto, H., Shiratuki, S., Tanaka, H., Monji, Y., Kuwayama, T., 2010. Effect of maternal age on the developmental competence and progression of nuclear maturation in bovine oocytes. Molecular reproduction and development 77, 595-1199.

Yamashita, Y., Okamoto, M., Kawashima, I., Okazaki, T., Nishimura, R., Gunji, Y., Hishinuma, M., Shimada, M., 2011. Positive feedback loop between prostaglandin E2 and EGF-like factors is essential for sustainable activation of MAPK3/1 in cumulus cells during in vitro maturation of porcine cumulus oocyte complexes. Biology of reproduction 85, 1073-1155.

Yang, X., Dunning, K., Wu, L., Hickey, T., Norman, R., Russell, D., Liang, X., Robker, R., 2010. Identification of perilipin-2 as a lipid droplet protein regulated in oocytes during maturation. Reproduction, fertility, and development 22, 1262-1333.

Yie, S., Collins, J., Daya, S., Hughes, E., Sagle, M., Younglai, E., 1996. Polyploidy and failed fertilization in in-vitro fertilization are related to patient's age and gamete quality. Human reproduction (Oxford, England) 11, 614-617.

Yu, Y., Dumollard, R., Rossbach, A., Lai, F.A., Swann, K., 2010. Redistribution of mitochondria leads to bursts of ATP production during spontaneous mouse oocyte maturation. J Cell Physiol 224, 672-680.

Zamah, A., Hsieh, M., Chen, J., Vigne, J., Rosen, M., Cedars, M., Conti, M., 2010. Human oocyte maturation is dependent on LH-stimulated accumulation of the epidermal growth factor-like growth factor, amphiregulin. Human reproduction (Oxford, England) 25, 2569-2647.

Zhang, M., Xia, G., 2012. Hormonal control of mammalian oocyte meiosis at diplotene stage. Cellular and molecular life sciences : CMLS 69, 1279-1367.

Zhang, X., Wu, X., Lu, S., Guo, Y., Ma, X., 2006. Deficit of mitochondria-derived ATP during oxidative stress impairs mouse MII oocyte spindles. Cell research 16, 841-891.

Zhao, J., Li, Y., 2012. Adenosine triphosphate content in human unfertilized oocytes, undivided zygotes and embryos unsuitable for transfer or cryopreservation. J Int Med Res 40, 734-739.

Zhong, S., Ye, W.P., Feng, E., Lin, S.H., Liu, J.Y., Leong, J., Ma, C., Lin, Y.C., 2011. Serum derived from zeranol-implanted ACI rats promotes the growth of human breast cancer cells in vitro. Anticancer Res 31, 481-486.

Zick, M., Rabl, R., Reichert, A., 2009. Cristae formation-linking ultrastructure and function of mitochondria. Biochimica et biophysica acta 1793, 5-24.

Zoller, L.C., 1984. A quantitative electron microscopic analysis of the membrana granulosa of rat preovulatory follicles. Acta Anat (Basel) 118, 218-223.

APPENDIX A
10 WORK FLOW FOR SEGMENTATION OF 3D DATA (MITOCHONDRIAL STAINING)

10.1 Preliminary steps to consider before performing deconvolution (in Imaris 7.4)

- Zeiss generates .lsm file. Open it with Imaris 7.4 and look at the 3-D dataset. Decide whether we can use the whole z-stack. In our volume sets (that was a 20 µm z-stack) there was a drop in intensity at the middle of the stack (due to photobleaching). If needed (as in our case) crop the 3-D volume set to the depth that can be used for further processing. In our case (Mitochondrial staining in oocyte), we went for 10 µm stack.
- Cropping the z-stack. Go to "Edit" and click on the "Crop data". This will prop up following window.

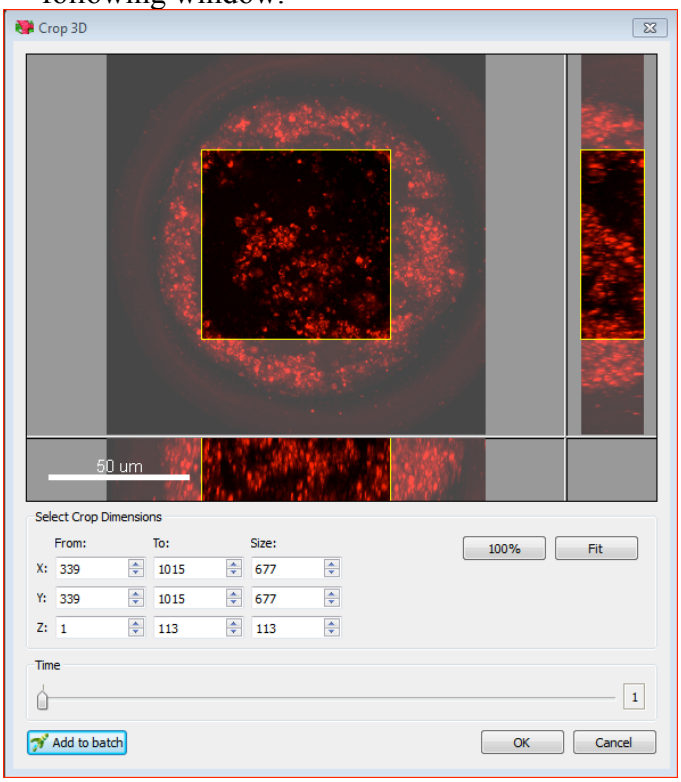

Windowpane 1: Cropping the 3-D volume sets.

For cropping, stretch the yellow box in the X-Y plane so that it aligns with the top, bottom, right and left sides. You select the depth in the z-direction by either moving the yellow box in the X-Z plane (bottom) or by changing the slice numbers for the z-axis. **I prefer doing the latter one, as it is faster and leaves little room for error.**

Note: This step is crucial to keep consistency across the different volume sets and also when you are adding a channel to existing dataset.

- Changing data type: This is needed to perform deconvolution as AutoquantX2 work with 32 bit images. Edit – Change data type – Make it "32 bit float data".

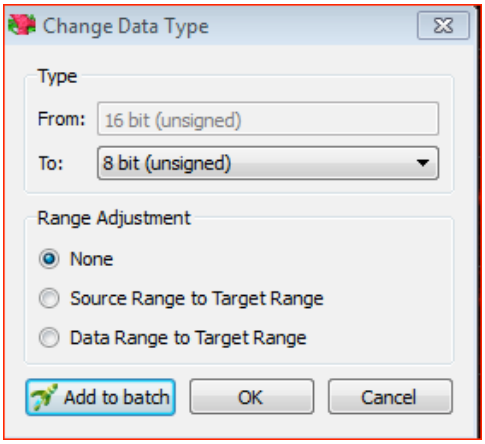

Windowpane 2 Changing 16 bit to 32 bitfloat image.

- Saving file for deconvolution: Saving as ".ids" file creates .ics and .ids (bigger) files for the same image. You will use ".ids" file to carry out deconvolution.

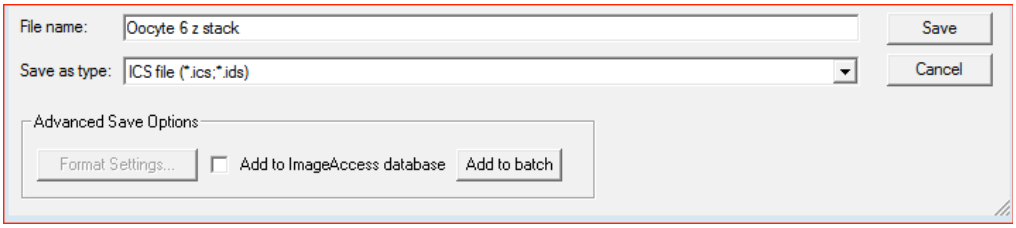

Windowpane 3: Saving image to .ids file format.

10.2 Deconvolution in Autoquant X2

- Import the ".ids" file (created as above). Pick the channel (if multichannel dataset) you want to deconvolute. Match up the following things to represent properties of image identical to those used for acquiring images. Check the size of voxel, type of microscopy, type of lens used and immersion medium used. Click on "Apply"

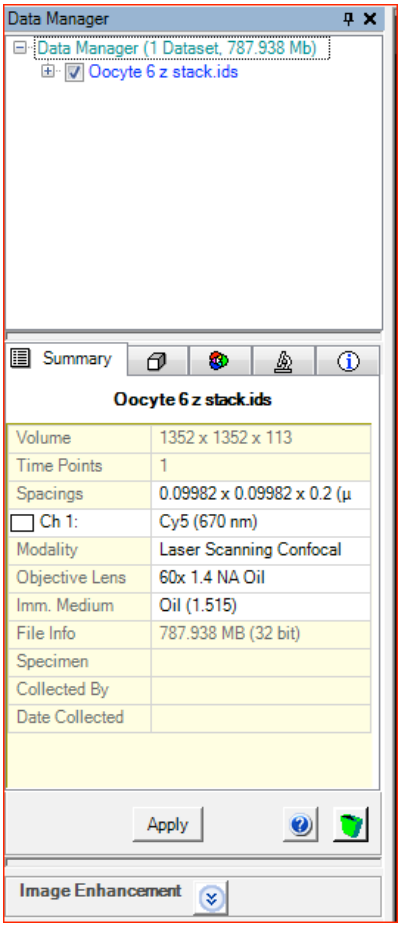

Windowpane 4: Summary of image properties.

Note: If you did something wrong here, it will show up under the 3-D deconvolution window (Window pane 9) and will be highlighted in red.

- Click on **3D button**  to initiate the deconvolution process.

Windowpane 5: Finding 3-D deconvolution button.

- This will open a side panel on the right side with 4 highlighted steps. The first two steps (Windowpane 6) designate the type of point-spread function we are going to use for deconvolution. We used blind method with theoretical PSF settings. We did try gathering acquired PSF but at this time that needs to be worked upon.

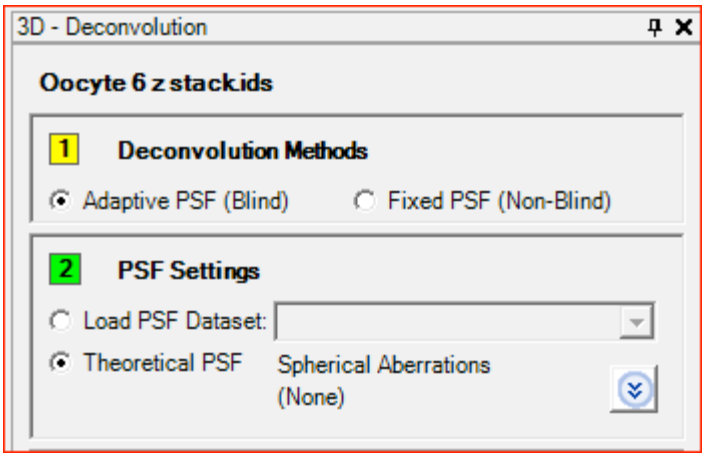

Windowpane 6: Point spread function.

- In the 3rd step (Windowpane 7), select deconvolution settings viz: iterations and noise level. This depends on the type of image you have. If you expect more noise:signal (as in my volume sets for mitochondria and lipid droplets), then go for higher number of iterations and high noise level (default setup is shown on the right). Unclick on the "use default" to go for manual settings.

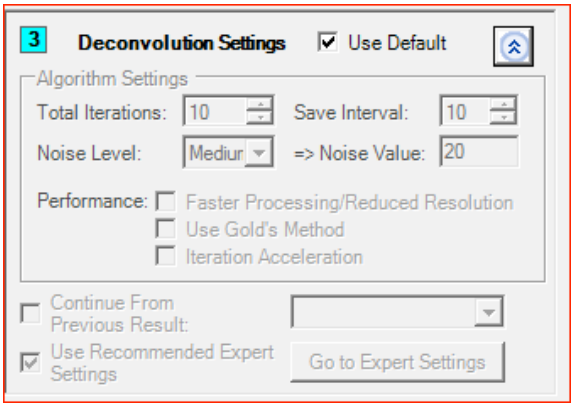

Windowpane 7: Changing the deconvolution settings.

- Under the output settings, choose the name, format (should be .lsm as you want to work latter in Imaris) and location of the output file.

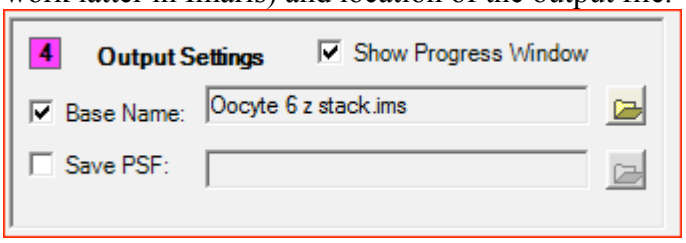

Windowpane 8: Saving the deconvolved image.

- Batch processing multiple images for deconvolution. I found this option very useful as it saves time and effort. But you need to make sure that all output files have been saved and you do not overburden the processing power of the computer. For the current processing power of the computer we have, you can batch process 12-15 images at a time. For batch processing, click 

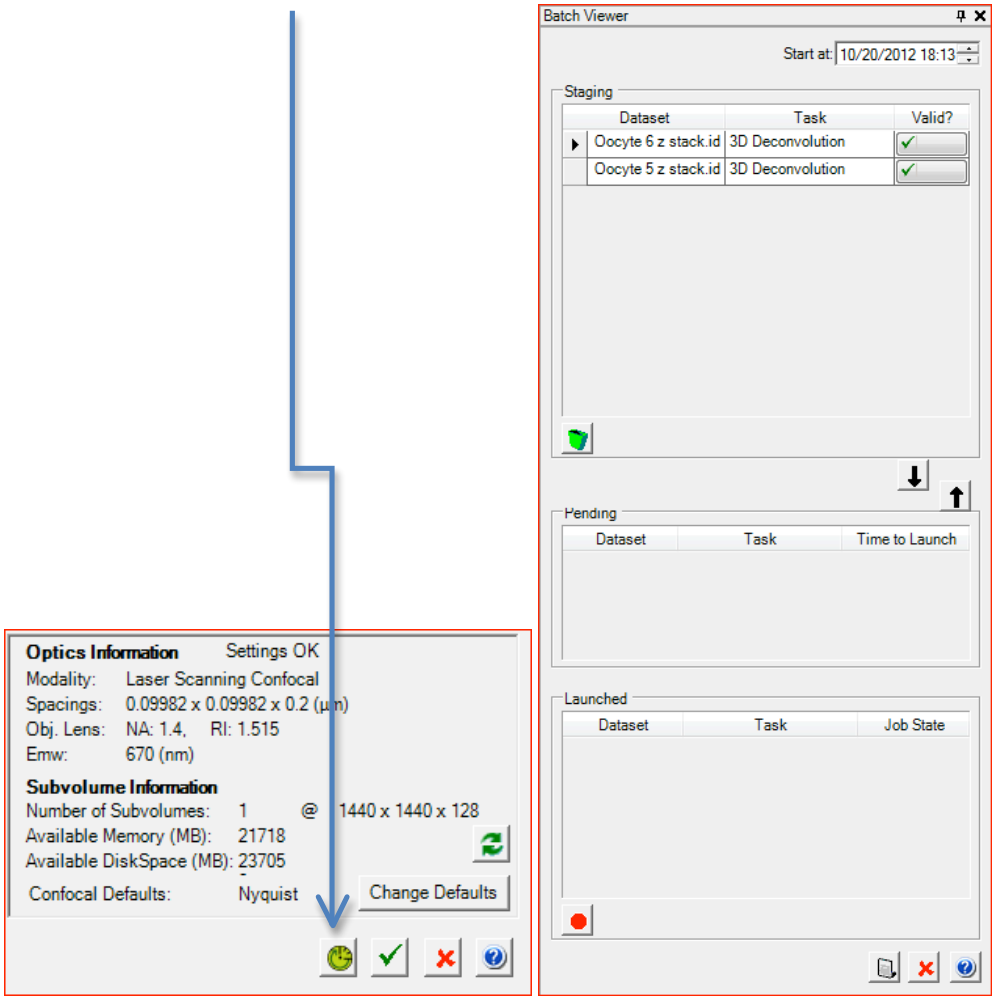

Windowpane 9: Processing multiple images for deconvolution.

- This will open up a new column on right side (as shown above) that will show all the images added to the batch. The middle and bottom thirds of this colum show the status of the images added to the batch. Clicking on the  launches the image for deconvolution. Clicking on the green arrow  starts the deconvolution process.

10.3 Segmentation of mitochondrial intensities

This involves using the deconvolved image to identify and classify mitochondria (individual/clusters) and getting the quantitative data regarding their number and distribution pattern.

10.3.1 Threshold cutoff (this is subjective)

- Go to Image processing – Thresholding – Threshold cutoff- Select channel – Select the background noise (here or through the Display Adjustment window, latter one is faster to do) – set the values below the selected threshold to “0”.

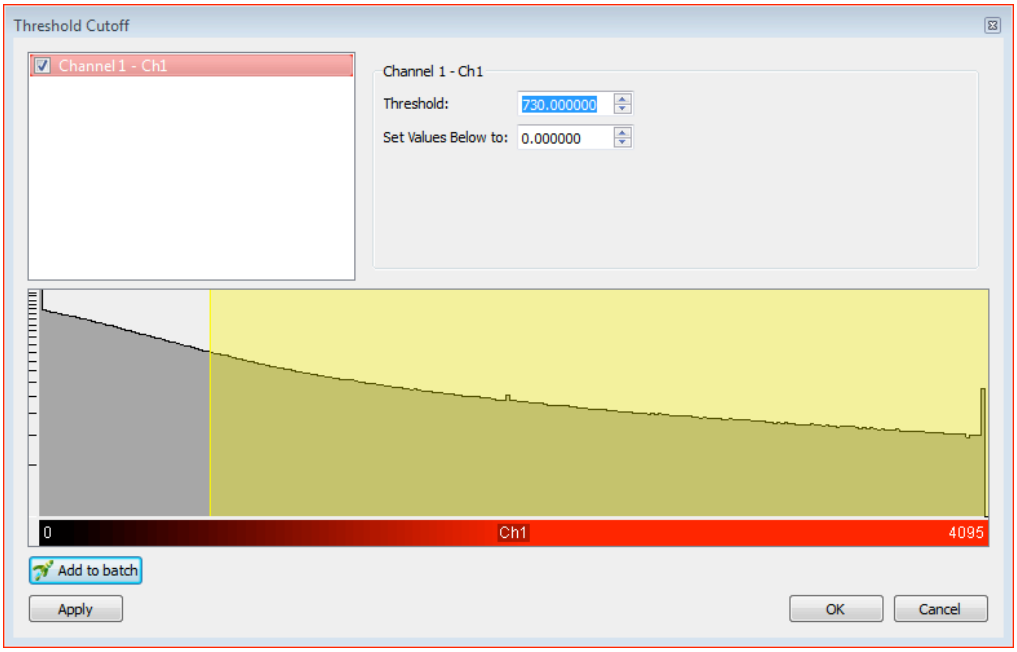

Windowpane 10: Performing threshold cutoff.

- Threshold selection- Display adjustment window- select the channel- go to the histogram and slide the slider on the left top of selected channel to make real time change in the image. This is purely subjective (idea is to keep the noise level to the minimum, a good reference will be to go through all the images and have an idea about the true signal and noise, identify a solitary spot that you think is mitochondria, measure its diameter in XY, should be between 1-1.5 micron).

10.3.2 Surface build up

- Click to start a new surface building process, uncheck segment only ROI and click “Skip automatic creation”

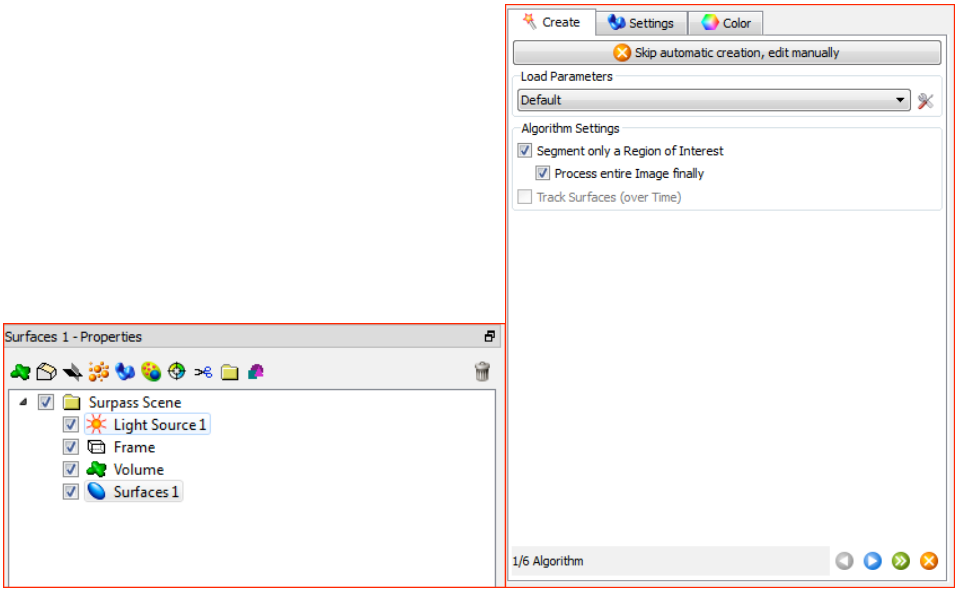

Windowpane 11: Surface creation to identify oocyte plasma membrane.

- Under "Contour" – Board- select XY orientation, Manual Resolution (946x946), Check preserve features

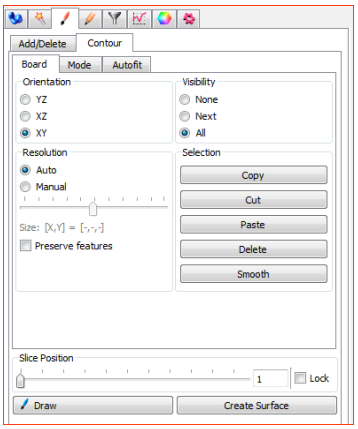

Windowpane 12: Manual creation of surface.

- Under "Contour- Mode – **select the channel you want to use,** select the "Distance drawing" – change vertex spacing to 0.5 μm. You may need to look at other modes for creating contour lines. The idea is to make the processing faster. If you feel that object has a circular outline then using the circle with >100 vertices is better. Other option is automatic detection of contour line with 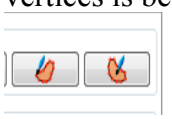 drawing modes, allow easy detection if there is enough clarity of signal. Other situation where it could be very useful is when we are concerned about identifying for say projections of oocyte plasma membrane.

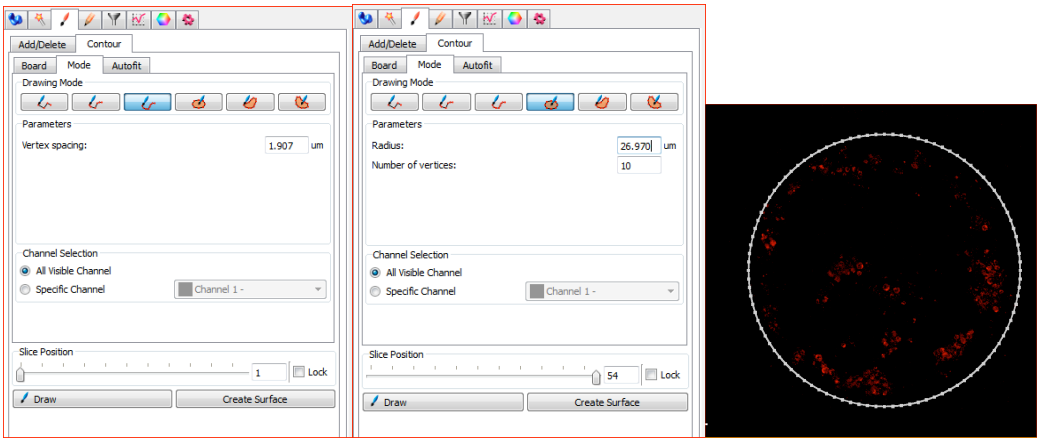

Windowpane 13: Different types of contour line for manually creating surface. Example of a circular contour line (with 100 vertices) is on the right.

- Bump up the intensities to have an idea of the oocyte plasma membrane (if you are not using the TPMT channel).

- Draw contour lines on the 1st, 2nd, 2nd last and last slices (you can copy paste the contour lines across the slices. Click on create surface.

- Mask (under pencil tab) all signal outside the surface as 0 (click on duplicate the channel before masking).

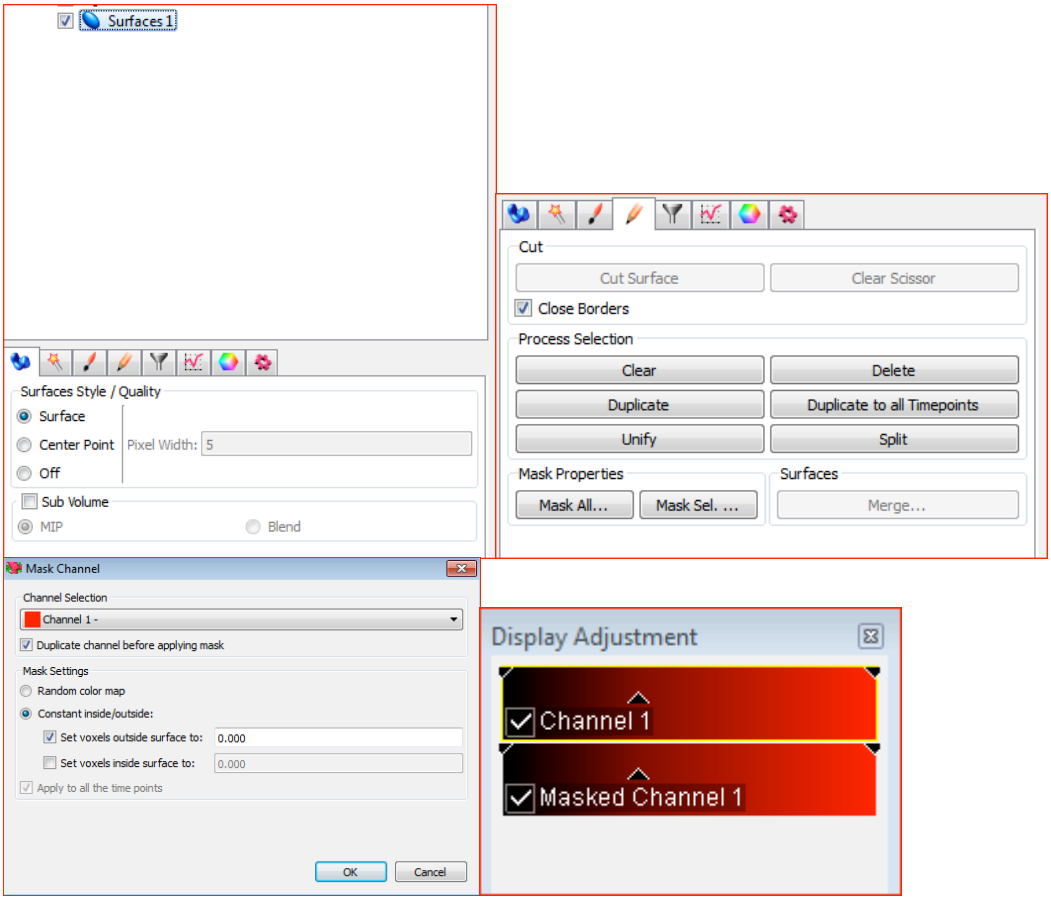

Windowpane 14: Masking the signal outside the surface to select the specified data set.

10.3.3 Distance transformation to surface

- Select the surface, click on the Tools button; click the “Distance transformation”, select the distance transformation from “inside the surface” and click OK.

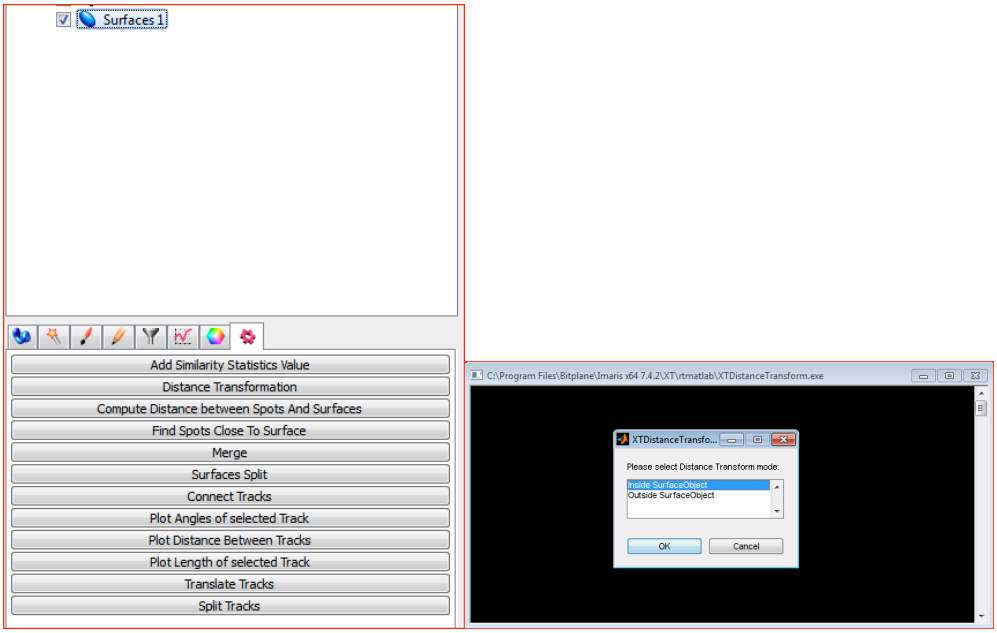

Windowpane 15; Distance transformation to surface.

- This will create another channel c/a Distance to Surface. Sometimes when we are creating new channel such as done here, it does not show up in the filters. In such cases save the image at the current step, close it and open it again.

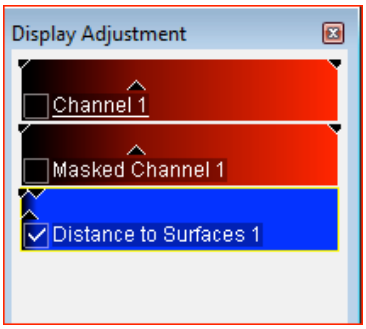

Windowpane 16: Channel created using distance transformation.

10.3.4 Identification of mitochondria as Spots

- Click on *spots* to create new set of spots (I call it Mitoall).

- Under the spots-, process entire image (unclick region of interest- Region of interest is very helpful in case of a very large dataset), click on different spot sizes (region growing).

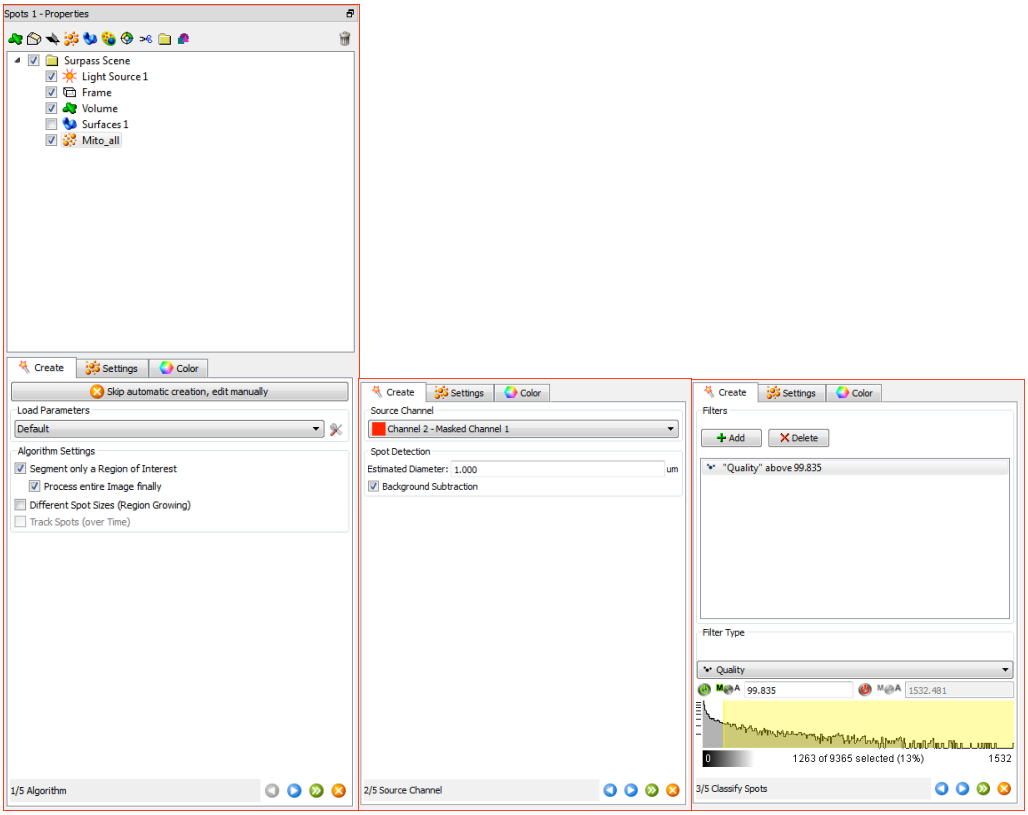

Windowpane 17: Spots creation to identify mitochondria.

- **Select the Masked channel** as you donot want to create spots outside the ooplasmic volume. You can always delete extra spots but it will be tedious job.

- Keep estimated diameter at 1 μm (this is based on the diameter of isolated intensity representing mitochondria under the Slice View). Check the "background subtraction". Click next.

- Under the quality filter work with lower range of intensities (power button is green and "M- Manual" mode is highlighted) let the button towards the higher range to be automatic (reflected by the power button being red). **Play with slider to the position where center points appear on the dimmest of the spots that you consider are representing the mitochondrial intensities.**

- Click next. Under Spot regions from, check the local contrast (Windowpane 18). Click next.

- Under spot regions, Diameter from: Region volume should be selected (Windowpane 18). Move the slices and play with the slider in order to pick the point that best represents the information you have. Always pay attention at the smallest/dimmest intensity and biggest/brightest intensity, this will tell the area that will be included in the spot. **For all my images I was using 1.45 value in the region volume.**

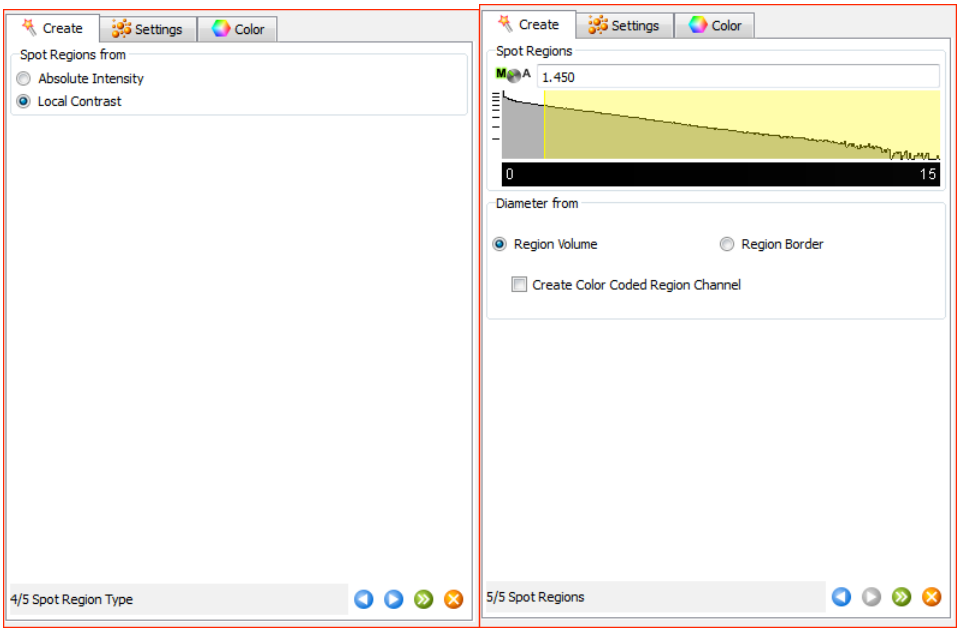

Windowpane 18: Settings for spots.

- Click on finish button and pick point style as Sphere (Windowpane 19).

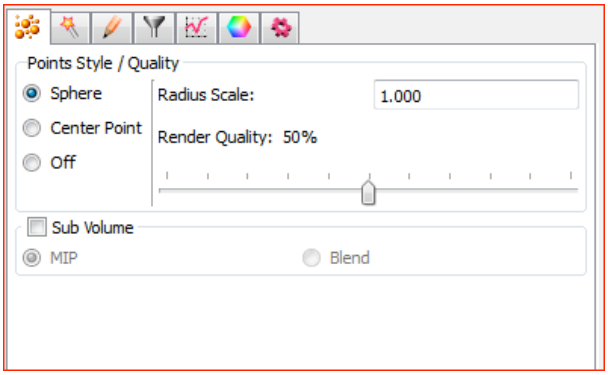

Windowpane 19: Changing the view option for spots.

10.3.4.1 Identification of spots in clusters or isolated spots (individual mitochondria)

- Click on the wheel button and select the Spots to Spots closest distance.
- Select the spots statistics and spots radius in the result mode.

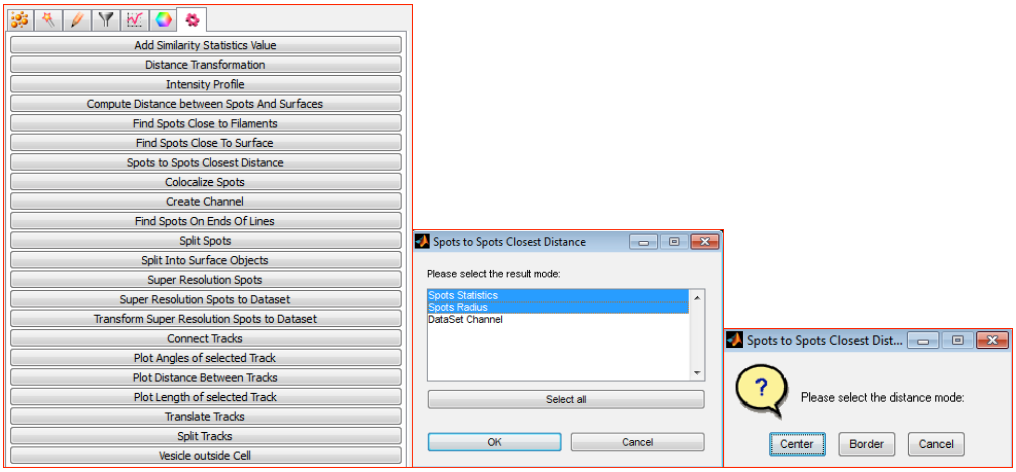

Windowpane 20: Identifying distance between spots.

- Click on the "center" under the distance mode.
- This creates the bubbles around the spots. The bubbles grow bigger until it touches bubble from other spot. This means bigger the bubble more isolated that is the spot.
- These bubbles are created as separate spots object.
- *Filter* these newly created according to the *Distmin*. You would like to select the bubbles that are not more than 2 micron *Distmin* from each other. These are the clustered bubbles. **Duplicate these as separate spots**.

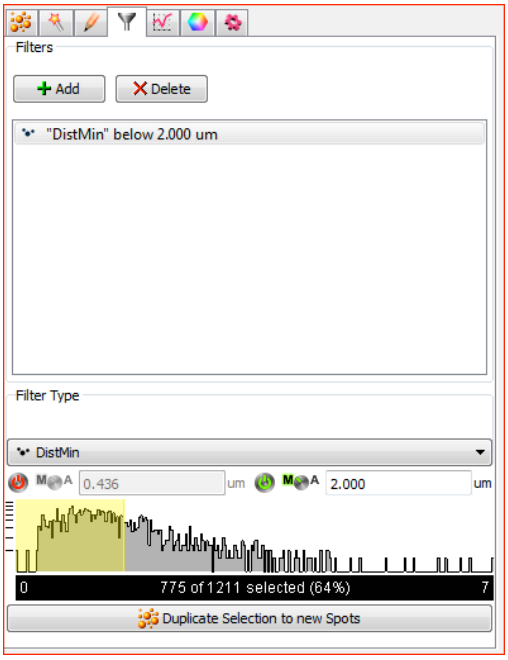

Windowpane 21: Identifying spots <2 µm from each other.

- Go to the wheels button again and click on the “create channel” and say “No” to *interpolation along the spots radius*. It is important because choosing “Yes” will create extra information (through interpolation) along the last slices (slices at the edge) in Z-direction.

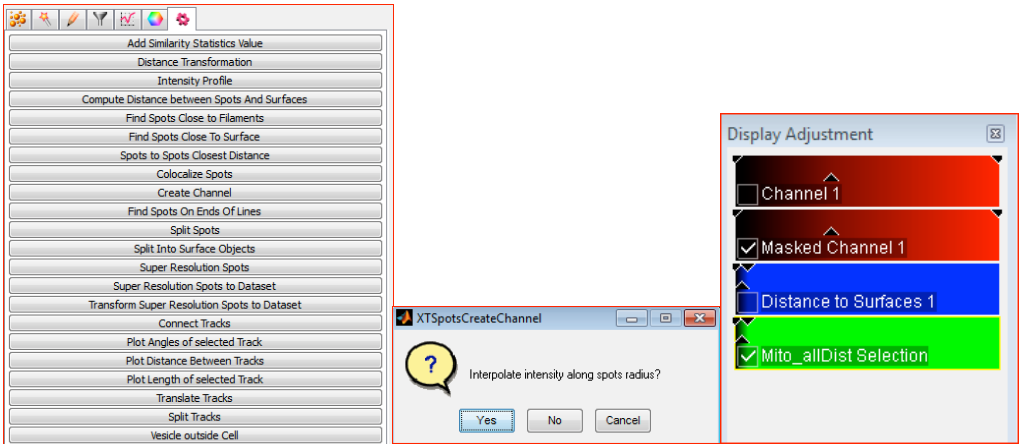

Windowpane 22: Creating a new channel for spots ≤2 µm distance to each other.

- Go to the original spots (Mitoall) and filter the spots according to the Intensity to center of Channel (Mito_allDist Selection) just created in the preceding step and duplicate the spots. Ideally these should represent the spots that were picked by the “spots to spots closest distance” step,

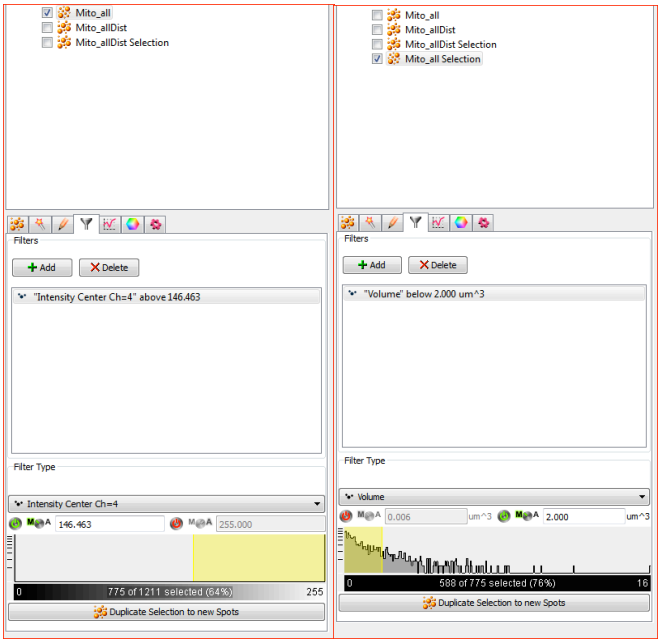

Windowpane 23: Filters to identify spots in clusters.

- Now in these duplicate set of spots (Mito_all selection) select the spots that are > 2 μm^3 volume and again duplicate these spots. These are the clusters. The

remaining spots are individual mitochondria. So the first filter was distance and 2nd is size. This is the best option we have right now to identify the clusters. I have tried "split spot" option for cluster analysis but that has problems and is more tedious to work along.

- Use these spots in clusters to create a channel (using the create channel option under the ____ button). This channel will be used to create surface around the clusters.

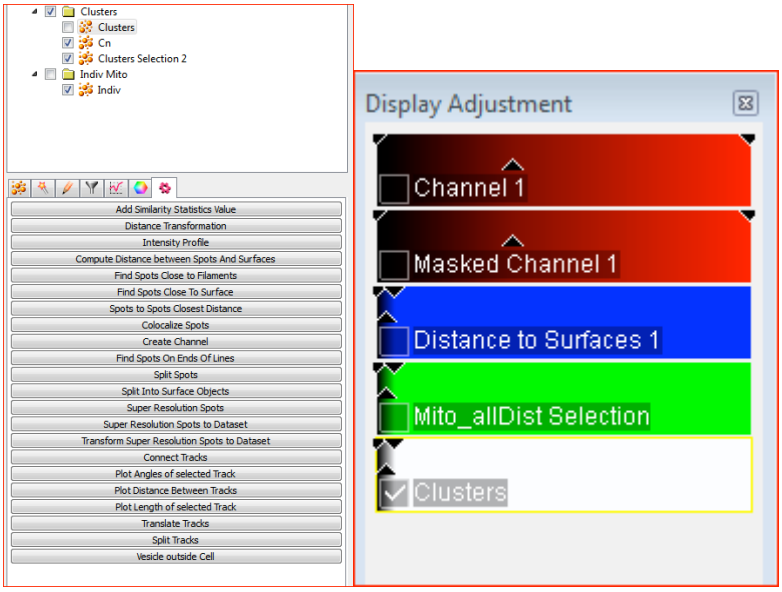

Windowpane 24: Creating channel for the mitochondria in clusters.

- Use the channel created above to create surface around the clusters (Windowpane 25). I used the settings (surface area detail at 0.2 µm and background subtraction set to 0.749 µm) identified by the software itself for creating this surface. Choose local contrast and keep other settings constant throughout all data sets.

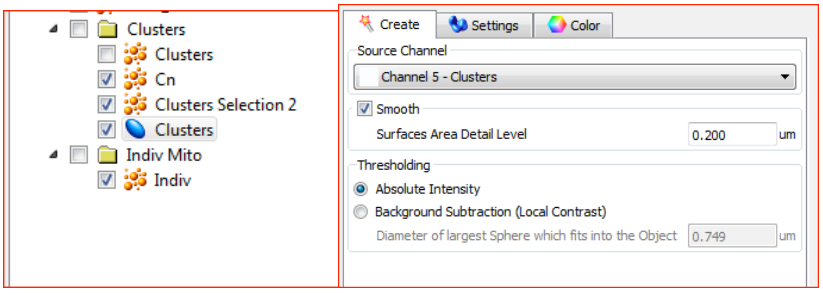

Windowpane 25: Settings for creating cluster surface.

- The remaining spots (volume ≤2 µm^3) are individual mitochondria. Also the mitochondria >2 µm distances to each other are individual mitochondria. Once you have these identified and duplicated into a separate folder group, you should merge them together.

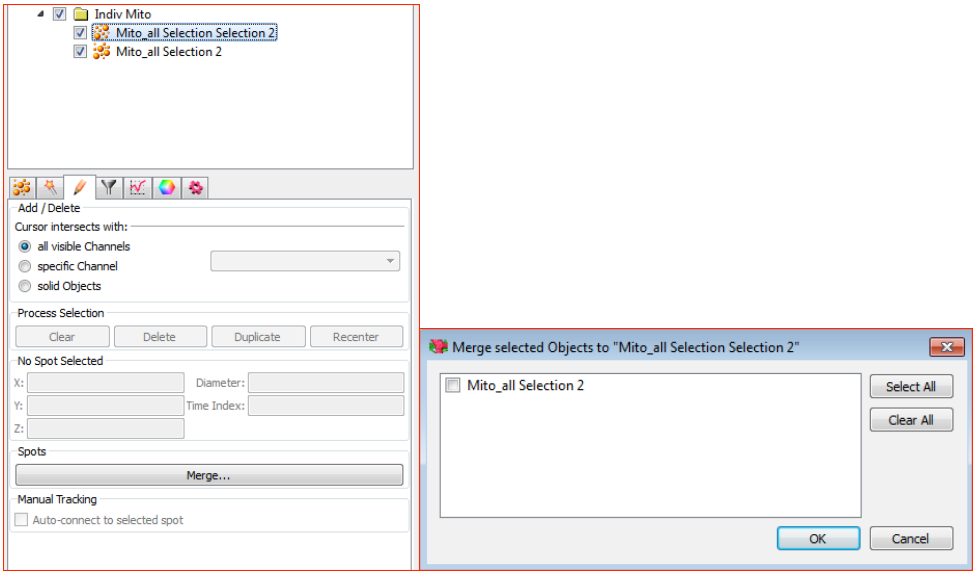

Windowpane 26: Merging spots (individual mitochondria) into one group.

10.3.5 Identification of peripheral vs central spots

- Go to the original spots and filter them according to the intensity of "Distance transformed channel" created for surface. This intensity is actually the distance from the surface towards the center. Select distance you want to say peripheral or central regions (we had 10 μm cutoff). Duplicate the selected spots. It is wise to make separate folders, as it will allow you to organize the selected spots and get the required information at the later stages.

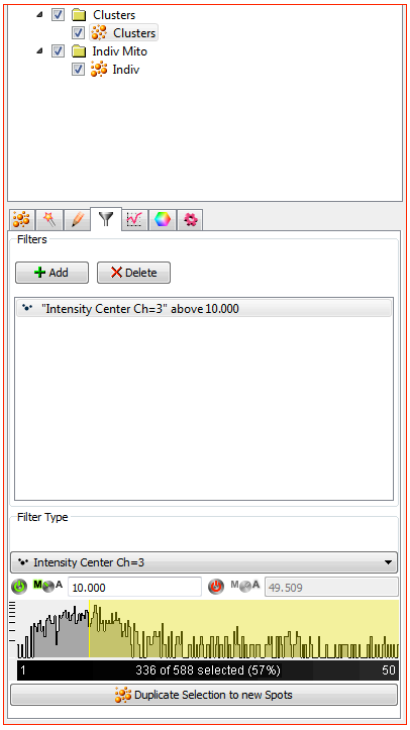

Windowpane 27: Filter for choosing peripheral/central spots.

- This applies to clusters also. Once the clusters

10.3.6 Identification of intensities in within the spots and clusters

- Import the original channel, in to the final image that you are working with, after changing it to 32 bit float. Make sure that you have this data set cropped to match up the one that you have used to identify the mitochondria.

- Then you can use the spots that you created to gather the information about the intensities